RECENT TRENDS IN THE CHANGING GEOGRAPHIC EXTENT OF CIÉNEGAS OF THE UNITED STATES/MEXICO BORDER REGION

by

Ian Wilson Housman

A thesis submitted to the faculty of
The University of Utah
in partial fulfillment of the requirements for the degree of

Master of Science

Department of Geography

The University of Utah

May 2011

Copyright © Ian Wilson Housman 2011

All Rights Reserved

The University of Utah Graduate School

STATEMENT OF THESIS APPROVAL

The thesis of **Ian Wilson Housman**

has been approved by the following supervisory committee members:

George F. Hepner	, Chair	**5-4-10** Date Approved
Andrea R. Brunelle	, Member	**5-4-10** Date Approved
Paul Maus	, Member	**5-4-10** Date Approved

and by **Harvey J. Miller** , Chair of the Department of **Geography**

and by Charles A. Wight, Dean of The Graduate School.

ABSTRACT

Wetlands, known as ciénegas, were once found throughout the basin and range physiographic province in southeastern Arizona, southwestern New Mexico, northern Sonora, and northwestern Chihuahua. These groundwater-dependent wetlands are now largely desiccated due to overgrazing, groundwater depletion, and the resulting incision of streams and rivers. This study consists of four components. First, a more complete inventory of the location of historical ciénegas is compiled. This is accomplished using peer-reviewed journal articles, historical maps, journals from explorers and pioneers, and USGS topographic maps. Second, the geographic extent of the documented ciénegas is hand-digitized through photo interpretation of aerial imagery. Each ciénega is divided by its activity status and the land cover succession path it followed. Third, the zonal statistics for a suite of Landsat Thematic Mapper (TM)-derived indices and elevation derivatives such as slope and aspect are compiled. Geospatial datasets that exhibit low variability among different succession paths are further analyzed as being possible predictor variables for the status or land cover type succession path of a ciénega. The two best predictor variables are the normalized burn ratio (NBR) and the thermal infrared (TIR) band. These two variables are used in a classification tree model to determine the location of other undocumented areas that are likely active ciénegas. The fourth component involves monitoring the trends of inactive, as well as active, ciénegas over the past 25 years using the two most sensitive predictor variables. The interannual variability is indicative of changes in vegetation cover, as well as the degree of saturation

of the soil. This component indicates that inactive and active ciénegas have experienced relatively uniform patterns of change that are highly correlated with annual precipitation patterns of the study region. This study results in a more complete inventory of the location and geographic extent of historical ciénegas, as well as a better understanding of the variables that can be used to identify different succession paths of ciénegas and possible undocumented active ciénegas. Additionally, for the first time, the recent trends of change for documented ciénegas have been analyzed using remote sensing techniques. This study serves as a preliminary inventory in what should be a series of studies to gain an understanding of the historical and paleodynamics of ciénegas, as well as possible restoration opportunities across a larger geographic area.

TABLE OF CONTENTS

ACKNOWLEDGEMENTS

I would like to thank the Southwest Consortium for Environmental Research and Policy (SCERP) for providing funding for this research. Without their funding, this study would not have been possible. I would also like to thank my Supervisory Committee for their guidance throughout the completion of this thesis. I would like to acknowledge Mr. and Mrs. A.T. and Cinda Cole and Dr. Raymond Turner for all of their help throughout my field work experience.

INTRODUCTION

Groundwater-dependent desert wetlands, known as ciénegas, serve as hospitable zones within a largely unforgiving environment. The geographic extent of these unique habitats has been diminishing since the late 1800s primarily due to the impacts of fire suppression, agriculture, overgrazing, groundwater depletion, and the resulting cycle of channel incision (Dobyns, 1981; Hastings, 1959). Ciénegas serve two key purposes. First, they provide a habitat for a diverse array of flora and fauna. Second, they absorb the temporally variable precipitation of the region, thereby reducing erosion and maintaining the height of the water table (Hastings, 1959; Hendrickson & Minckley, 1984). With their disappearance, the desert ecosystem is compromised.

A result of the concatenation of the Spanish words cien (one hundred) and agua (water), ciénega literally translates to "one hundred waters." In order to extend the understanding of the location and geographic extent of historical ciénegas, common attributes among succession classes, and recent trends of change, this study consists of four components. The first component (ciénega point location inventory) involves the creation of a complete inventory of locations of ciénegas across the study region since European settlement in the 19th century. This is necessary due to the current lack of knowledge of the location of historical ciénegas. The second component (ciénega areal extent inventory) uses aerial imagery interpretation to delineate the areal extent of documented inactive and active ciénegas. Each ciénega is classified based on its activity status succession path (active or inactive) and its land cover type succession path

(herbaceous, woody riparian, and agriculture). This creates areas of interest that are representative of their respective status and land cover type succession path for the third component. The third component (best predictor variable determination) involves the computation of the zonal statistics for each ciénega using a suite of different geospatial datasets. Some examples of these data include elevation, aspect, thermal infrared imagery, and Landsat Thematic Mapper (TM)-derived vegetation indices. These statistics are analyzed to find possible predictor attributes of both active and inactive ciénegas, as well as the land cover succession patterns exhibited by inactive ciénegas. Attributes that exhibit different values among the various succession paths of ciénegas will provide insight into possible influencing variables for ciénega desiccation and subsequent vegetation succession. The last component (monitoring recent trends of change) looks at change of vegetation health and wetness of ciénegas over the past 25 years based on the Landsat TM-derived normalized burn ratio (NBR) and thermal infrared (TIR) imagery. These results are analyzed to find any emerging patterns across the various ciénega succession paths.

Study Region and Anatomy of a Ciénega

The study region encompasses the geographic extent of ciénegas within the basin and range physiographic province of southeastern Arizona, southwestern New Mexico, northeastern Sonora, and northwestern Chihuahua (Figure 1). The general definition of a wetland used by the US Fish and Wildlife Service is based on the following three criteria:

1. The soil or substrate is saturated or covered by shallow water at some time during the growing season.

2. The plants in these environments are adapted to grow in water, soil or a substrate that is occasionally oxygen-deficient because of water saturation.
3. The hydric soils are saturated long enough during the growing season to produce oxygen-deficient conditions in the upper part of the soil occupied by plant roots.

(Baker, Lawrence, Montagne, & Patten, 2004)

Within the context of this study, ciénega refers to the specific type of wetland that results from perennial springs inundating flat basin areas in a desert environment. These perennial springs generally occur where one or both of the following underlying geological features occur:

1. There is a layer of clay-rich soil with a low hydraulic conductivity beneath the surface, thus limiting water flow. The water is not able to continue traveling downward, thus it is forced to the surface. This occurs where there are sudden changes in topography, such as at the edge of a basin as shown in Figure 1.
2. The underlying rock strata is fractured, usually due to a fault line. The fracture promotes the passage of ground water from a confined aquifer beneath to the surface. (Baker et al., 2004; Tiner, 2003)

Figure 2 depicts the groundwater flow patterns in the basin and range physiographic province. Recharge generally occurs in the mountains, while discharge occurs in the flat basin areas. Because the basins are generally flat and wide, discharge will not only occur directly into streams and rivers, but also at the edges of the basins. This is generally where perennial springs that feed ciénegas are found.

Ciénegas generally occur between an elevation of 1000 and 2000 meters within the study area (Hendrickson & Minckley, 1984). This results in an initial approximation of the study region (Figure 1).

The groundwater of the study region originates from its bimodal precipitation pattern, averaging between 250 and 400 mm precipitation annually (Etheredge, 2004). The range in precipitation is primarily elevation-dependent, with an increase in annual precipitation with increased elevation. Recharge to the hydrological system occurs during two periods throughout the year. During the winter, cyclonic frontal systems provide steady precipitation that accounts for about half of the usual precipitation in the northern portion of the study area. This proportion of the total precipitation decreases with latitude. Winter precipitation falls primarily as rain in the valleys and snow in the mountains (Etheredge, 2004), serving as the primary form of groundwater recharge for the perennial springs that feed ciénegas.

The remaining half of annual precipitation results from convective uplift of warm moist air from the south. Impacting the region from July through September, this is known as the North American monsoon (Etheredge, 2004). The strength of the North American monsoon increases as latitude decreases within the study region. The varying dependence on the monsoon can be seen in the variability in summer precipitation amounts of various cities throughout the study region in Figure 3. The North American monsoonal precipitation has more temporal variability than the winter precipitation, resulting in flash flood conditions (Etheredge, 2004). When torrents of surface flow from a flash flood encounter broad flat ciénegas, their energy is lost, thus depositing sediment.

This nutrient-rich sediment, along with constant inundation from ground water discharge, sustains a healthy ciénega (Minckley & Brunelle, 2007). The slow rate of surface flow in ciénegas serve as a natural groundwater recharge mechanism (Hendrickson & Minckley, 1984).

Permanently saturated hydrosoils provide a habitat for unique flora. These include, but are not limited to, shallow-rooted, semi-aquatic sedges (*Cyperaceae*), watercress (*Rorippa nasturtium-aquaticum*), and water-pennywort (*Hydrocotyle verticillata*) within the ciénega (Hendrickson & Minckley, 1984). The immediate surroundings of ciénegas are often saline, providing a habitat for salt grass (*Distichlis spicata*), yerba-mansa (*Anemopsis californica*), and various taxa of the Chenopodiaceae and Asteraceae families (Hendrickson & Minckley, 1984).

The sustainability of ciénegas' unique flora, as well as many endangered birds, amphibians, and fish, is largely dependent on the state of the subsurface hydrological system. Sustainability within a groundwater setting is when a system is recharged with an adequate volume of water to maintain the present ecosystem (Baker et al., 2004). When a system is not sustainable, the total volume of discharge, either due to evaporation, evapotranspiration, runoff, or anthropogenic causes, is larger than the volume of recharge (Baker et al., 2004). An unsustainable or a nonsteady state can result from a change in climate, a subsurface tectonic shift, a change in the flora or fauna of the region, or anthropogenic activities, such as the cultivation of crops or cattle grazing (Minckley & Brunelle, 2007). Because more water has been extracted from the study region than replenished, the water table has subsided, causing the majority of the region's

wetlands to disappear (Baker et al., 2004; Hendrickson & Minckley, 1984).

Current Restoration Efforts

Given the compromised state of desert ciénegas throughout the Southwest, numerous efforts to restore extinct ciénegas are taking place. The locations of these restoration efforts can be found in Figure 4. The most common restoration method for ciénegas has been to pump ground water to recharge the area while also building dams or dikes to retain the water (Minckley & Brunelle, 2007). Although the San Bernardino Ciénega in the San Bernardino National Wildlife Refuge does have several active perennial springs and seeps, the saturated portion of the historical ciénega is ultimately maintained through groundwater pumping.

Alternative approaches to ciénega restoration include introducing meandering flow patterns to slow the rate of surface flow, and small dams or gabions to impede surface flow. Each of these methods results in a reduction of arroyo incision, and an increase in water table levels. The introduction of meandering flow patterns is being used at the Pitchfork Ranch's Burro Ciénega near Silver City, NM, while the construction of a dam has been employed at the San Simon Ciénega on the Arizona/New Mexico border. Gabions have been used on the Rancho San Bernardino ciénega.

The San Simon Ciénega was restored in 1953, when the US Bureau of Land Management constructed a dam. Prior to this, the ciénega was continually deteriorating due to arroyo incision (Hendrickson & Minckley, 1984). Presently, there is a small reservoir in the lower part of the ciénega, with herbaceous vegetation dominating the area just above the completely flooded area. The reservoir does allow for groundwater

recharge of the area, but inhibits hydrophytes from growing. In addition to maintaining the ciénega's water table with a dam, the San Simon Ciénega uses the pumping of groundwater to ensure constant saturation (Hendrickson & Minckley, 1984). It should be noted that although Hendrickson and Minckley (1984) did classify this ciénega as being active, field observations and aerial photo interpretation in this study resulted in this ciénega not fitting the criteria necessary to be classified as active.

To the south of the San Bernardino National Wildlife Refuge is the San Bernardino Ranch Ciénega. This ciénega is a continuation of the same San Bernardino Ciénega in the National Wildlife Refuge. The active portion is located on the Mexican side of the border. There is a large section of the historical ciénega that has maintained a saturated state. This section can be seen in Figure 5. The ciénega in the photograph may appear as an open herbaceous area, just as many other grasslands. This area is actually fully saturated, with standing water just below the vegetation's surface. Hastings (1959) mentions this ciénega as being an anomaly because it is surrounded by areas of incision, yet has maintained a saturated, active state. This is likely due to the underlying geology of the site. More recently, many gabions have been constructed in some adjacent areas on the ranch to reverse the incision process, and elevate the water table.

The Burro Ciénega restoration project is a recent project that is making use of meandering channels for restoration. This method is effective, but much slower than dams, dikes, or gabions. By spreading flow through meandering paths, water's speed is slowed, thus inhibiting vertical incision and promoting sediment deposition. This method involves materials such as interwoven tree branches, and is therefore initially vulnerable

to flooding. As the channels become broader and shallower, the area becomes saturated once again. This restoration method takes advantage of the erosive forces of water to reestablish a new floodplain at the elevation of the incised channel, once again permitting sheet flooding and the establishment of a healthy ciénega. This differs greatly from dams, dikes, and gabions. Each of these structures raises the level of the surface, with the ultimate goal of back-filling the arroyo channel with sediment. In the first 5 years of restoration, the Burro ciénega has shown signs of increased saturation with areas that previously had ephemeral flow exhibiting perennial flow. The perennially flowing main channel, along with a control structure, can be seen in Figure 6.

Other active ciénegas that fall under some level of protection are the Arivaca ciénega (US Fish and Wildlife Service), Bingham ciénega (The Nature Conservancy), Canelo Hills (The Nature Conservancy), and the Sonoita Creek Preserve in Patagonia, AZ (The Nature Conservancy). Additional current restoration efforts include the Cloverdale ciénega (The Nature Conservancy and Sky Island Alliance).

The three restoration examples employ several different approaches to ciénega restoration. It is clear that all methods have their strengths and weaknesses. The reality is that ciénega restoration is a costly, time-consuming process. Nevertheless, the areas that have been restored serve as vital habitats in this arid region.

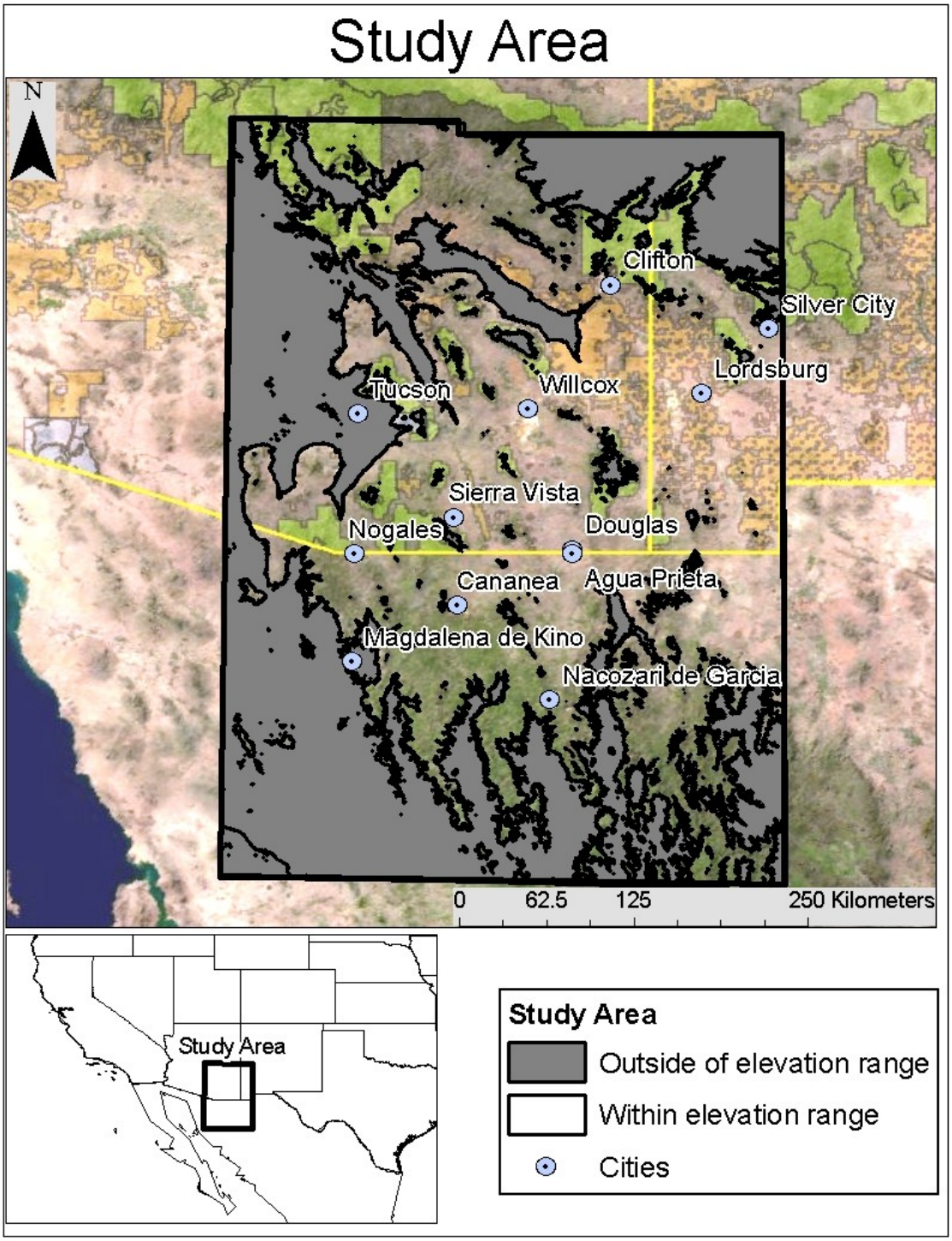

Figure 1: Outline of study area within basin and range physiographic province. The region is bound by the Sierra Madre Occidental to the south and the Colorado Plateau to the north. Areas that are >2000 or < 1000 m above mean sea level are masked out.

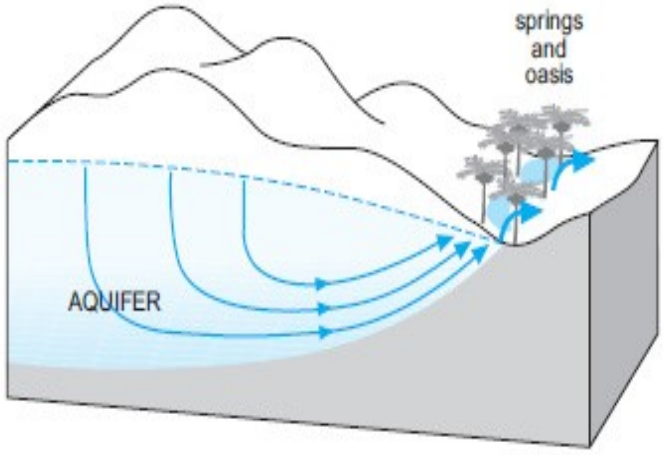

Figure 2: Hydrological flow diagram showing recharge in mountains and discharge in adjacent basins (Foster et al.,2006)

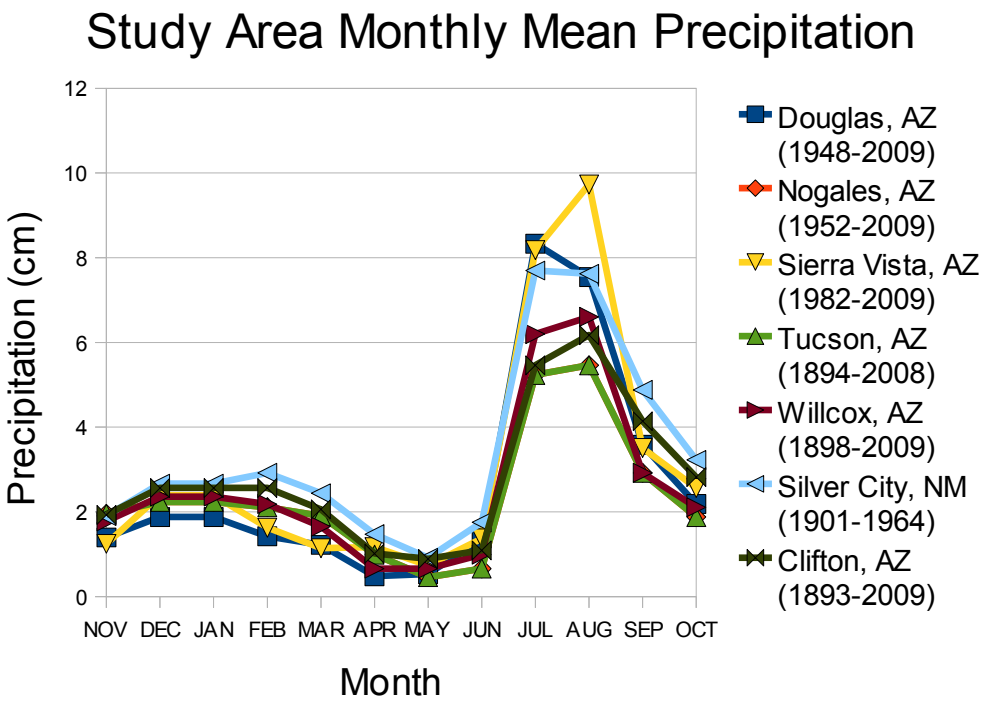

Figure 3: Graph of mean monthly precipitation in cities across the study region. The period of observation for each city is displayed in the legend. The influence of the North American Monsoon can be observed in the months of July, August, and September. (Precipitation data source: wrcc.dri.edu)

Restored Ciénega Locations

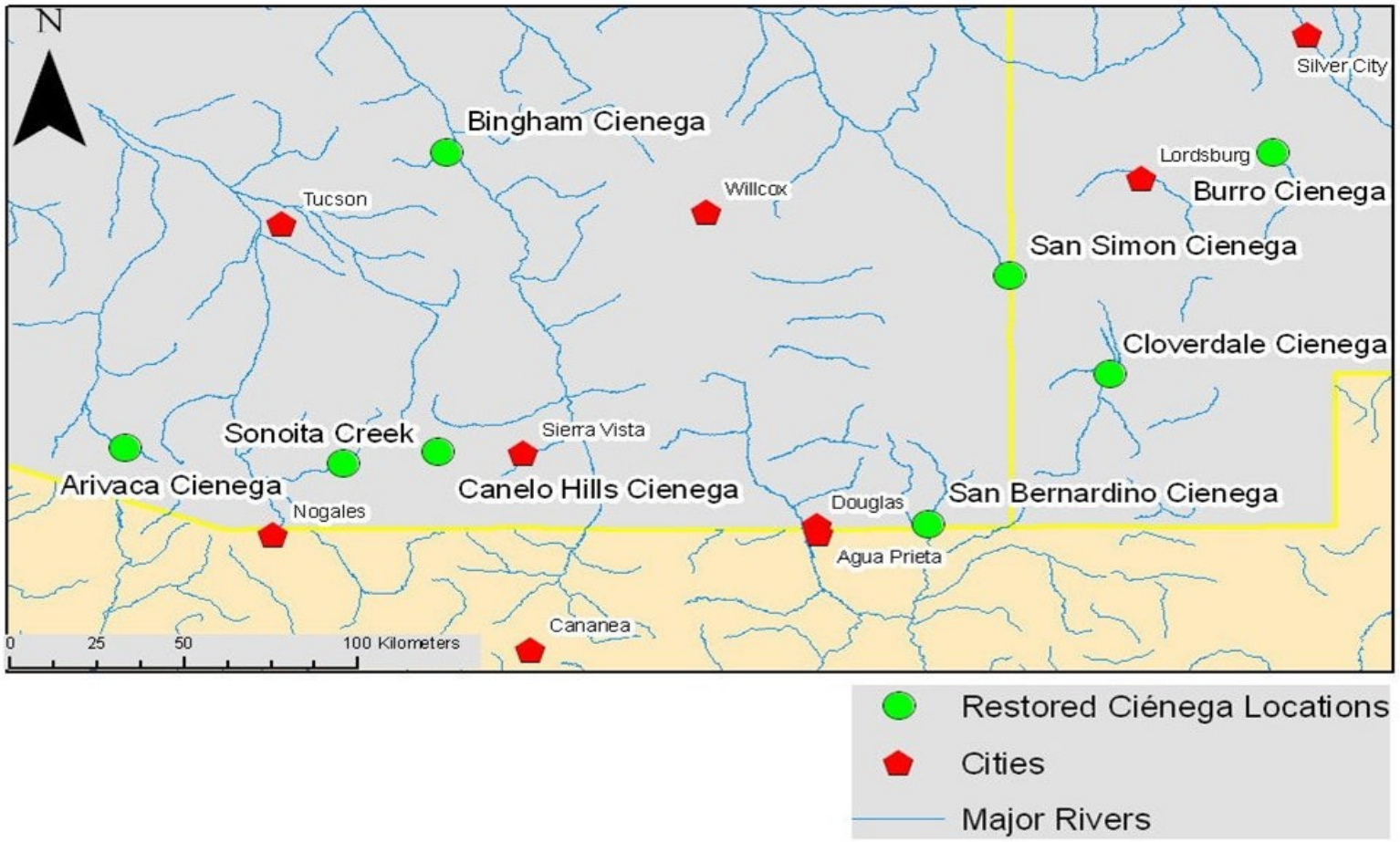

Figure 4: Locations of restored ciénegas throughout study region.

Figure 5: Active portion of Rancho San Bernardino Ciénega in January 2010

Figure 6: Pictures of Burro ciénega restoration (top) and perennially flowing channel (bottom)

LITERATURE REVIEW

The Extent and Patterns of Change of Ciénegas

Despite the important role ciénegas once played in erosion control, maintaining water table levels, and providing an ecotone for unique flora and fauna, there are relatively few studies on ciénegas. Recently, as the importance of ciénegas has come to light, the interest in ciénegas has increased. This has resulted in many more studies that are beginning to provide a greater understanding of these unique wetlands.

Although ciénegas were mentioned throughout army medical records, pioneers' journals, newspapers, and court documents throughout the European settlement of the study region, many of these records were not compiled to provide a greater understanding of where ciénegas had been located. Hastings (1959) began to change this in a paper entitled, "Vegetation Change and Arroyo Cutting in Southeastern Arizona." This paper looked to answer how exactly vegetation cover had changed since the European settlement of southeastern Arizona in the mid-19th century. One of most striking examples of documented land cover change was that of ciénegas. Within this compilation of pioneers' journals, newspaper articles, and court documents, Hastings identifies areas as historic ciénegas if they were referred to as ciénegas, marshy, or boggy (Hastings, 1959).

Such boggy areas are mentioned as being difficult areas to cross, or areas infested with malarial mosquitoes by pioneers. Hastings (1959) goes into great detail of how the entire San Pedro River valley was a continuous single ciénega. He adds that the Santa

Cruz, San Simon, and San Bernardino Rivers all had ciénegas on their margins. This paper served as the first publication that mentioned ciénegas as being a once widespread ecotone that had largely desiccated.

In 1965, Hastings and Turner published a book entitled *The Changing Mile*. The authors used 97 pairs of matched photographs from southern Arizona and northern Sonora between the late 19th century and the 1960s to arrive at four primary conclusions about vegetation change in the region:

1. Throughout the study region, a decrease in the frequency of desert scrub and cactus was observed.
2. Desert grasslands had been invaded by woody vegetation such as mesquite.
3. Areas that had once been dominated by oak, were now largely dominated by mesquite.
4. The xeric plant communities had moved upward in elevation (Hastings & Turner, 1965)

Hastings and Turner (1965) identified possible causes of these changes as cattle grazing, rodents and jackrabbits, wildfire suppression, and climate change. They concluded climate change could best account for the observed regional vegetation changes since the 1880s. This is because both the invasion of xerophytes such as mesquite and the more general displacement of mesic species by xeric species along an elevation gradient indicate a trend towards greater aridity. The reasoning for this trend will be revisited in future literature.

After "The Changing Mile" was published, the subject of arroyo incision and

causes of vegetation change in the Southwest continued to attract attention. Such papers include Cooke and Reeves (1976), and Dobyns (1981). Dobyns' paper, entitled "From Fire to Flood: Historic Human Destruction of Sonoran Desert Riverine Oases," deserves mentioning. This paper rekindled the debate over the ultimate cause of change in dominant vegetation types of the region, and arroyo incision. While Hastings and Turner (1965) ultimately concluded that looking at the patterns of vegetation change, climate change is most likely the primary driving force, Dobyns (1981) argues that the Native Americans controlled vegetation succession through the use of prescribed burning. He proposes that because areas were frequently burned, Native Americans were able to maintain herbaceous vegetation cover (Dobyns, 1981).

Whether the invasion of woody vegetation occurred due to historical wildfire suppression or not will be a recurring point of interest in the literature. Regardless of the cause of the invasion of woody plant species, the cause of the initial desiccation of ciénegas goes with little debate. The causes of ciénega desiccation should be separated from the causes of woody vegetation succession. Figure 7 displays both of these cycles, and how they differ. Although active ciénegas inhibit most woody species from growing due to saturated conditions, once desiccated, woody plant species succession can begin.

In 1984, Hendrickson and Minckley published the first and most complete inventory of historical ciénegas of southeastern Arizona to date. This paper, entitled "Ciénegas- Vanishing Climax Communities of the American Southwest" views ciénegas as an aquatic climax community. This hypothesis is based on paleoecological data that existed at the time of publication of this paper, thus viewing ciénegas across periods

without the influence of Native American fire prescription. Because these data indicate that ciénegas experience long periods of activity without incision, Hendrickson and Minckley (1984) attribute the historical cycle of arroyo incision and the subsequent ciénega desiccation to cattle grazing and ground water extraction (Figure 7).

Hendrickson and Minckley (1984) divide the ciénegas of North America into three categories based on elevation. The first category is found at elevations >2000m, in bog-like alpine settings. These areas are surrounded by conifer forest and are generally snow-covered throughout the winter months (Hendrickson & Minckley, 1984). The second category was found at elevations <1000 m, on the margins of major streams. These ciénegas form on oxbows of rivers, bound between uplands and the river's edge. Because this type of ciénega forms on dynamic floodplains, it is vulnerable to floods, thus exhibiting patterns of frequent change with respect to time (Hendrickson & Minckley, 1984). The third category was found between elevations of 1000 and 2000 m. This category is of primary concern to this study. Hendrickson and Minckley also limited their analysis of ciénegas to this category because ciénegas in this setting had exhibited little change over time prior to the end of the 19th century (Hendrickson & Minckley, 1984). Their vulnerability to scouring from floods is different from ciénegas at lower elevations because of their close proximity to streams' headwaters. These areas are sustained by groundwater discharge and sheet flooding from adjacent streams. The inventory that they provided only includes ciénegas that fall within this category.

The inventory Hendrickson and Minckley (1984) provided was geographically constrained to southeastern Arizona. This area was determined to be the region with the

highest concentration of ciénegas. In all, they identified approximately 35 ciénegas throughout southeastern Arizona. Each was given a brief description of where their description was found in the historic literature, as well as the ciénega's current condition.

Hendrickson and Minckley (1984) made it clear that further research was needed to evaluate whether ciénegas truly were climax communities that have been desiccated due to cattle grazing, and/or climate change, or whether a lack of Native American-prescribed fire was the culprit. Davis, Minckley, Moutoux, Jull, and Kalin (2002) used sediment analysis to reconstruct the vegetation history of six different ciénegas. They concluded that in all six ciénegas, there was a large transition in the flora present, as well as the frequency of fire at the beginning of the historical period. This was indicated by the pollen and charcoal present in the cores (Davis et al., 2002). They argued that Native Americans actively used fire to maintain herbaceous vegetation within ciénegas. Additionally, ciénegas were used by Native Americans for cultivation, indicated by the presence of corn (*Zea*) pollen. They finish by mentioning that Turner and Hastings (1965) dismissed this argument, in favor that climate change was the primary culprit for the historical change in vegetation cover. This was because of a lack of quantitative data to support the argument that Native Americans actively maintained the landscape through the use of fire. Davis et al. (2002) concluded by mentioning that they view their results as the quantitative data that Hastings and Turner (1965) were lacking.

Most recently, several papers have used coring techniques to assess the paleo conditions of several different ciénegas from the Davis et al. (2002) paper (Minckley & Brunelle, 2007; Minckley, Clementz, Brunelle, & Klopfenstein, 2009; Brunelle,

Minckley, Blissett, Cobabe, & Guzman, 2010). Minckley and Brunelle (2007) concluded that across a ~7000 year record sediment core from the San Bernardino ciénega, there was a correlation between times of rapid sediment deposition and moist periods. This also temporally correlated with periods of incision in the San Pedro and Santa Cruz river valleys. This indicates that the health of some ciénegas, such as the San Bernardino ciénega, was not temporally correlated with healthy periods in other documented areas such as the San Pedro and Santa Cruz basins. Regardless of the spatial variation in periods of aggradation and degradation, both are associated with periods of high runoff, thus indicating that incision and deposition are correlated with high precipitation regimes.

Minckley et al. (2009) analyzed the isotopes from a 4000 year sediment record from the San Bernardino ciénega and concluded that there has been a change in the source of organic matter from 850 calendar years before present. They attribute this change to an increase in moisture due to climate change, and vegetation evolution within the ecotone. Again, they mention that these records serve as valuable proxies to monitor paleoclimate change.

The most recent paper about ciénegas looked at an ~8000 year fire history of the San Bernardino ciénega (Brunelle et al., 2010). By looking at the fire patterns in charcoal data from times prior to Native American influence, this paper related fire frequency to the amount of winter precipitation received. Fire frequency increased with the start of the El Niño Southern Oscillation (ENSO). ENSO results in years with increased precipitation during the winter months for the study region. Additionally, the pollen data indicated that winter-dominated precipitation regimes corresponded to greater fire

frequency, thus supporting the charcoal data (Brunelle et al., 2010). By relating fire regimes to climate cycles such as ENSO, the ability for Native American burning to serve as the chief mechanism for controlling plant succession appears to be an oversimplification.

The studies reviewed provide a good foundation for an understanding of historical ciénegas, and their paleodynamics. This study will build on this body of literature by using remote sensing techniques to map historical ciénegas, and monitor recent patterns of change. The locations of historical ciénegas will enable future paleostudies of historical ciénegas.

Remote Sensing of Ciénegas

The use of remote sensing as a technique for monitoring the trends of change of ciénegas, as well as identifying any common attributes, has never been performed. Although ciénegas have not been studied using these techniques, wetlands have been studied using a number of remote sensing techniques.

Remote Sensing Techniques for Wetland Identification

The ability to use remote sensing techniques to classify areas as wetlands allows for a more efficient, geographically continuous analysis than field-based techniques. This application of remote sensing has a large body of literature behind it, with nationwide products such as the National Wetlands Inventory resulting from the synthesis of many of these studies.

One such classification method was explored by Baker et al. (2006). Using

Landsat Enhanced Thematic Mapper Plus (ETM+) imagery, they explored the ability of two decision-tree models to identify wetlands and riparian areas in the imagery. They used the classification tree analysis (CTA) and stochastic gradient boosting (SGB) classification algorithms. Each algorithm resulted in a high level of accuracy, with CTA having an overall accuracy of 73.1% and SGB having an overall accuracy of 86.0% at identifying wetlands and riparian areas. Additional studies have also had encouraging results. Rodemaker and Heidel (2008) used a Classification and Regression Tree (CART) model with ASTER imagery to map peatlands in the Shoshone National Forest. Variables used included image-derived variables, and elevation derivatives such as slope and aspect. The results were then compared to the NWI of similar peatland vegetation. They concluded that both the NWI, along with the techniques their study used, provide useful data to land managers.

Another similar study looked at the possibility of using Landsat TM-derived variables, along with ancillary GIS layers, to classify different types of palustrine wetlands (Wright & Gallant, 2007). They used a classification tree algorithm to classify the different types of palustrine wetlands found in Yellowstone National Park. This methodology resulted in error rates from 7.8%-17% depending on the level of classification. They finished by mentioning that a spatially discrete classification of palustrine wetlands may be insensitive to the variability in wetlands' extent with respect to time. By creating a wetland probability surface, this variability, along with the overall likelihood of the existence of a wetland, would be accounted for.

Remote Sensing Techniques for Groundwater Monitoring

Each of the previous studies used surface attributes as predictors for the existence of wetlands. The assumption that vegetation, slope, aspect, and other ancillary attributes of an area are indicative of the presence or absence of a wetland is often times correct. However, in some scenarios, such as springs and seeps within a canopy, or homogenous herbaceous areas where some flora are dependent on hydric soils while others find such conditions uninhabitable, these methods result in large errors of omission. The underlying geology greatly influences the subsurface hydrology, thus presenting anomalies when only surface data is used. These shortcomings of using traditional shortwave remote sensing techniques have resulted in the use of alternative approaches.

The prospect of using remote sensing to monitor groundwater dependent features has gained attention in recent years. It was not until 2006 that preliminary analyses of the potential of using satellite remote sensing to monitor groundwater were published (Becker, 2006; Jha, Chowdhury, Chowdary, & Peiffer, 2006). Jha et al. (2006) mentioned that at the time, there were six major areas of remote sensing and GIS applications in groundwater hydrology. From this list, the most closely related to the identification of groundwater-dependent ecosystems (GDEs) such as ciénegas was the, "exploration and assessment of groundwater resources" (p. 427). It is mentioned that although at the time there were six primary applications, each was limited with its level of success. This is inherent with the difficulties of measuring subsurface flow using proxies from above the surface. Becker (2006) proposed using remote sensing techniques as a proxy to infer ground water behavior. Additionally, he looked into the possibility of using a suite of

different datasets that would more adequately account for subsurface geological heterogeneities to model groundwater flow. This paper, although rather indirectly related to the remote sensing of GDEs, does provide the framework for subsequent analyses.

Large-area Remote Sensing of GDEs

Large-area remote sensing of GDEs has been attempted using a number of different techniques. Munch and Conrad (2007) used a combination of a GIS model and Landsat-derived biomass indicators to classify areas as GDEs. They were successful at identifying large-area GDEs, while the 30 m resolution of the biomass indicators limited the level of success at identifying small-area GDEs (Munch & Conrad, 2007). Numerous other studies have used satellite remote sensing to monitor or identify larger wetlands over large areas with a high level of success (Hansen, 2008; Krankina, Pflugmacher, Friedl, Cohen, Nelson, & Baccini, 2008; Pflugmacher, Krankina, & Cohen, 2007; Roshier & Rumbachs, 2004; Soti, Tran, Bailly, Puech, Seen & Begue, 2009).

Small-area Remote Sensing of GDEs

Small-area mapping of GDEs and other types of wetlands have proven somewhat more difficult using remote sensing and GIS techniques. This is largely because the spatial resolution of most space-borne sensors is too coarse to identify small land cover features such as GDEs. Additionally, canopies often times mask the presence of small spring-fed GDEs. Powell, Pflugmacher, Kirschbaum, Kim, and Cohen (2007) presented an analysis of different sensors that have moderate spatial resolution. They concluded that although Landsat TM/ETM+ are successful sensors, offering a large archive of

temporally continuous data, there are other sensors, such as SPOT, IRS, CBERS, ASTER, and ALI, that have similar capabilities. This study does not look at high resolution sensors, thus limiting its relevance to small-area GDE mapping.

Thermal Infrared Remote Sensing Techniques

The most promising approach for the remote sensing of GDEs uses the Thermal infrared (TIR) band to identify areas with high levels of evapotranspiration and/or saturation (Allen, Robison, Garcia, Kjaersgaard, & Kramber, 2008; Kustas, Anderson, Mecikalski, & Hain, 2009; Southworth, 2004) . Southworth (2004) used Landsat TM band 6 to classify succession stages of forest growth. It was found that despite compromised spatial resolution, TIR's sensitivity to variation in evapotranspiration rates made it a more accurate classifier than many individual spectral bands that had 16 times greater spatial resolution. This finding is very encouraging, but still relies on data that lack sufficient spatial resolution to be sensitive to many small GDEs.

Allen et al. (2008) showed that the sensitivity of the TIR band and the normalized difference vegetation index (NDVI) were correlated. Because NDVI is derived using the near infrared (NIR) and red bands with the Landsat TM sensor, it inherits the 30 m spatial resolution. Through the relation of the TIR and NDVI, Allen et al. (2008) increased the 120m spatial resolution of the TIR band to 30 m. Providing that the assumption that the TIR value is correlated with the NDVI value is true, this allows for the identification of smaller GDEs. This paper shows the most promise of the applicability of remote sensing techniques for identifying GDEs with the current sensors available for use. Unfortunately, this correlation is most safely assumed for cultivated agricultural areas,

thus limiting its applicability to this study.

Each of these studies has progressed the understanding of how to use remote sensing techniques to monitor wetlands. Because all these studies are interested in monitoring the present state of the system, they do not solve many of the difficulties of identifying historical ciénegas. This difficulty will need to be circumvented using alternative techniques.

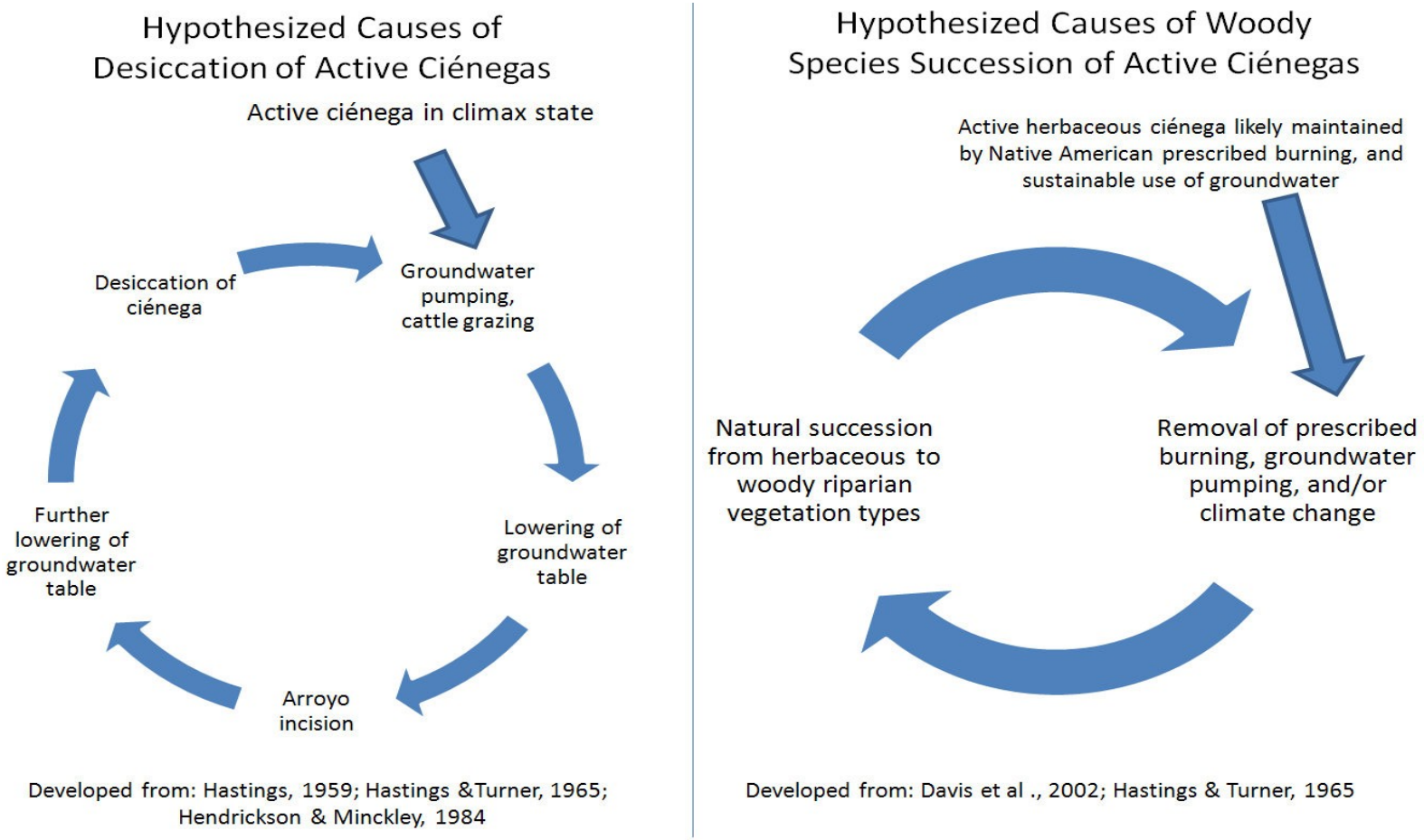

Figure 7: Depiction of the cycle of desiccation of active ciénegas. The separation of ciénega desiccation, from woody species succession illustrates that the influencing variables of these two patterns of change are likely different.

METHODOLOGY

This study consists of four components, using a combination of different techniques. The general flow of the methodology can be followed in Figure*s* 8, 9, and 10. The first component is referred to as the point location inventory (Figure 8). It involves integrating several different historical analysis techniques to create a more complete inventory of historical ciénega locations. These techniques include the review of historical maps, pioneers' and explorers' journals, published literature, and USGS topographic maps. The second component is referred to as the ciénega areal extent inventory (Figure 9). This component involves the use of aerial imagery interpretation to delineate the areal extent of documented inactive and active ciénegas. Because the activity status and land cover succession paths of ciénegas are divergent, each ciénega is classified by status (active or inactive) and by land cover type succession path (herbaceous, agriculture, woody riparian). This creates homogeneous historical ciénega segments that serve as representative areas of interest for the third component. The third component is referred to as the best predictor variable determination component (Figure 10). It involves the computation of the zonal mean, median, and variety (variety is the count of unique values within each polygon) using Landsat TM-derived datasets, along with elevation and various elevation derivatives. These statistics are analyzed using data mining techniques to find possible predictor attributes of various succession paths. Attributes that exhibit distinctly different values among the various succession paths of ciénegas may provide insight into possible influencing variables for ciénega desiccation

and subsequent vegetation succession. The two best predictor variables are used in a classification tree model to identify possible undocumented active ciénegas. The last component is referred to as the monitoring recent trends of change component (Figure 10). By analyzing patterns of change of the best predictor variables, any emerging patterns across the various ciénega succession paths become evident. These predictor variables are then compared against precipitation data for the study region, indicating whether precipitation can explain the variation in the trends of change.

Creation of the Point Location Inventory

The goal of the point location inventory is to create a more complete inventory of the locations of historical ciénegas than provided in Hendrickson and Minckley (1984). A historical analysis method is used because the majority of these ciénegas are presently extinct. This component involves three different techniques in compiling the locations of documented historical ciénegas:

1. Review of published literature that specifically mentions the location and/or extent of historical ciénegas (Davis et al., 2002; Hastings, 1959; and Hendrickson & Minckley, 1984).
2. Review of historical maps at the Arizona Historical Society, and the University of Arizona's Special Collections in Tucson, AZ, for the word ciénega (also spelled cienaga and cienagua). Because the scale of the maps is often small, the exact location is first approximated using landmarks such as cities, borders, rivers, and other features delineated on the map that are also present within the GIS. Next, the location is more specifically identified by finding the location that is along a

flood plain. When the same ciénega is mentioned in different maps, the presence of a ciénega, as well as the identified location, is reinforced.

3. A thorough review for locations with the word ciénega, and/or an area indicated as being a marsh is performed using 1:60000 USGS topographic maps (Figure 11).

Dale Turner of The Nature Conservancy in Tucson, AZ is compiling an inventory of ciénega locations. He queried geographic names databases in the US and Mexico for the word "ciénega." These databases include hydrological datasets, such as the National Hydrological dataset's streams, springs, and flowlines database, the USGS topographic map word database, as well as the Mexican equivalents. The result is a complete inventory of every instance of the word ciénega within the digitized records in both the US and Mexico. This inventory was provided for possible inclusion with this inventory, but is largely excluded because of the vastly different methods used to compile the inventory. The apparent errors of commission were quite high using database querying techniques, while the more hands-on approach used for this study likely results in errors of omission. It was decided that the best use of this valuable dataset would be for a method of visual validation for coincident locations of ciénegas.

Creation of the Ciénega Areal Extent Inventory

The techniques employed for the ciénega areal extent inventory are very different from those originally proposed. The preliminary research evaluated several approaches to the identification and measurement of ciénegas' historical extent. These approaches used Landsat Thematic Mapper (TM) imagery and derived vegetation indices.

Traditional supervised classification and unsupervised classification was performed using the known ciénegas' extents as training data. Also, an object-oriented approach to delineate ciénegas as objects within the landscape was evaluated using Visual Learning Systems, Inc.'s *Feature Analyst*. All of these methods proved very accurate for identifying vegetated active wetlands, cultivated fields, and riparian corridors. This is expected due to the lack of photosynthetic vegetation cover in the surrounding uplands during the time of image acquisition. All classification methods have two common limitations. First, they cannot identify inactive, sparsely vegetated ciénegas. Second, they cannot consistently differentiate between active ciénegas and woody riparian areas. These limitations are due to the diverging succession paths of desiccated ciénegas. The hierarchy of all succession paths of historical ciénegas is shown in Figure 12. Areas that had once been dominated by herbaceous ciénega vegetation desiccated over 100 years prior subsequently following one of three primary succession paths:

1. The area is still dominated by herbaceous vegetation that is tolerant of unsaturated soils such as giant sacaton (S*porobolus wrightii*);
2. The area became dominated by woody riparian vegetation such as mesquite (P*rosopis glandulosa*) or cottonwood (P*opulus deltoides*);
3. The area is actively farmed.

All areas in these categories are more likely to not have been a historical ciénega. This is because the succession paths of many areas that were historically unsaturated also experienced an encroachment of woody vegetation, as well as agriculture (Hastings & Turner, 1965). Additionally, many areas that once were maintained as grasslands,

possibly through prescribed burning by Native Americans, were not historically saturated. Thus, classifying areas based strictly on their spectral signature yields errors of commission. The spectral signature of these succession paths simply are too similar with that of areas that are riparian or upland herbaceous in nature. This similarity among spectral signatures can be seen in Figure 13. The similarity between woody riparian vegetation and active ciénegas, and inactive herbaceous and upland herbaceous, is evident. An accuracy assessment was not performed on the preliminary analyses that led to this conclusion due to a lacking of ground-truth points. A qualitative assessment of known active and inactive areas led to this conclusion.

To circumvent the difficulties heterogeneous succession paths with similar spectral signatures pose for automated classification techniques, high resolution aerial imagery interpretation is employed. Baker et al. (2006) mentions that aerial image interpretation of wetlands is both labor intensive, and difficult to reproduce. Despite these apparent drawbacks, aerial image interpretation is the most practical, effective technique available.

Image interpretation involves the ciénega point inventory, 1 meter resolution imagery from the 2006 National Agricultural Imagery Program (NAIP), NHD flowlines, and a slope dataset. The following are the steps taken in ciénega areal extent delineation:

1. Locate point of documented ciénega location in the ciénega point inventory. Because these locations are a point location, the extent is larger.
2. Identify areas with a slope of <4 degrees, within an national hydrography dataset (NHD) flowline floodplain. A threshold of 4 degrees was determined based on

field observations. Areas that were observed as being historical wetlands all had a slope of <4 degrees. The extent of ciénegas is limited by surface slope, and subsurface hydrology. Areas with a shallow slope allow for sheet flooding, while reducing the likelihood of arroyo incision. The threshold of four degrees allows for the inclusion of areas where springs and seeps are likely to occur on the margins of floodplains. The NHD flowline dataset identifies areas that are prone to have a water table that intersects the surface.

3. If the area is "near" a documented ciénega location, has a slope of <4 degrees, and is within a floodplain, it may be an inactive or active ciénega.
    i. If the area appears to be a fallow open area dominated by herbaceous vegetation, but lacks row patterns, outline the area, and label status as "inactive." Label the vegetation type of these areas as "herbaceous." Open herbaceous areas within a floodplain that do not exhibit row patterns are likely not agricultural areas. These areas have experienced a simple succession from a saturated, active ciénega dominated by herbaceous vegetation, to an unsaturated, inactive ciénega, dominated by herbaceous vegetation that does not depend on hydrosoils.
    ii. If the area appears to have row patterns, or a circular shape, outline the area, and label status as "inactive." Label vegetation type as "agriculture." Areas that exhibit row patterns, or circular shapes are most likely agricultural areas. Because of the fertile soil found in historical ciénegas, many of these areas are actively farmed. There is evidence that agriculture was also practiced in

ciénegas by Native Americans (Davis et al., 2002).

iii. If the area is covered by woody riparian vegetation, but still meets the criteria above, outline area, and label status as "inactive." Label vegetation type of this area as "woody_riparian." These areas were succeeded by woody riparian vegetation after desiccation. Because these areas fall within a floodplain, and are near an area that was documented as a historically active ciénega, it is likely that they were part of the historically active ciénega.

iv. If the area appears green, with herbaceous vegetation that has not undergone senescence, possibly with small areas of open water, label area as "active." Label vegetation type of this area as "herbaceous." Active ciénegas have a much longer photosynthetic period than unsaturated herbaceous vegetation. Although herbaceous vegetation dominates much of the uplands, active ciénegas are photosynthetic during the spring months. This difference, along with their location within a floodplain, allows for the easy delineation of active ciénegas.

4. For each polygon delineated, a level of confidence of the perimeter outline and status is noted. The scale is a qualitative "high," "medium," and "low."

   i. The confidence of the perimeter outline is based on the source of the point within the ciénega inventory, the homogeneity and vegetation type of the polygon (areas that have homogeneous, herbaceous vegetation cover are more likely to be extinct ciénegas than areas with shrub/woody vegetation).

   ii. The confidence of the status of the ciénega is based on the source of the status

(if one is provided), and the appearance within the imagery.

Most resulting ciénega outlines have several separate polygons in order to identify representative succession paths. Inactive and active areas of a ciénega are always within separate polygons (Figure 14). Ciénegas with heterogeneous vegetation cover were divided among areas of homogeneous vegetation cover type.

The same techniques are applied for areas where NAIP imagery is not available. Google Earth, with its streaming high resolution aerial/satellite imagery, serves as a practical, cost-effective analysis tool for the delineation of these ciénegas. The same methodologies are used within the Google Earth environment, and then combined with the ciénega outlines created within ArcMap. The imagery streamed from Google Earth for the ciénegas delineated is GeoEye-1 2010 imagery. The spatial resolution is pan-sharpened 0.41 m. Despite the resolution differences between GeoEye-1 and NAIP, the scale (~1:10,000) at which ciénega extent delineation is performed made this difference largely negligible.

Best Predictor Variable Determination

The ciénega areal extent inventory resulted in 211 separate polygons of numerous different ciénegas. Each of the steps outlined above is necessary for the third component of the study: calculating zonal statistics of each polygon using a suite of geospatial datasets. Proposed statistics included distance of ciénegas from springs, wells, NHD flowlines, roads, cities, and various other features. Because these data are given with varying degrees of detail, as well as different naming conventions in Mexico, there was an apparent information gap for many of the ciénegas located in Mexico. The initial

calculations using the US data showed no significant trends in the location of ciénegas from any of the features mentioned above, and its status and/or land cover type succession path. This resulted in the decision that using continuous data that are available across international boundaries serves this study better.

Zonal statistics are a technique for identifying representative statistics for an areal extent. In this case, the zonal statistics are calculated for each polygon within the ciénega areal extent inventory. The calculation of zonal statistics has two separate objectives. The first is to see if there is a dependence of the ciénega's succession path on any of the Landsat TM- derived vegetation indices, thermal infrared band (TIR), or digital elevation model (DEM) derivatives. The second is to monitor the patterns of change of the ciénegas over the last 25 years: 1984 to 2009. This time period was chosen for three primary reasons. First, it is the largest time frame available for the Landsat 5 TM sensor. This sensor began operation in 1984, offering the only dataset of its quality for that time period. Second, this time frame captures change since the last in-depth inventory of ciénegas across southeastern Arizona (Hendrickson & Minckley, 1984), to provide insight into the recent changes. Third, the precipitation/temperature regime after 1984 has been cited as being significantly different from before this time period. Many scientists use 1984 as the cutoff point for before and after global climate change began (Barnett & Pierce 2009). Although somewhat arbitrary, this break is evident in both the precipitation data, as well as the temperature data over this relatively short time frame.

The date of image acquisition coincides with the spring dry season of the study region. The spring dry season is the only time that all regional grasslands are not

photosynthetic, while ciénegas are (Figure 15; Figure 16). Unfortunately, during this period, woody riparian vegetation is also photosynthetic, limiting the ability to differentiate between active ciénegas and woody riparian vegetation (Figure 16). Nevertheless, May and June are the best months for image acquisition due to the relative high contrast between ciénegas and surrounding vegetation.

The study region encompasses a total of nine Landsat path/rows. Each path row is about 185 km x 185 km. Due to the size of the study area, the number of time frames within the 25-year total time window is limited to three. This involves a total of four image sets. The images are chosen based on their vacancy of clouds, as well as their proximity in time to the desired date of June 21. With the summer monsoon beginning shortly after this date, but the photosynthetic activity of ciénegas being very high, this date was determined to be the best date. If cloud-free imagery is not available for this date, imagery from before is chosen. The resulting image sets do differ in dates of acquisition, thus introducing some inherent differences in the reflectance of vegetation. The normalized difference vegetation index (NDVI) values in Figure 15 indicate that the variation between late May and early June is minimal, thus ensuring minimal offset between images.

The years of the image sets are chosen to capture the decadal fluctuations in precipitation that are evident throughout the area. With an initial image set in 1984, subsequent years are 1990, 2000, and 2009. All of these image sets are reflectance corrected, and orthorectified. Cloud masking is not necessary, since all ciénega outlines were assigned to images that do not have clouds in the area. This is possible due to the

aridity of the region during the spring dry season.

The following vegetation indices with their respective algorithms are used from the Landsat imagery:

1. Normalized difference vegetation index (NDVI):

((NIR-red)/(NIR+red))

2. Normalized burn ratio (NBR):

((NIR-SWIR)/(NIR+SWIR))

3. Thermal index (TI):

(NIR-TIR)

4. Normalized thermal index (NTI):

((NIR-TIR)/(NIR+TIR))

5. Tasseled cap- brightness, greenness, and wetness transformations:

6. First principal component (All bands were included except for the TIR band)

7. Band 6- thermal infrared

Thermal index (TI) simply uses the absolute difference between the values of the NIR band 4 and the TIR band 6, while the NTI normalizes this value by the sum of the two bands. Most vegetated areas experience a negative correlation with NIR and TIR values. It was noticed in the preliminary analysis that many active ciénegas' spectral signatures were outliers in this relationship. Active ciénegas, as well as irrigated agricultural areas, had relatively low TIR values for their given NIR value. Therefore, the difference was able to distinguish such areas, masking out the vast majority of vegetated areas as having a relatively small difference between NIR and TIR.

All imagery derivatives are calculated for the 1984 imagery. Additionally, once the best two predictor variables are determined, all four image years are included for both of these variables. Additional datasets are derived from a DEM from the National Elevation dataset (NED). These include:

1. Elevation
2. Slope
3. Aspect
4. Heatload (McCune & Keon, 2002)
5. Topographic roughness index (Stambaugh & Guyette, 2008)

All datasets listed above are used to calculate the zonal statistics for each polygon. Since each polygon involves delineating homogeneous areas, it is assumed that each is representative of its status and land cover type. The status confidence level is used in the evaluation process in order to filter out any possible errors of commission in the zonal statistics calculations. Initial evaluation of the polygons over the Landsat-derived datasets exhibited large amounts of pixel mixing at the edges of the polygons. This was because the polygons are delineated on 1 m resolution imagery, while Landsat imagery is primarily 30 m spatial resolution, with the thermal infrared band having a 120 m spatial resolution. Because the objective of this component is to calculate representative zonal statistics, a negative buffer is used on all polygons, to avoid the heterogeneity introduced by the pixel mixing at the edges (Figure 17).

The resulting zonal statistics are the mean, median, and variety. Mean and median are included because they represent the best approximation of the representative value of

each polygon. Median needs to be included in addition to the mean because some polygons have a small number of pixels to sample from, and therefore do not have a normal distribution needed for the mean to be a representative value. Variety is predicted to be the best measure of variability to pick up on the heterogeneity found in rough, woody riparian areas. Standard deviation is not included for many of the same reasons that the mean is often times not the best measure of a representative value. Data that are floating point cannot have the variety or median computed because there are an infinite number of possible values. When possible, the data are converted to integer type by multiplying the value by 1000. The only data that cannot be converted to integers are the elevation data, along with the various elevation derivatives.

The resulting table of data is analyzed using the open source data mining software *Orange*. This software package offers numerous visualization tools, as well as many classification methods for analyzing the resulting zonal statistics. It was determined that the best approach with this software is to first identify the best predictor variable for three levels of succession paths that are given to the ciénegas. The variables that prove to consistently limit the variability in the data among the various succession paths are determined to be the best predictor variables (BPV). This is determined using the "VizRank" tool within the "Scatter Plot" tool. This tool compares each variable to every other variable iteratively, giving each comparison a score of how well it is able to limit the variability in the data with respect to a given succession path (Leban, Zupan, Vidmar, & Bratko, 2006).

The total number of times each variable appears in the top projections within

"VizRank" is assessed. Because the BPVs are best able to separate the data based on different levels of succession (activity level, and land cover type), it is assumed that they are best able to monitor the underlying variables that impact the status and/or land cover type succession of the ciénega. The best predictor variables' sensitivity to ciénegas' status was used to create a classification tree model to identify possible active ciénegas. The model uses the top BPVs from VizRank across the status succession path. Because the change detection component of the study is interested in assessing the ways in which ciénegas have changed over the past 25 years, the best predictor variables are also assumed to be the best variables at monitoring the underlying influencing variables of change.

Monitoring Recent Trends in Change

The change detection component of the analysis involves the use of the top two best predictor variables to monitor recent trends in change. Zonal mean values of NBR and TIR for 1984, 1990, 2000, and 2009 are calculated. Each of these years accounts for different changes in the regional precipitation patterns. Preliminary studies indicated that NBR is more sensitive to the changes in vegetation cover of ciénegas due to its sensitivity to vegetation and bare soil, while NDVI is not as sensitive to bare soil. The NBR is more sensitive to inactive ciénegas that are dominated by senesced herbaceous cover. This often occurs in inactive ciénegas during dry years. The NBR's proficiency is a result of using both the near-infrared (NIR) as well as the shortwave infrared (SWIR) bands, while NDVI uses the NIR and red bands. This finding is inconsistent with some of the literature on remote sensing of wetlands (Allen et al., 2008), so the 1984 NDVI is

included in the zonal statistical analysis section. Additionally, thermal infrared (TIR) imagery is used to monitor change. Landsat TM TIR band 6 has proven proficient at identifying wetlands in various studies (Allen et al., 2008; Kustas et al., 2009; Southworth, 2004).

The mean values with respect to time across different succession paths are compared to evaluate whether there is a dependence on the pattern of change over time on the status, or land cover succession type. Additionally, the correlation of these mean values with annual precipitation is evaluated using linear regression. All of these individual analyses allow for an increased understanding of how ciénegas are reacting to recent trends in climate change.

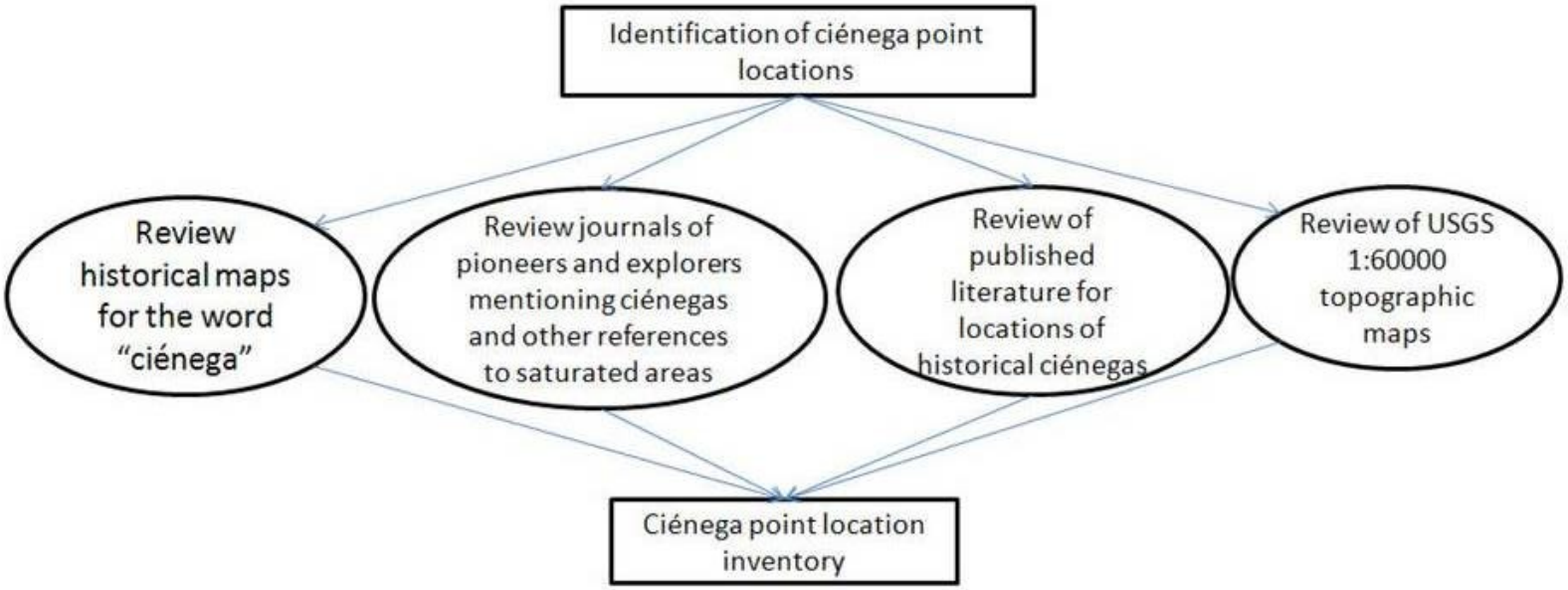

Figure 8: Flowchart of Ciénega Point Inventory method

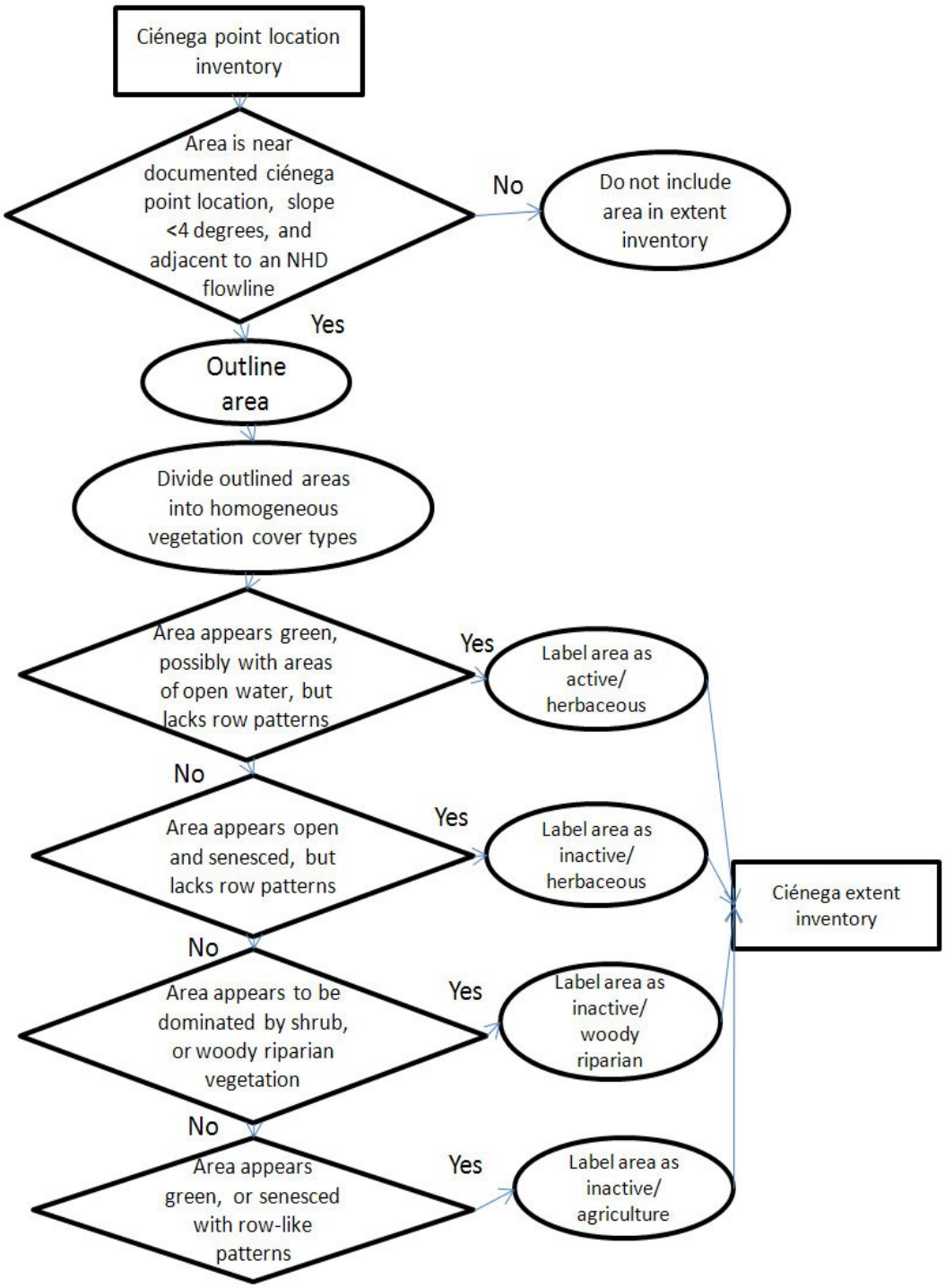

Figure 9: Flowchart of Ciénega Areal Extent Inventory method

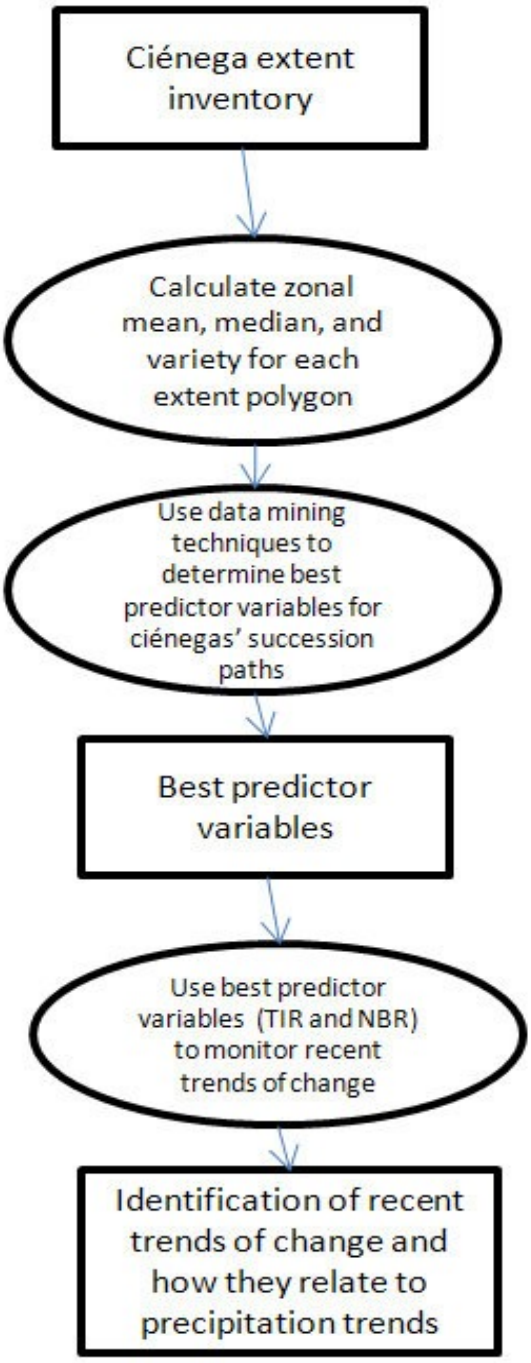

Figure 10: Flowchart of Best Predictor Variable Determination component, followed by the Recent Trends of Change component methods

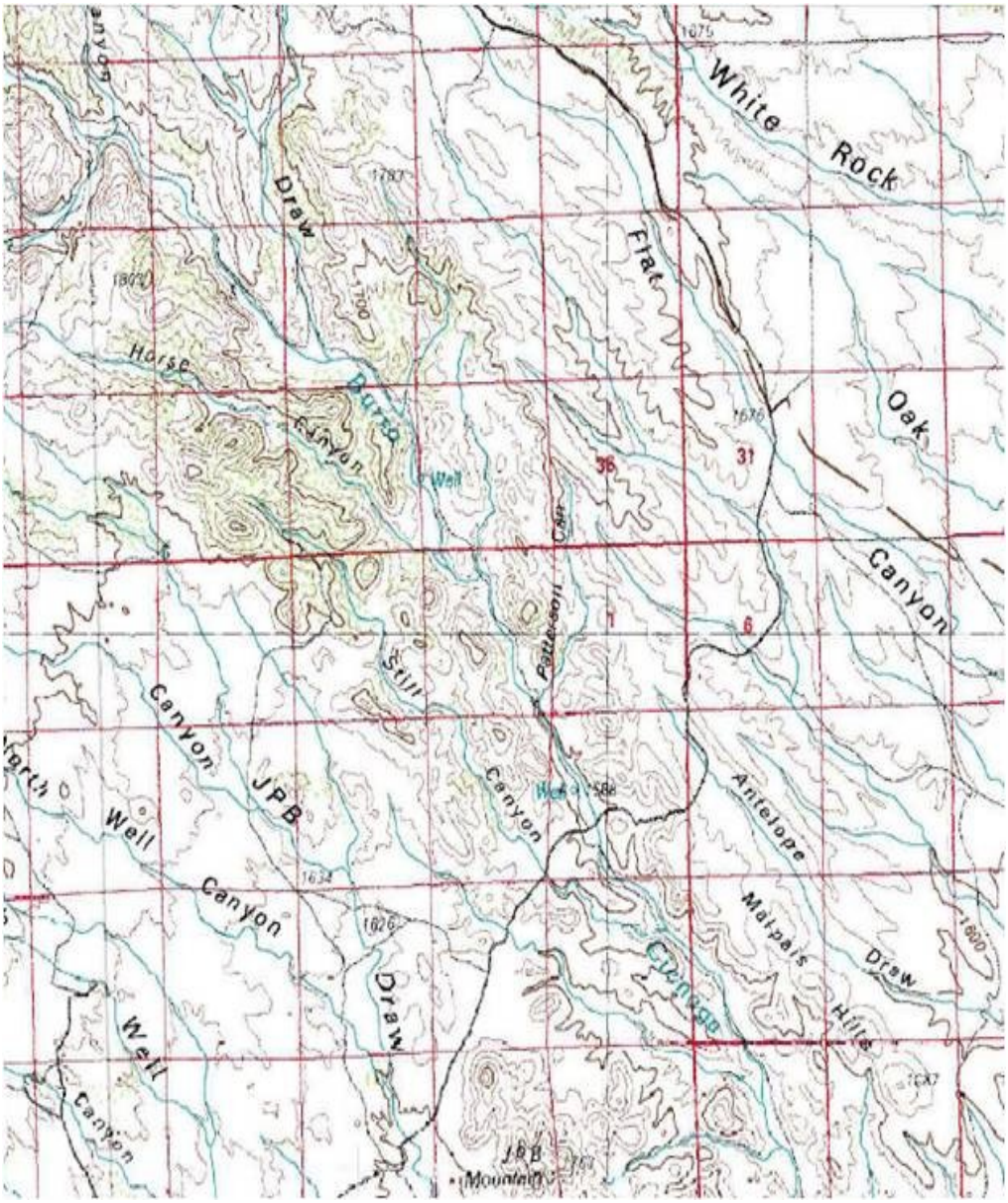

Figure 11: Examples of a topographic map with the word ciénega in it (Source: U.S. Geological Survey).

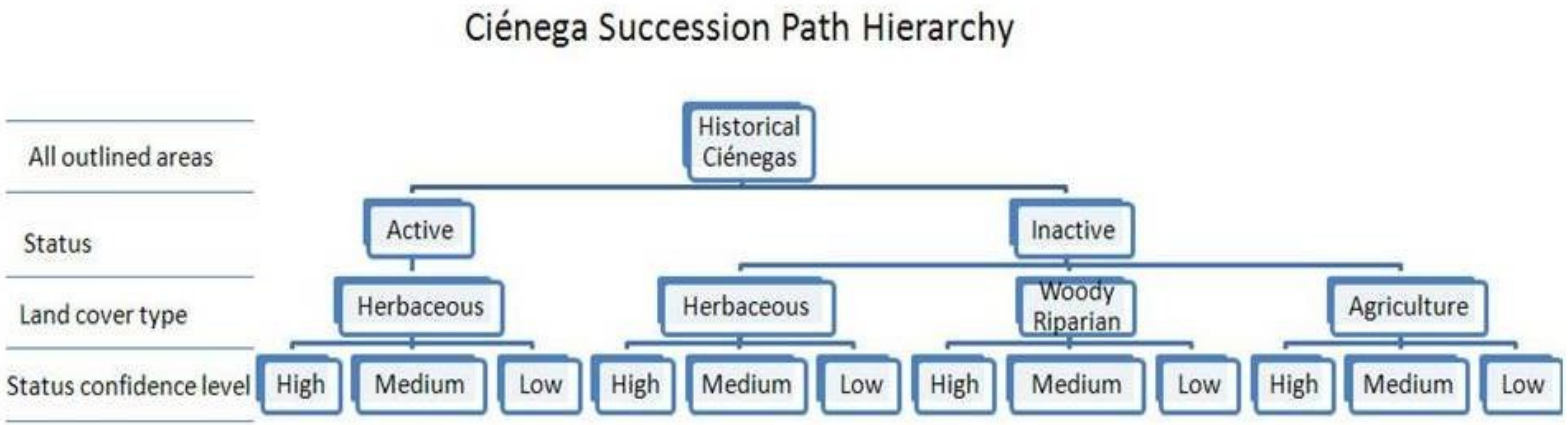

Figure 12: Hierarchy of succession paths of historical ciénegas. The status confidence level was included in order to identify anomalies in the zonal statistics.

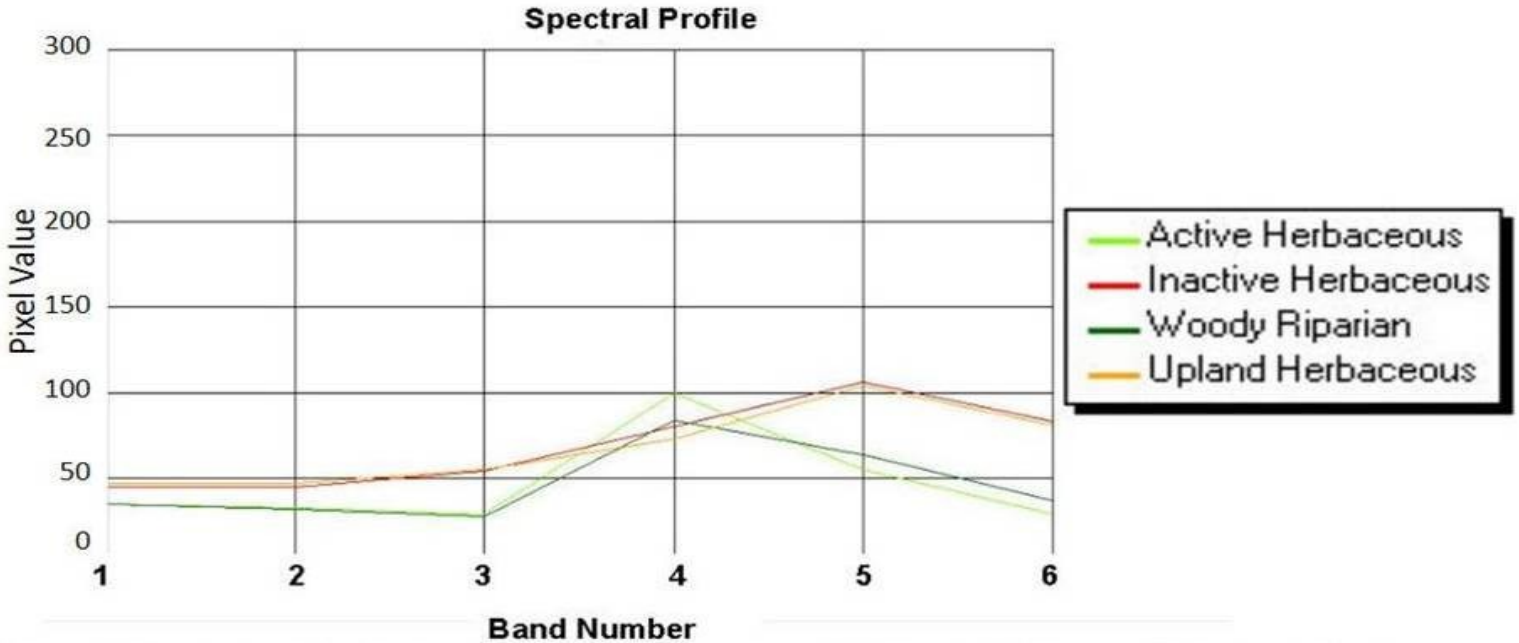

Figure 13: Spectral profile of various succession classes using a 1984 Landsat TM image. Notice the similarities among the active/herbaceous and woody riparian profiles, and the inactive/herbaceous and upland herbaceous profiles. This similarity made automated classification methods inadequate for this study.

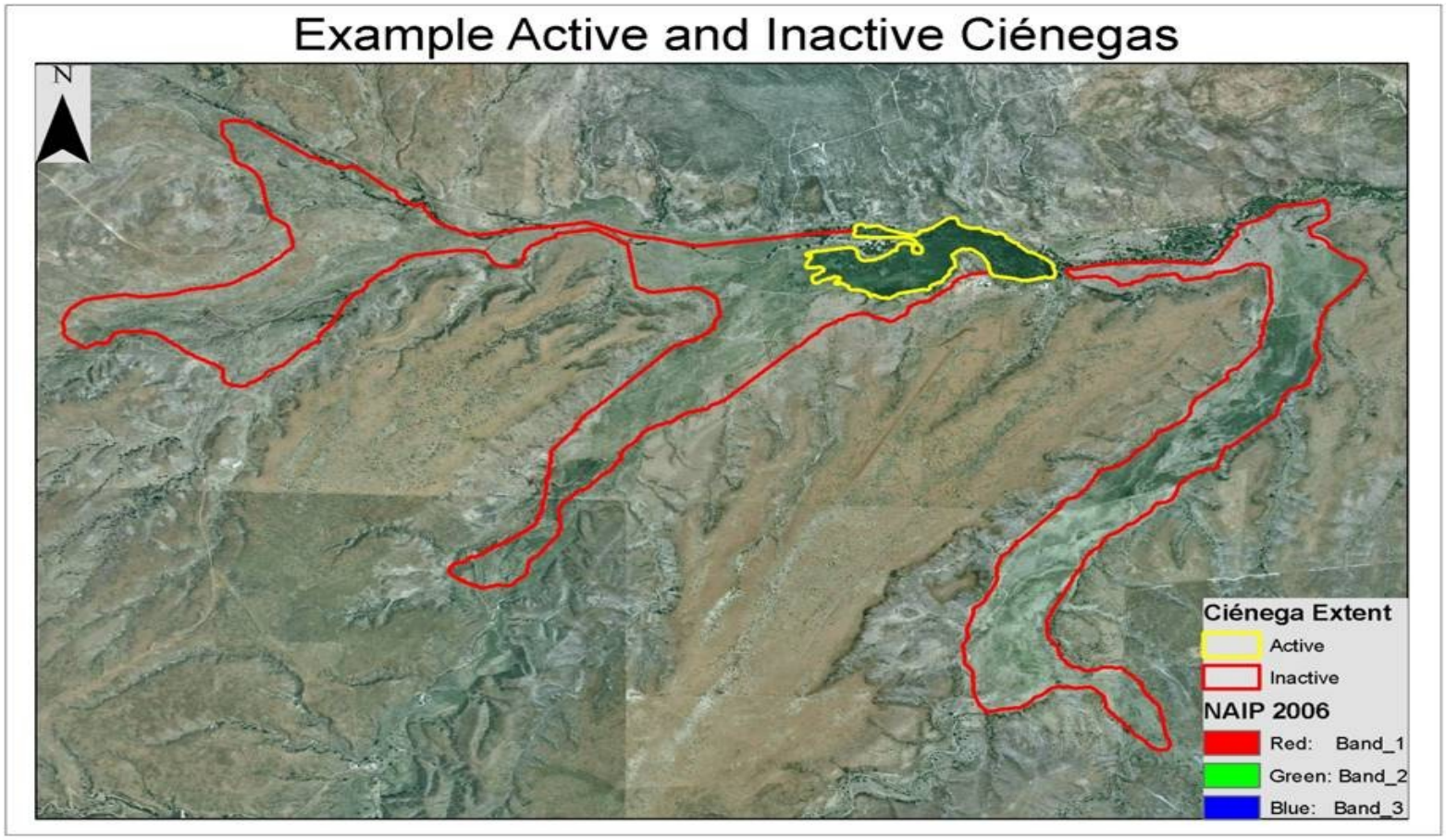

Figure 14: Example of ciénega with a remaining active area, along with inactive areas. Intra-ciénega divergent succession paths are captured by outlining individual areas of each succession path type.

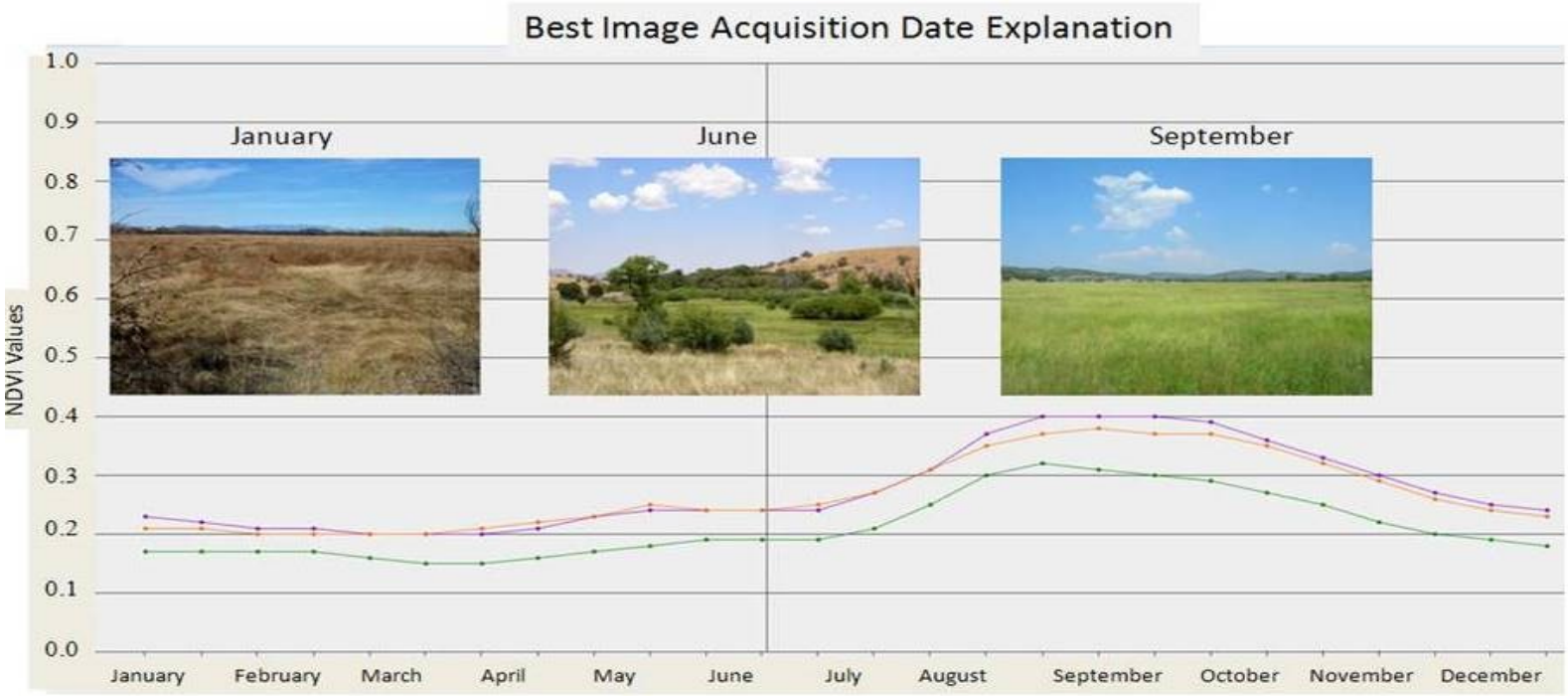

Figure 15: A graph of NDVI over the course of the year 2000, across different vegetation cover types (glovis.usgs.gov). Pictures are taken from various ciénegas in the study region, representing the photosynthetic state of vegetation at that time of the phenological cycle. Notice how the vegetation of the ciénega is green in June, while the surrounding upland areas are still in senescence.

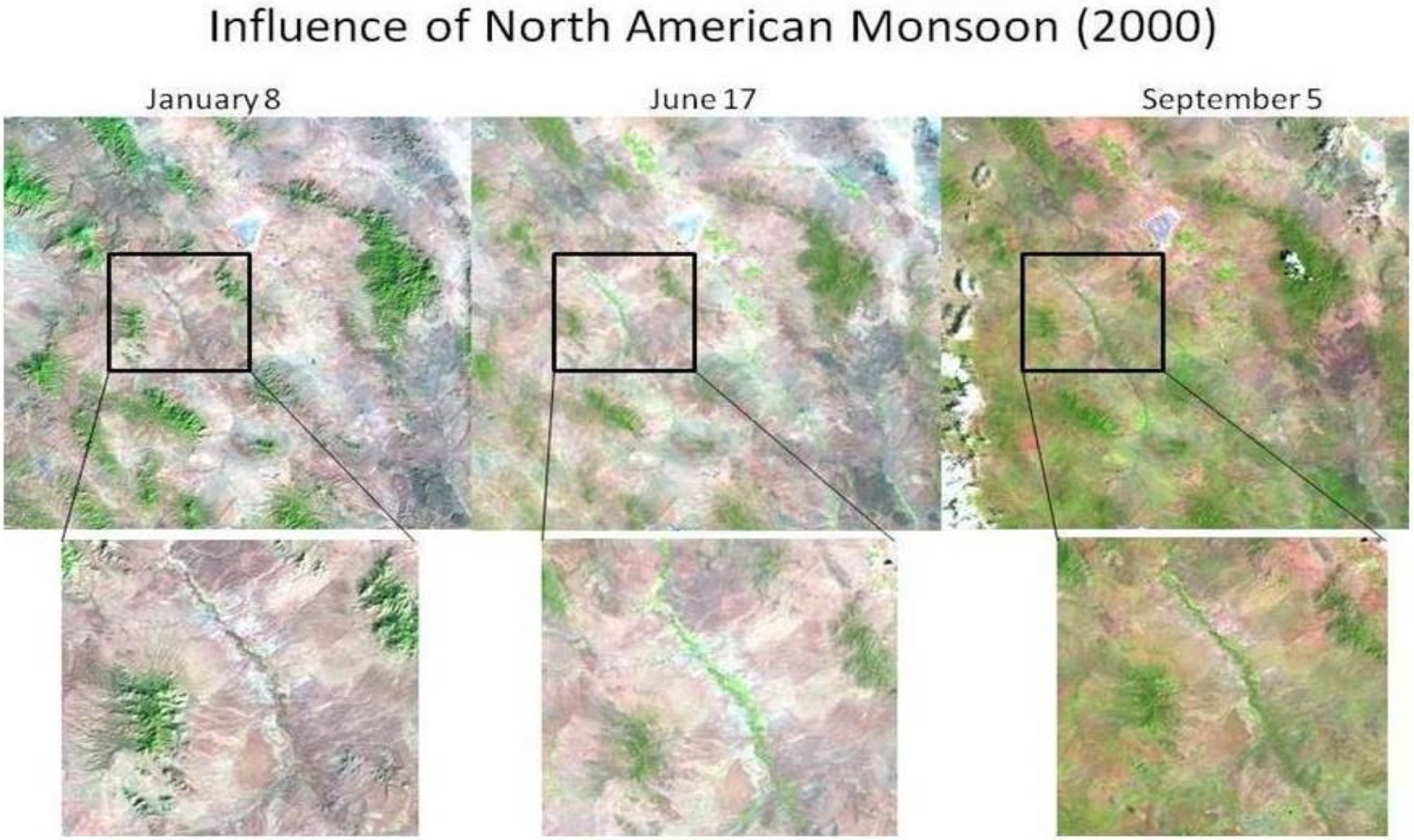

Figure 16: Landsat TM imagery for central portion of the study area, illustrating the spatial distribution of photosynthetic vegetation at three different times of year. Notice that June is the only image time when riparian/wetland corridors are photosynthetic, while upland herbaceous areas are not.

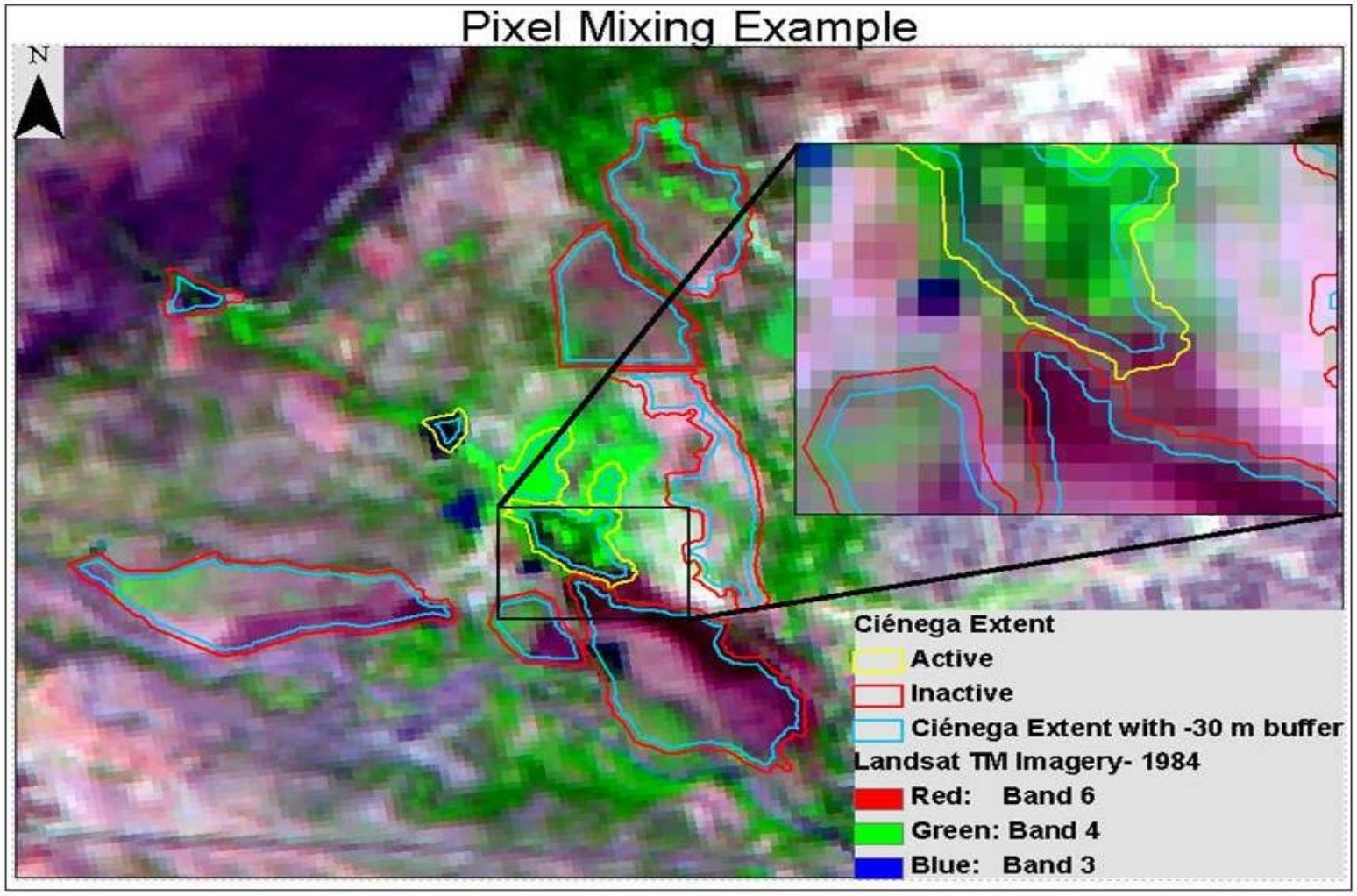

Figure 17: Example of pixel mixing at the active/inactive ciénega interface. A -30 m buffer depicted by the blue line demonstrates the avoidance of the inclusion of such pixels.

ANALYSIS AND RESULTS

Ciénega Point Inventory

Ciénega Point Inventory Analysis

The ciénega point inventory component of this study results in a more complete inventory of historical locations of ciénegas. This inventory serves as a vast improvement over the past inventory. Due to the impracticalities of reviewing every historical document within the time frame of this study, the errors of omission are likely high. Additionally, errors of commission may be higher than expected. By including areas that indicated the presence of a ciénega by labeling the area with the word "ciénega," inclusion of an area that is more loosely defining a moist area is possible. Additionally, this inventory follows the Hendrickson and Minckley (1984) definition of a ciénega, with most of the ciénegas being found between 1000 and 2000 m in elevation. This limits the inclusion of all areas historically known as ciénegas.

Ciénega Point Inventory Results

A total of 63 ciénegas are identified throughout the study area. The locations of the ciénega point locations are presented in Figure 18 as a map and Table 1 as a table with the ciénega's name, source, longitude, latitude, and elevation.

Ciénega Areal Extent Inventory

Ciénega Areal Extent Inventory Analysis

The goal of the ciénega areal extent portion of the inventory process is to delineate representative, homogeneous ciénegas across status and land cover type succession paths. Therefore, all ciénegas are divided into homogeneous segments.

The extents of historical ciénegas are undoubtedly greater. The image interpretation techniques used were prone to errors of omission. This was chosen over the possibility of including more areas as historical ciénegas, resulting in large errors of commission. Such a bias is necessary in order to create a dataset that is representative of the various succession paths. With this in mind, the resulting inventory extents should be evaluated with their primary purpose in mind- identifying the best predictor variables of various succession paths, and representing recent trends of change across different succession paths. An additional reason for avoiding errors of commission is the lack of a field accuracy assessment. An accuracy assessment involves coring extinct ciénegas, thus proving impractical for the scope of this study. This prevents the accuracy of the ciénegas' extents from being evaluated quantitatively. The confidence level is merely indicative of the ciénega's location source, and appearance within the imagery, thus lacking a true validation.

Ciénega Areal Extent Inventory Results

This inventory results in a total of 211 different polygons. Figure 19 shows the extents of the documented ciénegas, while Figure 20 shows the count statistics of various succession path categories of the ciénegas. These count statistics do not account for

differences in area among different polygons. Each polygon is treated as a single sample regardless of its area. These statistics show that 82.5% of ciénegas within the areal extent inventory are inactive. The majority (59.7%) of historical ciénegas presently have herbaceous land cover. When the status confidence level is included (not displayed on map), it becomes evident that ciénegas that are inactive are identified as such with greater confidence. Areas that are not documented as being active, but appear active in the NAIP imagery, account for 67.5% of the active ciénegas. Only 24.32% of the active ciénegas are given a high level of status confidence.

Best Predictor Variable Determination

Introduction to the Analysis

The first step taken within *Orange* is to analyze which attribute was able to explain the variability of the data most proficiently. The zonal statistics chosen are mean, median, and variety. These statistics show the most true sensitivity to the various succession paths, while other attributes are often times sensitive due to chance. These variables are compared to every other variable iteratively to find relationships among the different variables to the discrete classes. The "VizRank" tool as described in Leban et al. (2006) compares each variable, and finds the optimal variables for splitting the data with a given discrete class. This is performed using the k-Nearest Neighbor method, where variables that minimize the distance between the closest 10 values receive a higher score. One hundred percent of the data is used, with a 10-fold cross validation testing method. The succession paths that are used are status, land cover type, and the combination of status, land cover type, and the confidence level of the status.

Best Predictor Variable of Status Succession Path Analysis

The top 10 attributes displayed in Figure 21 exhibit the best ability to separate the data based on the chosen succession path. In this case, each attribute listed is best at identifying the status succession path indicated by the color of the bar. This yields a relationship between inactive ciénegas, and the TIR band 6, while active ciénegas appear to be more dependent on elevation. All top 10 attributes yield a >80% proficiency at properly classifying the values, using a 10-fold cross validation. The dependence of TIR on inactive ciénegas is somewhat unexpected, because the TIR band has been used exclusively as a tool for identifying active wetlands in past studies (Allen et al., 2008; Kustas et al., 2009; Southworth, 2004). The dependence of active ciénegas on elevation is expected, but likely not due to a globally influencing variable in this case. Despite the small sample size in this category, areas higher in elevation do receive more precipitation, and generally are less impacted by human influence. Because the sample size for active ciénegas is small, this dependence could be an anomaly in the data. A larger sample group of active ciénegas simply does not currently exist, thus limiting the ability to test this relationship.

Because TIR and NBR are the best predictor variables for a ciénega's status succession path, the distribution of values of TIR and NBR are analyzed (Figure 22). The first row of graphs (A and B) shows the distribution of the mean value of TIR band 6 in 1984, while the second row (C and D) shows the distribution of the mean value of NBR in 1984. The probability of obtaining a given value at the 95th percentile confidence interval is shown in the dark black line. The outer lines are the 90th and 99th percentile

confidence intervals. The left-hand column (A and C) of distributions within Figure 22 shows the probability of identifying an active ciénega at a given TIR or NBR value, while the right-hand column (B and D) shows the probability of identifying an inactive ciénega at a given TIR or NBR value. The apparent differences in the probabilities for both variables is quite large. This indicates that using the TIR band 6 and NBR is possibly a good method for identifying inactive areas and active areas. Because this study was interested in identifying inactive ciénegas, and not all unsaturated areas, these graphs are somewhat misleading. While both TIR band 6 and NBR are proficient at separating active and inactive areas, most inactive areas are not historical ciénegas. This sensitivity of active wetlands to TIR (Figure 23) does concur with the present body of literature, that TIR is a very good tool for identifying saturated areas, and areas with high evapotranspiration rates (Allen et al., 2008; Kustas et al., 2009; Southworth, 2004). What this does not provide is a best predictor variable for separating the inactive ciénega succession path from all other unsaturated areas within a flood plain.

Best Predictor Variable of Land Cover Type Succession Path Analysis

The second succession path is land cover type. Because all active ciénegas are dominated by herbaceous vegetation cover, this made the land cover type a succession path among inactive ciénegas. This section can possibly identify common attributes for the three primary succession paths of inactive ciénegas. With this goal in mind, the status is included in the path name, yielding four separate paths: active/herbaceous, inactive/herbaceous, inactive/woody riparian, and inactive/agriculture.

Each of the succession paths is sensitive to a variety of different attributes. This is

evident with the numerous different paths represented within the top 10 attribute table in Figure 24. The most notable is the mean elevation, an experimental index named the thermal index (TI), and the NBR. Additionally, TIR band 6, the normalized thermal index (NTI), and tasseled cap brightness are also sensitive to various land cover types. Once again, the elevation dependency is likely due to the relative pristine nature of the small number of active, upper elevation ciénegas. The NBR values for both 1990 and 2000 prove to be useful for identifying active/herbaceous status/land cover types.

The TI (denoted "NTI diff" in graph) and NTI are an experimental index created for this study. The goal of NTI is to be able to identify areas of herbaceous land cover with high soil moisture content. Irrigated agricultural areas are easily masked out using land cover classifications such as the National Land Cover Dataset (NLCD). The fact that TI was a top 10 attribute in only identifying agricultural areas and not active herbaceous areas indicates that using the TIR band 6 is better for identifying active ciénegas than NTI or TI.

Best Predictor Variable Analysis

The final succession path incorporates the confidence level of the status of the ciénega with the status and land cover type. This results in a total of 12 paths, of which 11 have values. There are no inactive, woody riparian areas with low confidence of their status. This is because any area that is dominated by woody riparian vegetation cover is inherently inactive, resulting in a status confidence level of medium or high. If an active ciénega has woody riparian vegetation present, it would have a low density in canopy cover, thus being classified as an herbaceous land cover type.

Because of the increased number of different succession paths, the projection scores are lower, with the best projections having a score in the low 30s. This is expected, because it is unlikely that any one attribute is sensitive to the status, land cover type, and the confidence of the status. Most difficult to identify with any of the given attributes is the confidence of the status. Since this confidence is based on the source of the data, how it appears in the NAIP imagery, along with inputs from experts from around the study area, it is likely that any of the attributes calculated cannot be used for a proxy to such a qualitative process. Nevertheless, these results do shed some light on what variables the ciénegas, their respective succession paths, and the level of confidence of the ciénega's status are sensitive to (Figure 25*)*.

Once again, the elevation dependence of active ciénegas is displayed. Elevation is sensitive to the active ciénegas with a medium level of confidence of their status. Because there are only three ciénegas that fall into this category, it is likely that this relationship is due to very specific circumstances, rather than a more global phenomenon. If this relationship appeared across all three status confidence levels of active/herbaceous ciénegas, then this relationship may be more representative. Some possibly representative relationships are with the NBR values, as well as the tasseled cap wetness and greenness indices. The NBR's sensitivity to a ciénegas' status is the primary reason the index was chosen over NDVI as a best predictor variable. Additionally, this index demonstrates a sensitivity to inactive herbaceous cover. Tasseled cap greenness is sensitive to both inactive/agriculture/medium, and active/herbaceous/low succession paths. This can be expected because of its sensitivity to vegetation cover. Additionally,

during the land cover classification process, areas that appear as agricultural areas sometimes also share many characteristics with active ciénegas. Sometimes the characteristics are sufficiently similar that it necessitates the status to be given as active, with a low status confidence level. This is evident by the shared sensitivity among these two succession paths.

Best Predictor Variable Determination Results

Through comparing each attribute using the "VizRank" tool within *Orange,* it is apparent that TIR band 6, NBR, and elevation are the most consistently sensitive to the various succession paths of ciénegas. The most consistent relationships that are likely due to global driving forces, and not local impacts, are NBR and TIR band 6. Figure 26 depicts the distribution of elevation values across the status/land cover type/status confidence level succession paths. Notice the skewed distribution of the three "Active/Herbaceous/Medium" ciénegas. Because of this, elevation is not considered a good predictor variable. Because NBR and TIR band 6 appears in the top rankings across different succession paths, they are used in a study area-wide binary classification of possible active ciénega extents.

A classification tree model is developed using the results from VizRank. The goal of the classification is to locate possible ciénega extents throughout the study region for future studies. While most active ciénega locations within the United States are known, many locations with the Mexican portion of the study area remain local knowledge. The classification tree (Figure 27) limits the areas that are classified to having an elevation between 800- 2200 m, and a slope of less than 5 degrees. If the area meets these criteria,

then the best predictor variables are used to determine whether the area is likely an active ciénega. Through the results in VizRank, it is determined that areas with a TIR digital number (DN) value less than 190 are likely to be sufficiently saturated to be a ciénega. Also, an NBR index value greater than 400 is likely to be an active ciénega. This classification tree results in the inclusion of agricultural areas, woody riparian vegetation, and active ciénegas. The inclusion of woody riparian and agricultural areas is a result of the similar spectral signatures between the three different land cover types. An example of the Babocomari Ciénega is shown in Figure 28 demonstrating the difference in the perimeter resulting from the classification tree, and the areal extent inventory methods.

The purpose of this classification is to provide future studies a resource to identify other possible ciénegas. These locations will largely be identified visually from this classification. Masking of agricultural and woody riparian areas without field verification may result in masking out many adjacent saturated areas, thus decreasing the effectiveness of this classification.

Monitoring Recent Trends of Change

The zonal means from 1984, 1990, 2000, and 2009 datasets of TIR band 6 and NBR are used to assess the patterns of change of the ciénegas in the inventory over the past 25 years. Additionally, these statistics are compared to the precipitation trends of the study region using linear regression. Precipitation trends are able to explain most of the variation in the changes in the mean values of NBR and TIR.

Trends of Change of Status Succession Path Analysis

The first results demonstrate the dependence of the NBR index values and TIR band 6 on the status succession path (Figure 29). The trend for lower NBR values and higher TIR values for inactive ciénegas is upheld across all four time frames. The difference in values among different status succession paths across time is relatively uniform. This indicates that NBR and TIR sensitivity to the influencing variables is uniform across the status succession path. Uniformity among paths is upheld with the notable change in both the NBR index values and TIR in 2009. The change in 2009 is the only change of its kind within the study period. The decrease within the NBR index values are not as significant as the increase in TIR values. This increase of 9.68 in the active TIR mean, and 11.77 in the inactive TIR mean, is well outside the standard deviation of the mean values over time of 4.23. This elevated sensitivity to change with TIR is likely a result of the cumulative effect of a decade of below average groundwater recharge. The NBR shows greater variability over all time periods, suggesting a greater dependence on interannual precipitation variation.

Trends of Change of Land Cover Type Succession Path Analysis

The next graph analyzes the sensitivity of NBR and TIR to the land cover type succession path (Figure 30). Because all active ciénegas have an herbaceous land cover type, the status needs to be included. If active/herbaceous ciénegas are grouped with inactive/herbaceous ciénegas, heterogeneity is introduced into the herbaceous classification. These results indicate that there is a greater dependence of TIR radiance on whether the ciénega is active or inactive, rather than its land cover succession path.

This is evident in the close proximity of all inactive ciénegas, while active/herbaceous ciénegas exhibit a significantly lower value across all time intervals. By dividing the ciénegas by the land cover type succession path, it becomes evident that the sensitivity of the NBR is not simply between active and inactive ciénegas, but rather, active/herbaceous and inactive/herbaceous ciénegas. Both inactive/woody riparian and inactive/agriculture do not exhibit differing trends. This supports the preliminary studies that indicated NBR's sensitivity to photosynthetically active and inactive herbaceous vegetation makes it a valuable index for monitoring change in active and inactive/herbaceous ciénegas.

Trends of Change Analysis

The final succession path involves status, land cover type, and the status confidence level. By separating the data based on these criteria, any hidden trends in the dependencies of TIR and NBR are unveiled. The TIR graph (Figure 31) shows that both inactive/woody riparian/medium and active/herbaceous/medium are outliers from the overall trend. This is likely because the sample size of these paths is four and three, respectively. Because these two paths do not follow the global trend, it is likely that local influencing variables are responsible for these anomalous trends. All other trends appear to resemble the trends based on the ciénegas' status, thus indicating that TIR is highly dependent on the saturation of ciénegas. This agrees with the body of literature, but does not solve the problem for identifying the overwhelming majority of ciénegas that have desiccated, and apparently share similar TIR radiance values across different succession paths. It should be noted that all of these statistics do not account for the spatial variability that result due to a number of complex influencing variables. This variability

can be seen in Figure 31. The NBR results appear to have some of the same difficulties as the TIR results. Most notably is that of the inactive/agriculture/low category. This category is represented by only one ciénega, thus likely being due to local effects (Figure 32). All other trends appear to follow the trends found when ciénegas were separated by land cover type.

Recent Trends of Change Results

These results indicate a dependence of TIR radiance values on the level of saturation of a ciénega, while the NBR values indicate the relative health of vegetation.

Precipitation Correlation Analysis

Because saturation and vegetation health are dependent on precipitation, it was hypothesized that there would be a significant correlation between TIR radiance/ NBR index values, and precipitation. In order to evaluate whether there is a significant correlation between the precipitation of the study area, annual total precipitation data is compiled from Douglas, AZ, Sierra Vista, AZ, Tucson, AZ, Willcox, AZ, Nogales, AZ, Clifton, AZ, and Lordsburg, NM from 1980-2009 from the Western Regional Climate Center (wrcc.dri.edu). The mean for all data is calculated to represent a mean precipitation for the study area for each year. The precipitation trend from 1980-2009 can be viewed in Figure 33. The general downward trend in precipitation is evident in the trendline and its respective function.

The relationship between the mean total annual precipitation and TIR values is evaluated using linear regression (Figure 34). The lower *r*-squared value of active

ciénegas is expected since active ciénegas are dependent on groundwater, which is more closely related to the long-term precipitation patterns and hydraulic conductivity of the subsurface. In order to assess if a multiyear precipitation pattern is responsible for these trends, the mean annual precipitation from the 2 years prior, along with the year of image acquisition, is used.

The lower *r*-squared values of the multiyear precipitation mean demonstrates that the influencing variables for presently active ciénegas are somewhat more complex than inactive ciénegas. This indicates that understanding what makes a ciénega resilient to change requires more than precipitation data. Resilient ciénegas, such as the Rancho San Bernardino ciénega, result due to a relative lack of historical disturbance, along with proper underlying geology to ensure that far-reaching disturbances to the subsurface do not impact them.

Precipitation Correlation Results

The linear regression analysis (Figures 34 and 35) results in active ciénegas having *r*-squared values of 0.67 and 0.84 for TIR and NBR, respectively. Inactive ciénegas have *r*-squared values of 0.80 and 0.84 for TIR and NBR, respectively. The relatively similar *r*-squared values across TIR and NBR indicate that both are sensitive to the variability introduced by precipitation. The NBR *r*-squared values indicate that 84% of the variability can be explained by precipitation trends in the active ciénegas, and 72% can be explained in inactive ciénegas. The stronger relationship among active ciénegas is likely because active ciénegas are more homogeneous than the different succession paths of inactive ciénegas and therefore are more uniformly sensitive to precipitation. The high

r-squared values indicated that 80% of the variability found with the mean TIR values of the inactive ciénegas, and about 67% of the variability found with the mean TIR values of the active ciénegas, can be explained by the trends in precipitation. Although there is a strong relationship between precipitation and both TIR and NBR values, none of the correlations are significant at the 95% confidence interval. At the 90% confidence interval, only the NBR values of active ciénegas had a significant relationship to precipitation. This lacking of significance is likely due to the limited number of sample years. A total of 4 years were chosen, thus limiting the total samples across time. If each year from 1984-2009 was included in this analysis, it is likely that a significant relationship would be exhibited. This is not practical for this study because this would require 468 images (9 path rows * 26 years * 2 best predictor variables).

The mean annual precipitation from the 2 years prior, along with the year of image acquisition, do not show a significant relationship to the NBR or TIR values (Figure*s* 36 and 37). With a significant decrease in *r*-squared values, the results indicate that the multiyear precipitation mean does not explain the variability in the trend of TIR or NBR mean values as well as the precipitation mean of the year of acquisition. None of the *r*-squared values are significant at the 95% or 90% confidence intervals.

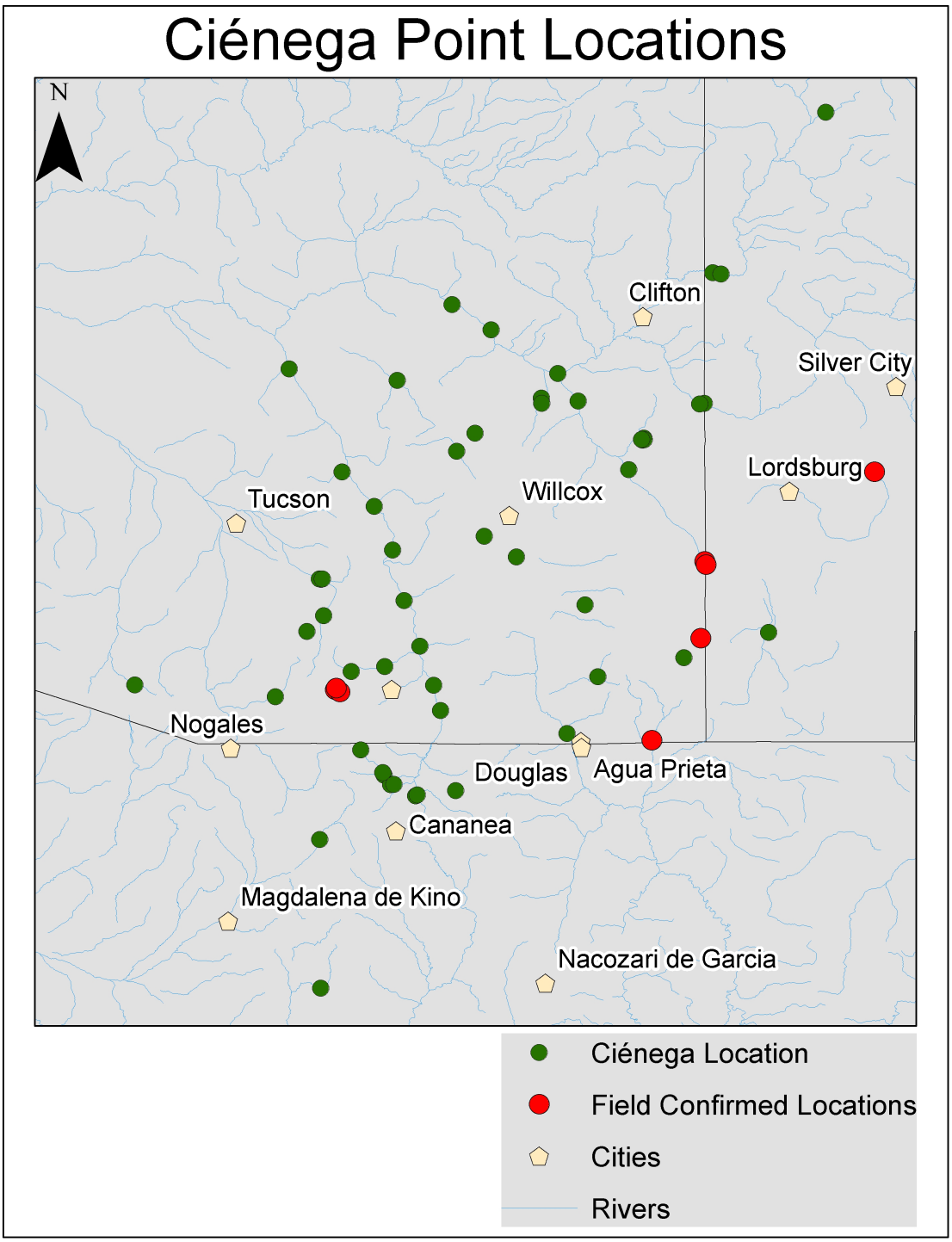

Figure 18: Map of resulting ciénega point location inventory

Table 1. Ciénega Point Location Inventory Table

Name	Source	Longi-tude	Lati-tude	Elevation
Animas	Minckley & Brunelle, 2007	-108.79	31.78	1418.01
Arivaca Ciénega	US Fish and Wildlife Service	-111.33	31.57	1102.09
Artesia	Hendrickson & Minckley, 1984	-109.70	32.70	991.75
Babocomari Ciénega	Hendrickson & Minckley, 1984	-110.47	31.63	1403.33
Babocomari River	Hendrickson & Minckley, 1984	-110.33	31.65	1294.43
Burro Ciénega	USGS Topo Quad- Lordsburg, NM	-108.37	32.43	1638.73
Canelo Hills	The Nature Conservancy	-110.53	31.56	1506.63
Cascabel- San Pedro	Hendrickson & Minckley, 1984	-110.37	32.29	961.00
Cienaga de Heradia	Southern Arizona, Northern Sonora	-110.21	31.13	1400.00
Cienaga de los Pinos	Old Territory and Military Department of NM	-110.59	32.00	1066.57
Cienaga de Saiz	Old Territory and Military Department of NM	-109.04	32.05	1186.46
Cienaga del Cuervo	Old Territory and Military Department of NM	-109.02	33.23	1310.19
Cienaga- Town	Old Territory and Military Department of NM	-109.05	32.70	1163.80
Cienaga- Unnamed	Old Territory and Military Department of NM	-108.56	33.87	2008.42
Ciénega Bonita	Military Map of New Mexico- 1864	-109.30	32.56	1073.01
Ciénega de Heredia	Mapa General de la Localidad	-110.20	31.13	1393.37
Ciénega de los Pinos	Map of Pioneer Trails 1541-1867	-110.58	32.00	1072.52
Ciénega del Guiso	Military Map of New Mexico- 1864	-108.98	33.22	1459.37
Ciénega Ranch	1958 Usgs Topo Quad- Empire Mtn 15 min series	-110.58	31.85	1293.35
Ciénega Springs	Hendrickson & Minckley, 1984	-109.70	32.72	967.68
Ciénega- Unnamed	Mapa General de la Localidad entre	-110.30	31.17	1392.94
Ciénega- Unnamed	Military Map of New Mexico- 1874	-109.07	32.70	1122.45
Cocospera Ciénega	Mapa Oficial del Estado Sonora Republica de Mexico	-110.59	30.95	1080.00
Croton Springs	Hendrickson & Minckley, 1984	-109.93	32.17	1262.30
Douglas Valley	Hendrickson & Minckley, 1984	-109.60	31.38	1201.40
El Jarral Ciénega	Southern Arizona in the late '70s	-110.34	31.22	1426.11
Empire Ranch	1958 Usgs Topo Quad- Empire Mtn 15 min series	-110.64	31.79	1401.56
Fairbank- San Pedro	Hendrickson & Minckley, 1984	-110.19	31.73	1175.51

Table 1. Continued

Name	Source	Longi-tude	Lati-tude	Elevation
Feldman- San Pedro	Hendrickson & Minckley, 1984	-110.71	32.84	663.54
Geronimo-Bylas	Hendrickson & Minckley, 1984	-110.06	33.10	800.73
Grant	Hendrickson & Minckley, 1984	-109.97	32.58	1379.25
Hooker Ciénega	Hendrickson & Minckley, 1984	-110.04	32.51	1337.78
Horseshoe Canon	Southern Arizona in the late '70s	-109.06	31.76	1282.96
La Fresna Ciénega	Antonio Esquer- TNC, and Trevor Hare- SIA	-110.43	31.31	1539.85
Leslie	Hendrickson & Minckley, 1984	-109.48	31.61	1450.23
Lewis Springs- San Pedro	Hendrickson & Minckley, 1984	-110.14	31.57	1234.98
O'Donnell Creek	Hendrickson & Minckley, 1984	-110.53	31.55	1530.19
Redington- San Pedro	Hendrickson & Minckley, 1984	-110.50	32.43	874.38
San Bernardino Ciénega	Minckley & Brunelle, 2007	-109.26	31.35	1147.38
San Pedro- Complex	Hendrickson & Minckley, 1984	-110.11	31.47	1257.58
San Simon	Hendrickson & Minckley, 1984	-109.56	32.71	957.28
San Simon	Hendrickson & Minckley, 1984	-109.05	32.07	1177.21
San Simon 2	Hendrickson & Minckley, 1984	-109.35	32.44	1042.00
San Simon-Gila	Hendrickson & Minckley, 1984	-109.64	32.82	900.71
Saracachi Ciénega	Sky Island Alliance	-110.59	30.36	940.00
Sonoita	Minckley & Brunelle, 2007	-110.77	31.53	1226.77
St. David- San Pedro	Hendrickson & Minckley, 1984	-110.25	31.91	1092.87
Sulphur Springs	Hendrickson & Minckley, 1984	-109.80	32.09	1272.01
Sycamore	Minckley & Brunelle, 2007	-111.60	33.66	482.29
The Narrows- San Pedro	Hendrickson & Minckley, 1984	-110.30	32.11	1022.33
Turkey Creek	Hendrickson & Minckley, 1984	-110.51	31.54	1525.62
Unnamed	Hendrickson & Minckley, 1984	-109.13	31.68	1332.22
Unnamed Ciénega	Estado de Sonora Estados Unidos de Mexico- 1924	-110.33	31.21	1419.59
Unnamed Ciénega	Estado de Sonora Estados Unidos de Mexico- 1924	-110.31	31.17	1400.41
Unnamed Ciénega	Mapa Oficial del Estado Sonora Republica de Mexico	-110.05	31.15	1482.24

Table 1. Continued

Name	Source	Longi-tude	Lati-tude	Elevation
Unnamed Ciénega	New Map of the Territory of Arizona....	-110.59	32.00	1069.9
Unnamed- Gila	Hendrickson & Minckley, 1984	-109.91	33.00	843.95
W. Turkey Ck.	Hendrickson & Minckley, 1984	-109.53	31.89	1430.82
Water of the Dead-Klondike	Hendrickson & Minckley, 1984	-110.28	32.80	1103.79
Whitlocks Cienaga	Old Territory and Military Department of NM	-109.29	32.56	1073.25
Whitlock's Ciénega	Map of Pioneer Trails 1541-1867	-109.29	32.56	1070.99
Whitlock's Sink	Hendrickson & Minckley, 1984	-109.30	32.56	1070.66

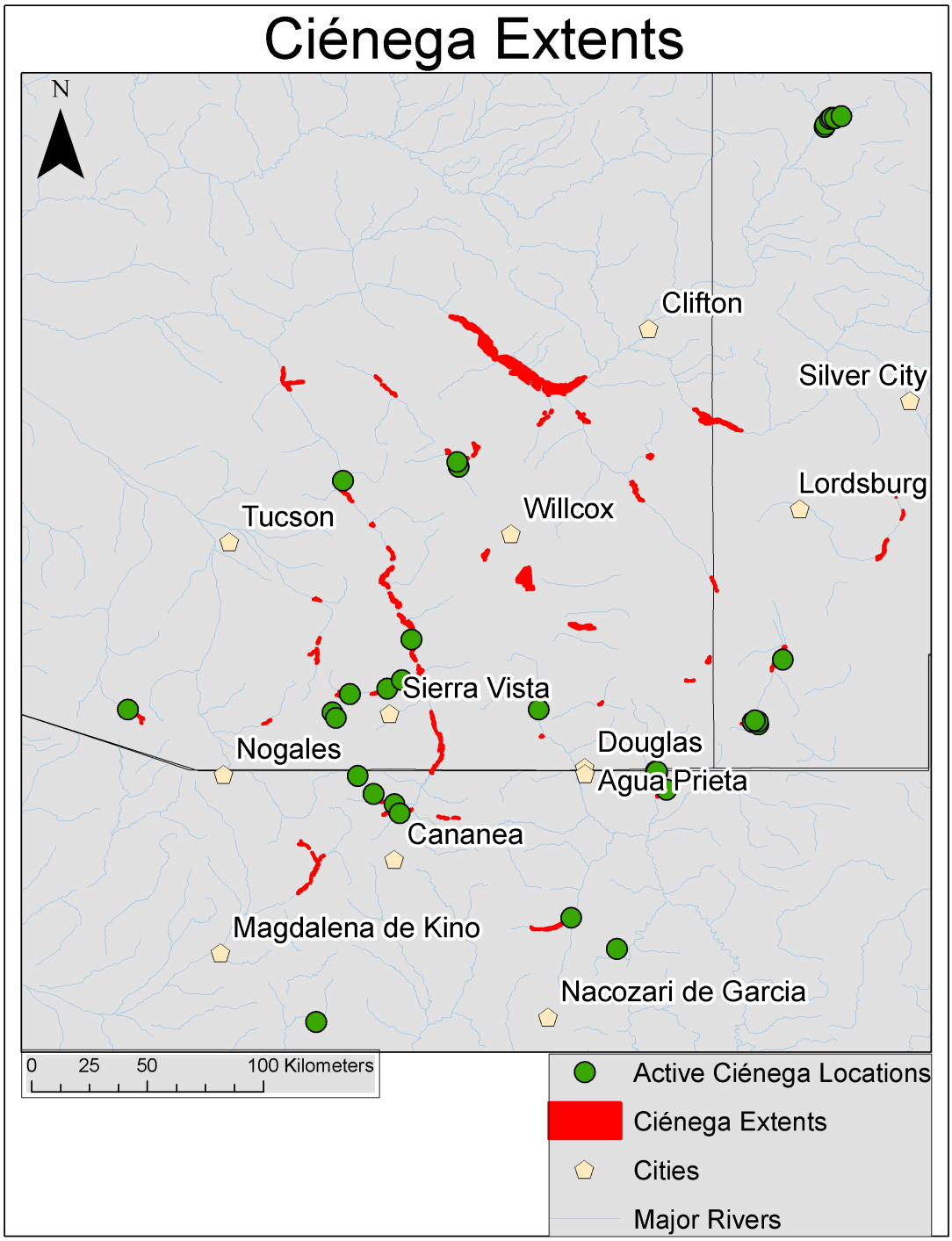

Figure 19: Map of delineated ciénega extents

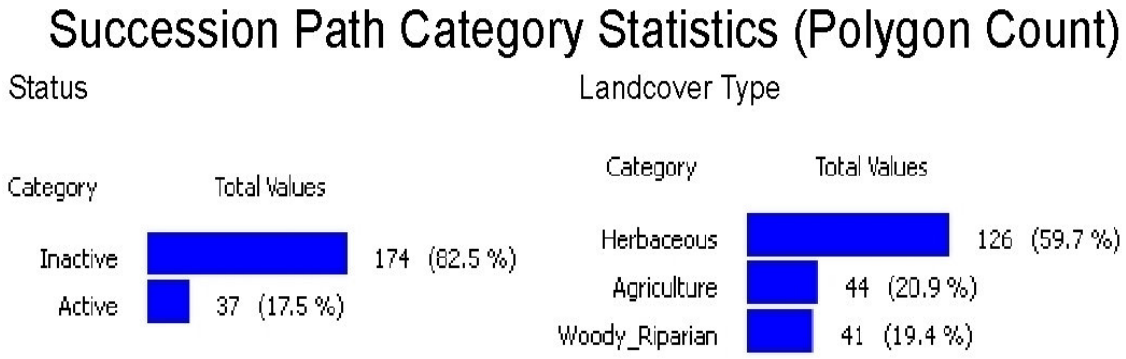

Figure 20: Count statistics across different succession path categories. The statistics are a count of the number of polygons of each succession path category. The status confidence level represents the number of ciénegas that had status confidence levels across different succession paths.

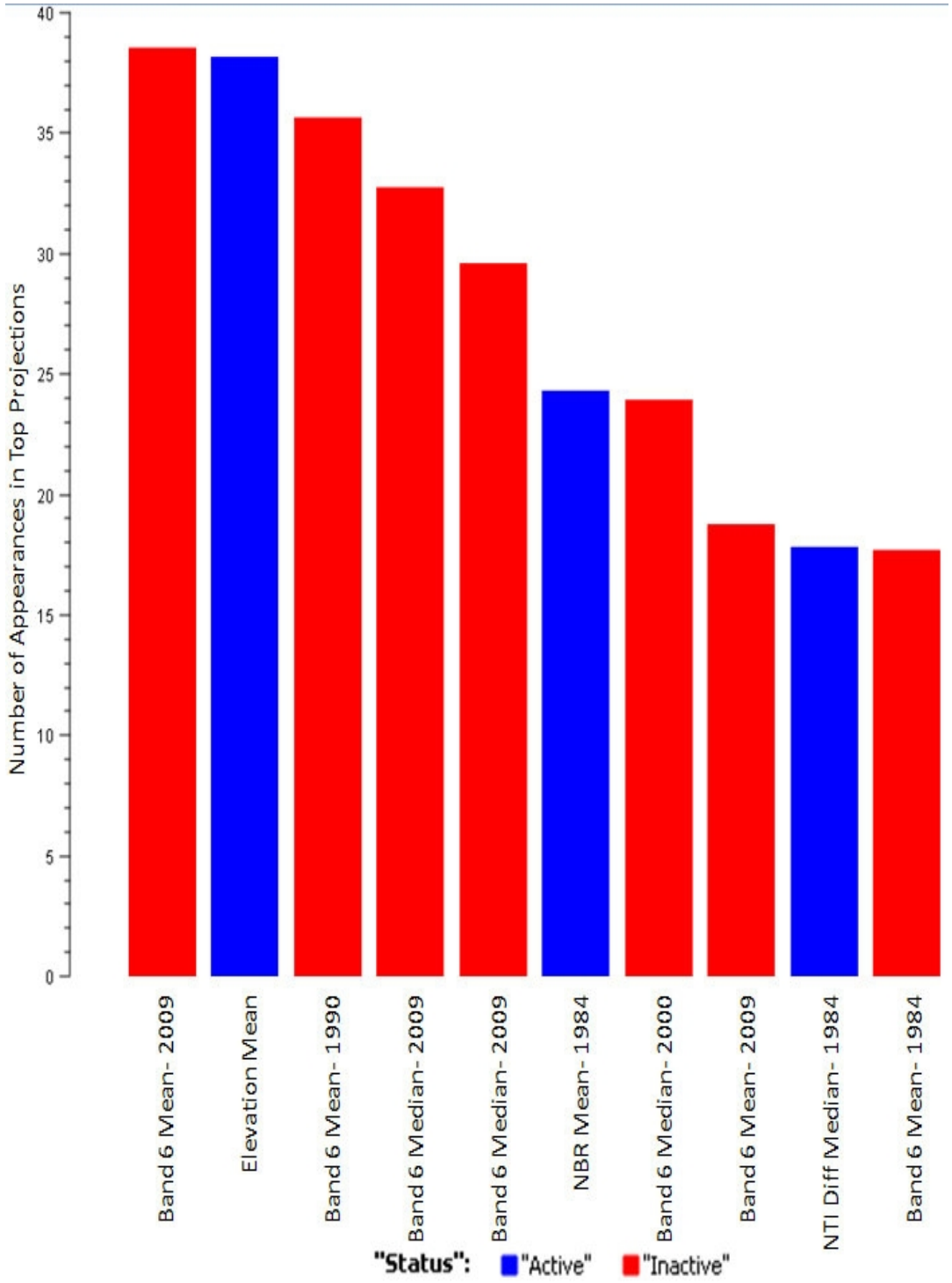

Figure 21: Top 10 most commonly used attributes with the number of times they appear in the 1035 projections in "VizRank" across the status succession path.

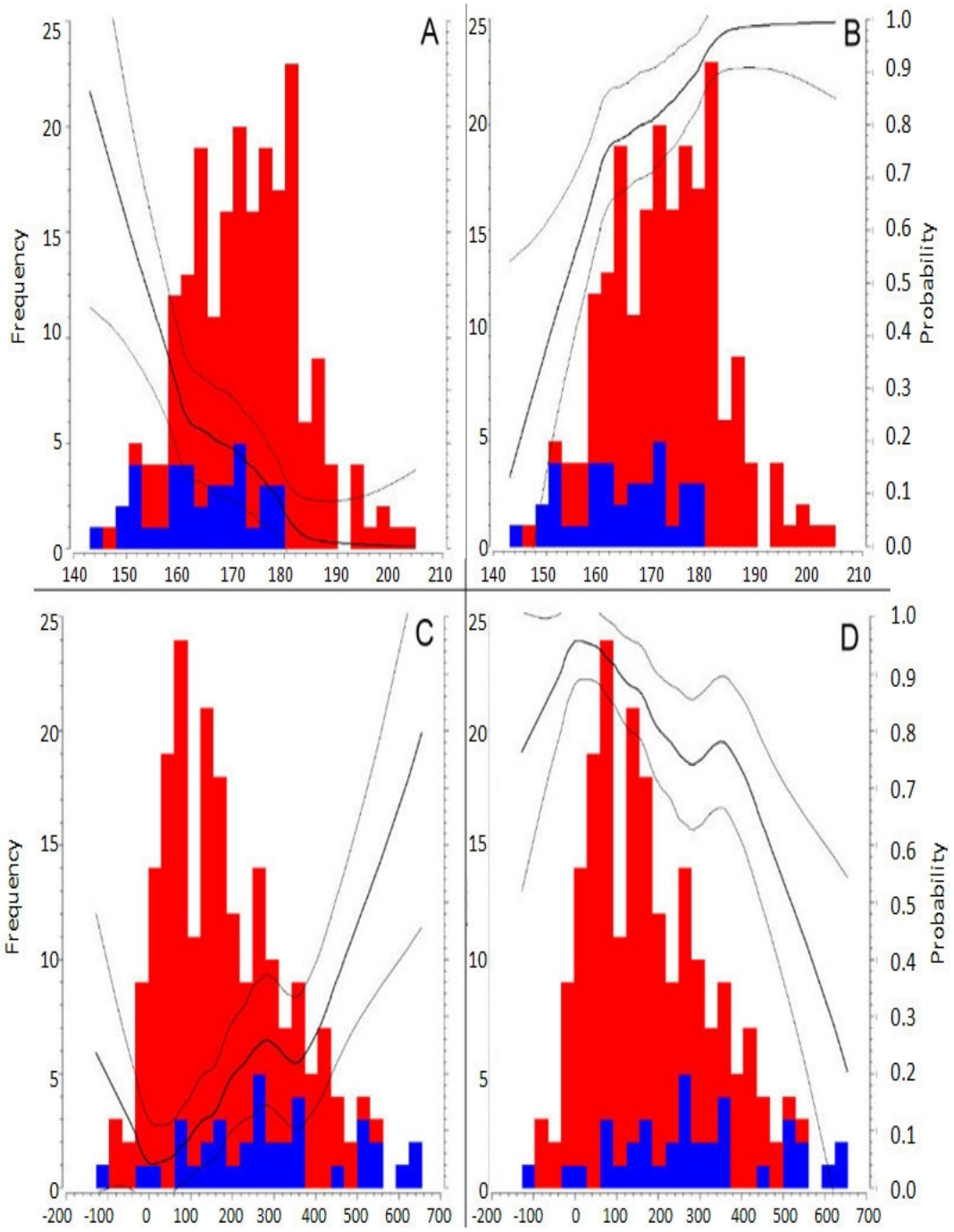

Figure 22: Distributions represent mean TIR band 6 (A and B) and NBR (C and D) frequency distributions. Lines represent the probabilities at the 90th, 95th, and 99th percentile of obtaining an active ciénega in distributions A and C, or inactive ciénega in B and D. The significant difference in the probabilities across different values of TIR and NBR can be observed.

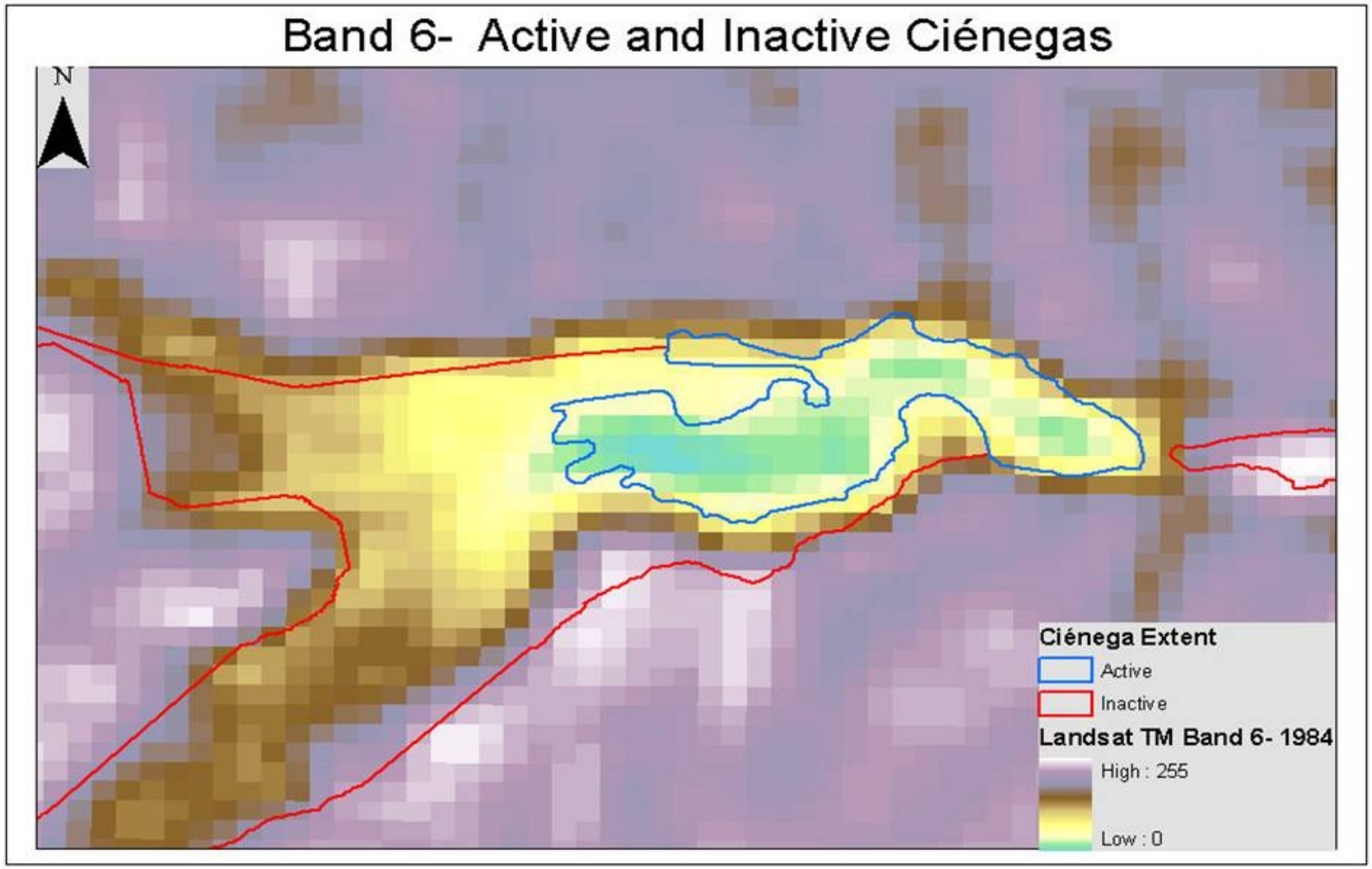

Figure 23: Example of sensitivity of TIR to active and inactive sections of ciénegas. Low values are apparent within the active portion, while the inactive portion is dominated by higher values.

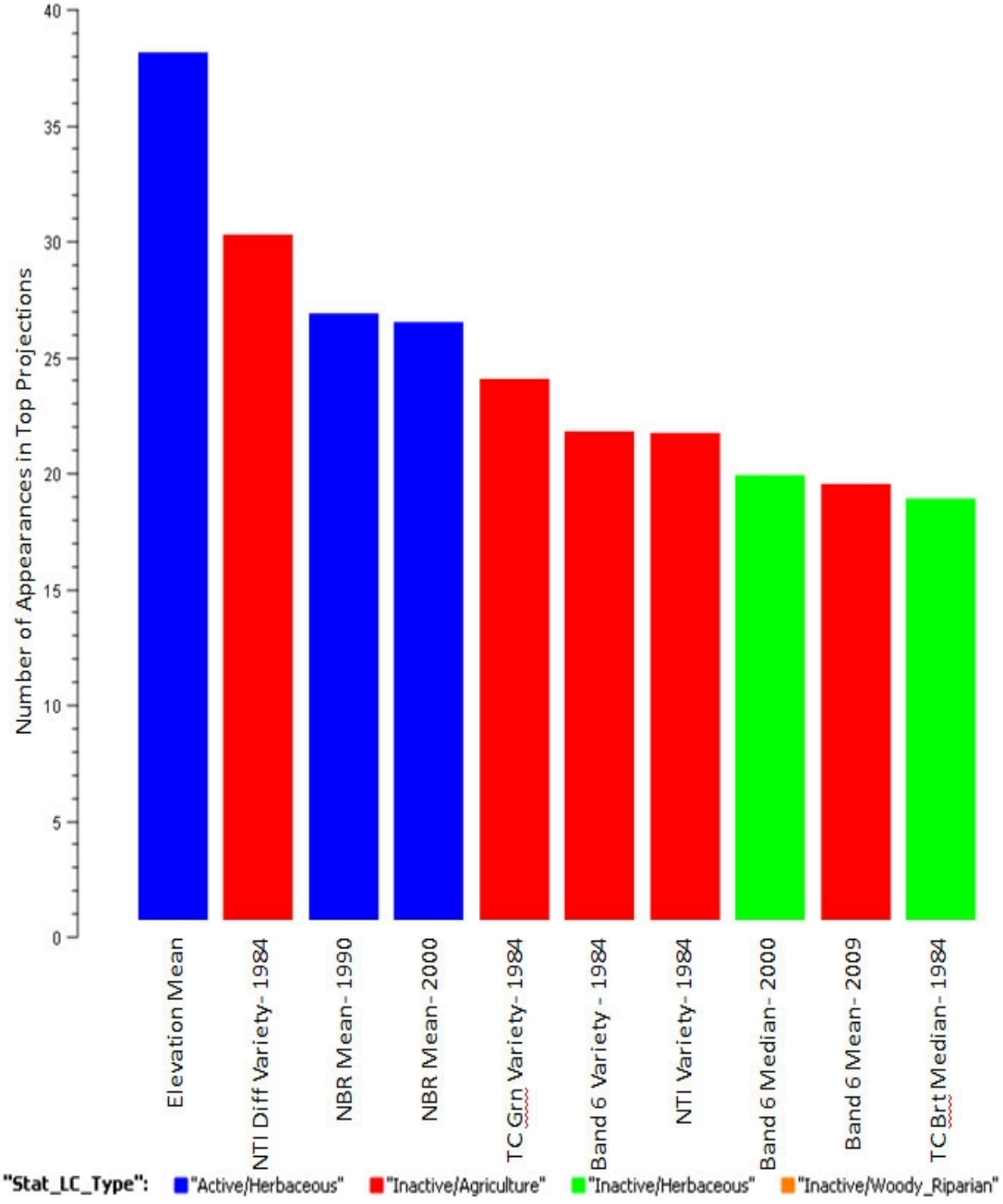

Figure 24: Top 10 most commonly used attributes with the number of times they appear in the 1035 projections in "VizRank" across the land cover type succession path.

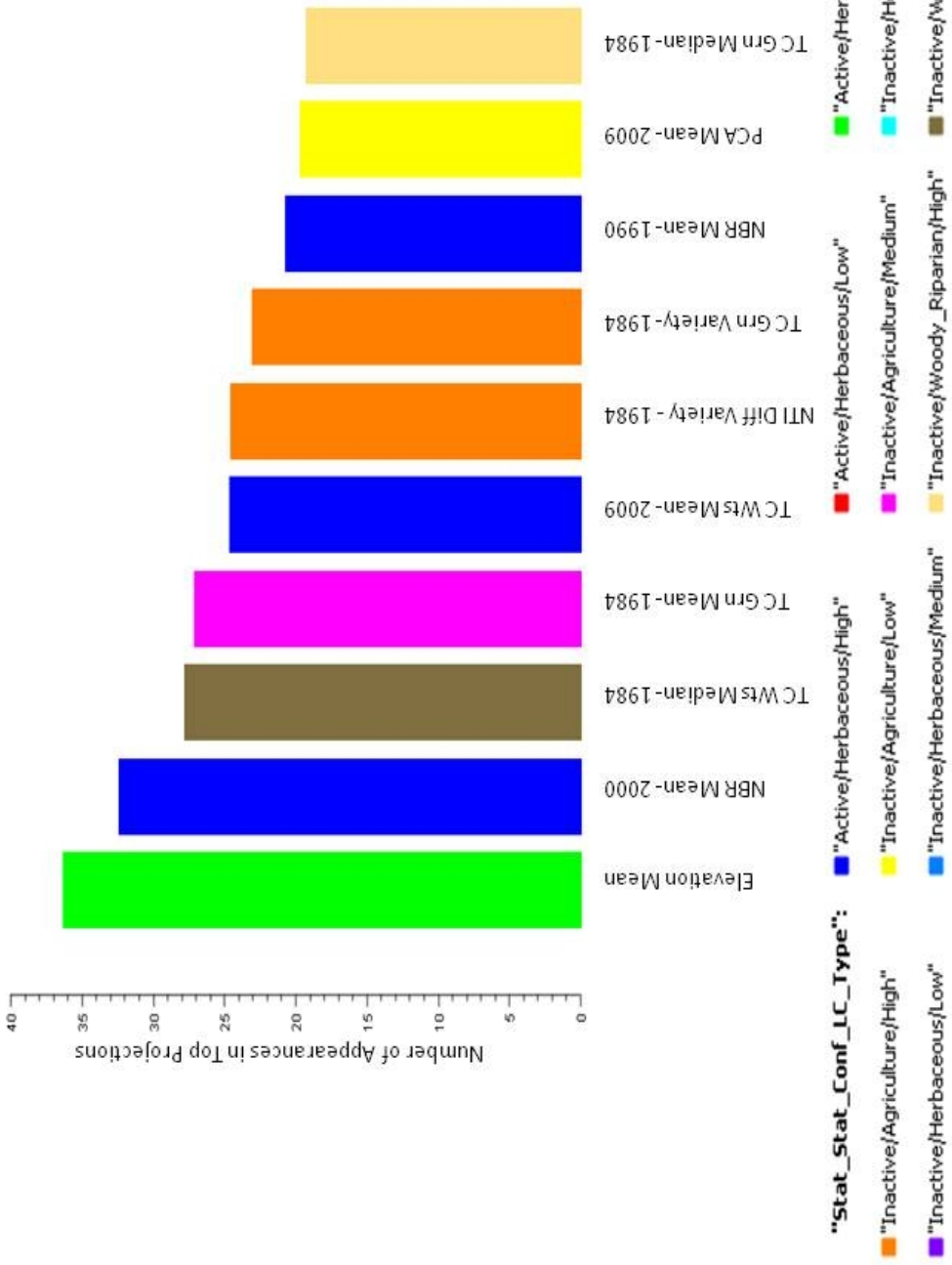

Figure 25: Top 10 most commonly used attributes with the number of times they appear in the 1035 projections in "VizRank" across the status, land cover type, and status confidence level succession path.

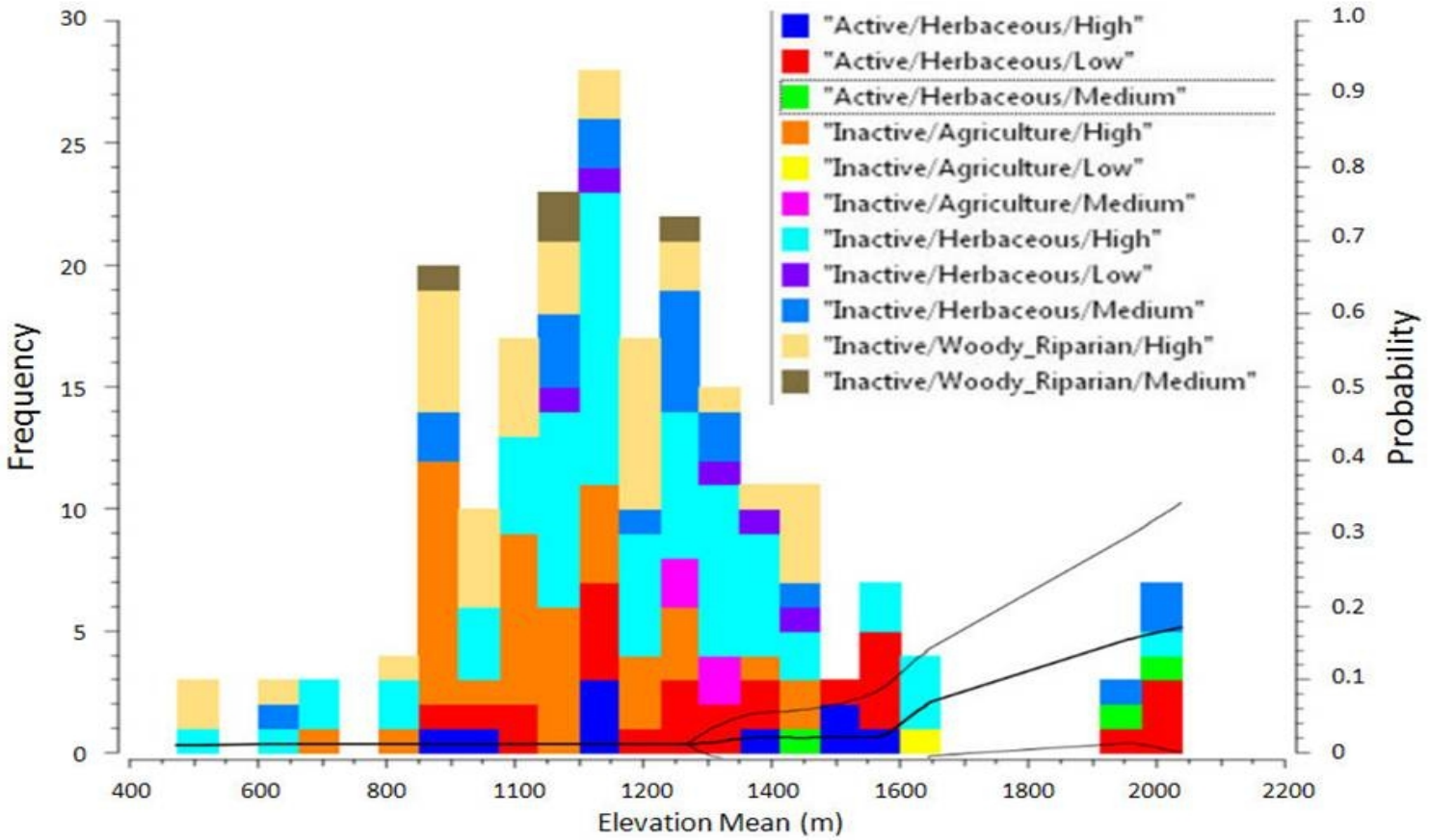

Figure 26: Distribution of mean elevation values of each polygon across the status, land cover type, status confidence level succession paths. Probability shown is that of the active/herbaceous/medium class. This class was the most sensitive to elevation. This is likely because of its small sample size being easily leveraged with what are likely outliers from the global trend.

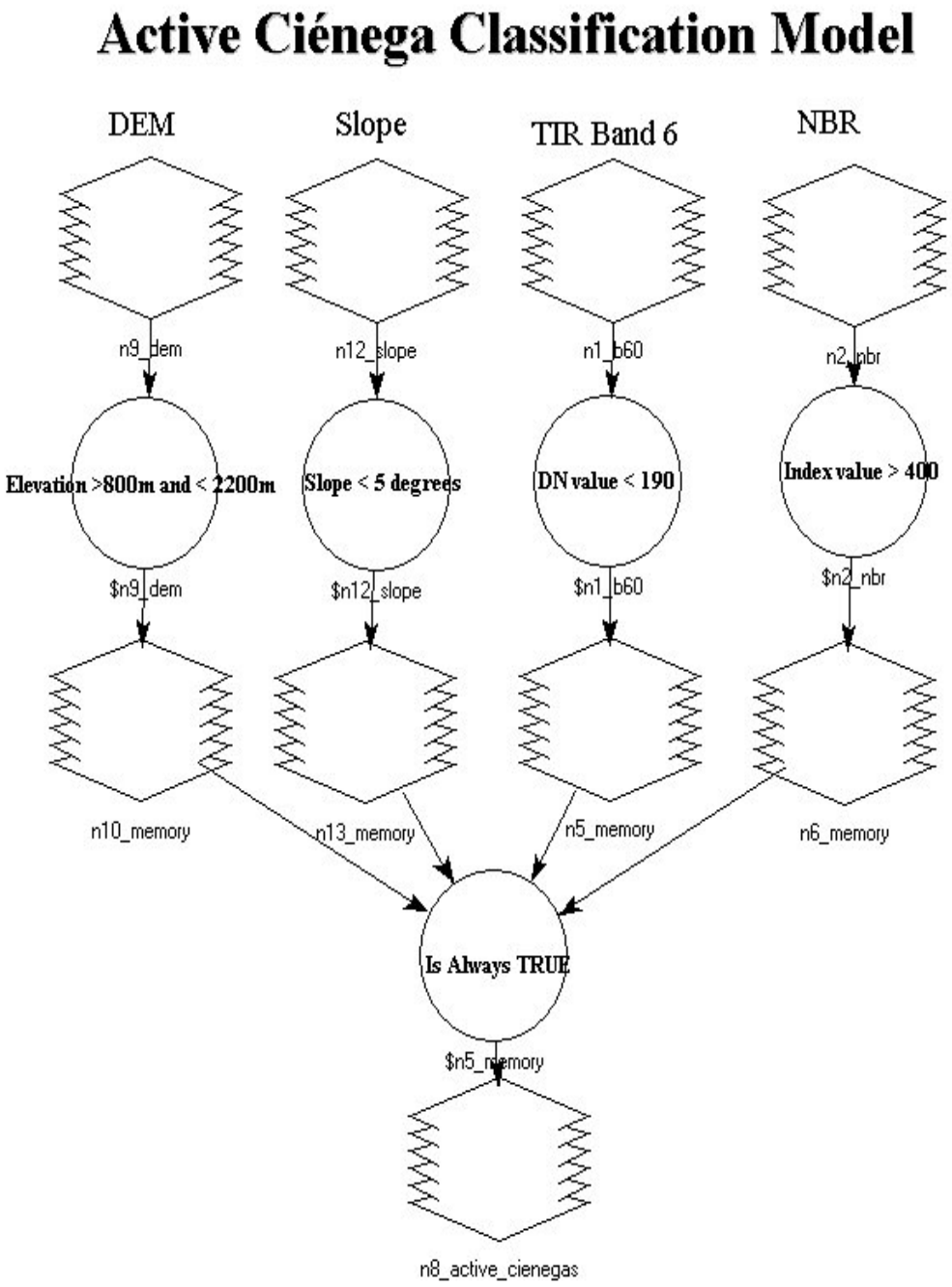

Figure 27: Flow of model to identify areas that are likely active ciénegas according to the natural breaks values in the data within VizRank.

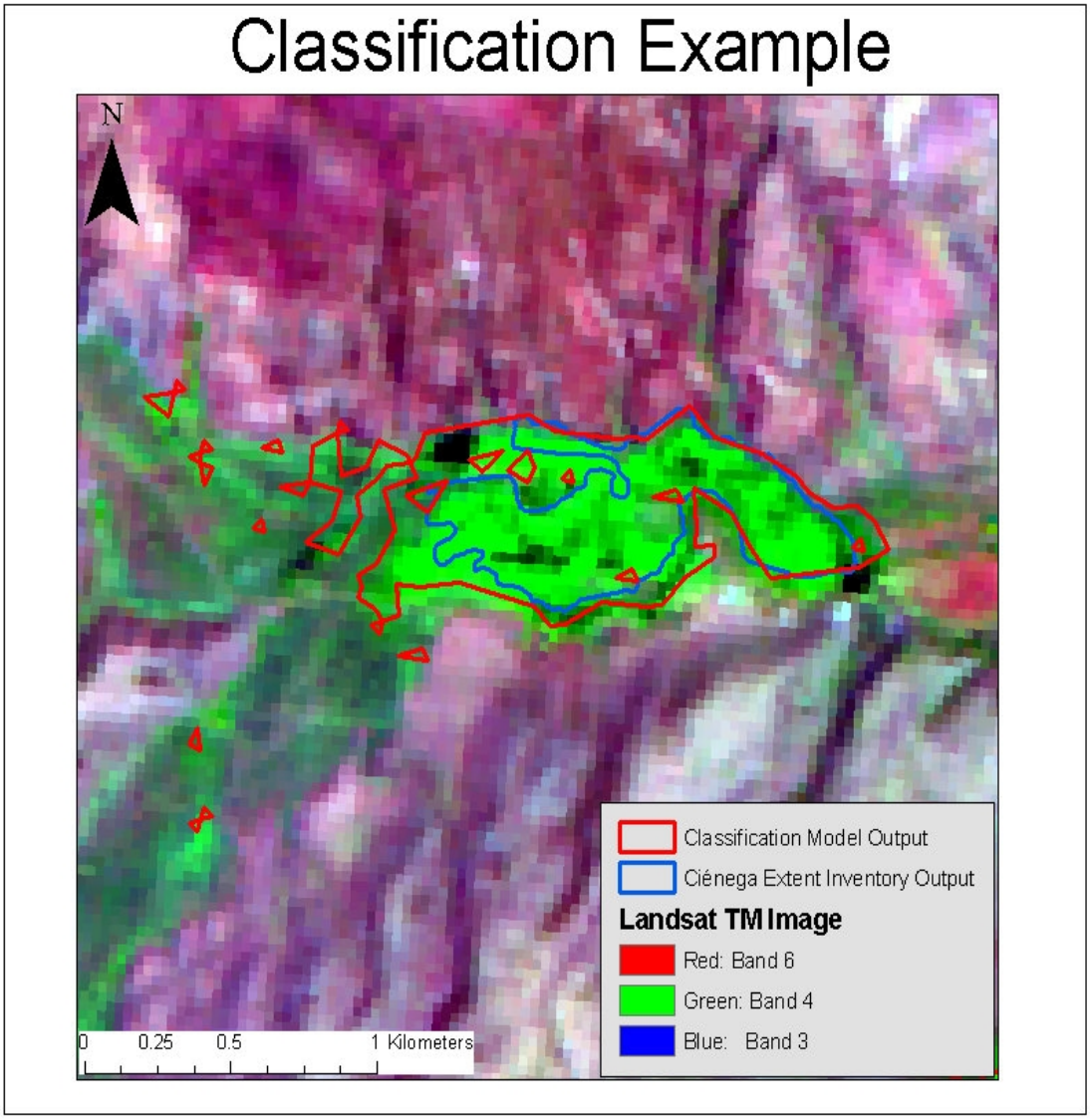

Figure 28: Example of delineated extent from the classification model, compared to the manually delineated extent of the active portion of the Babocomari Ciénega.

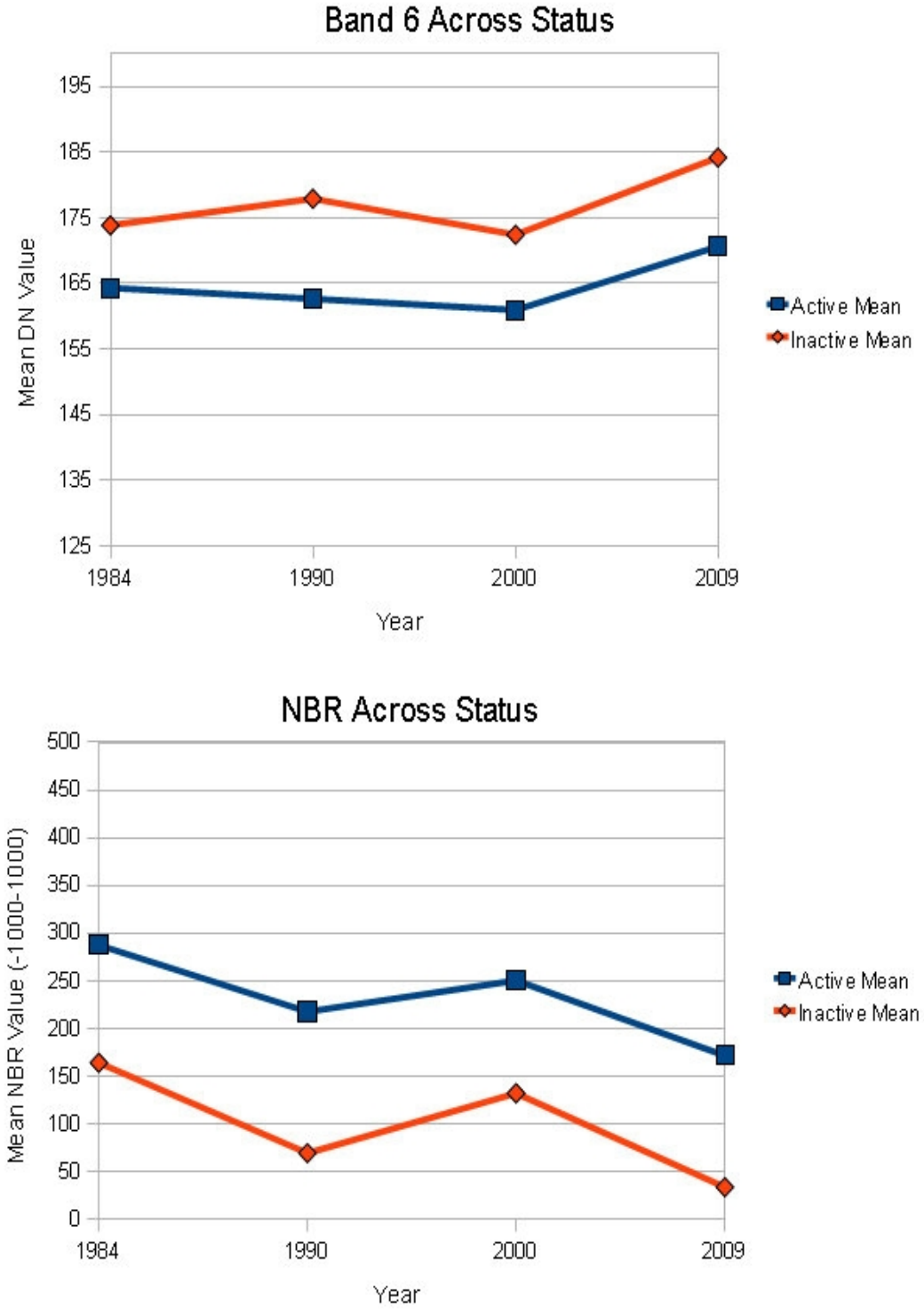

Figure 29: Mean TIR band 6 and NBR values from 1984-2009 of ciénegas classified based on the status succession path

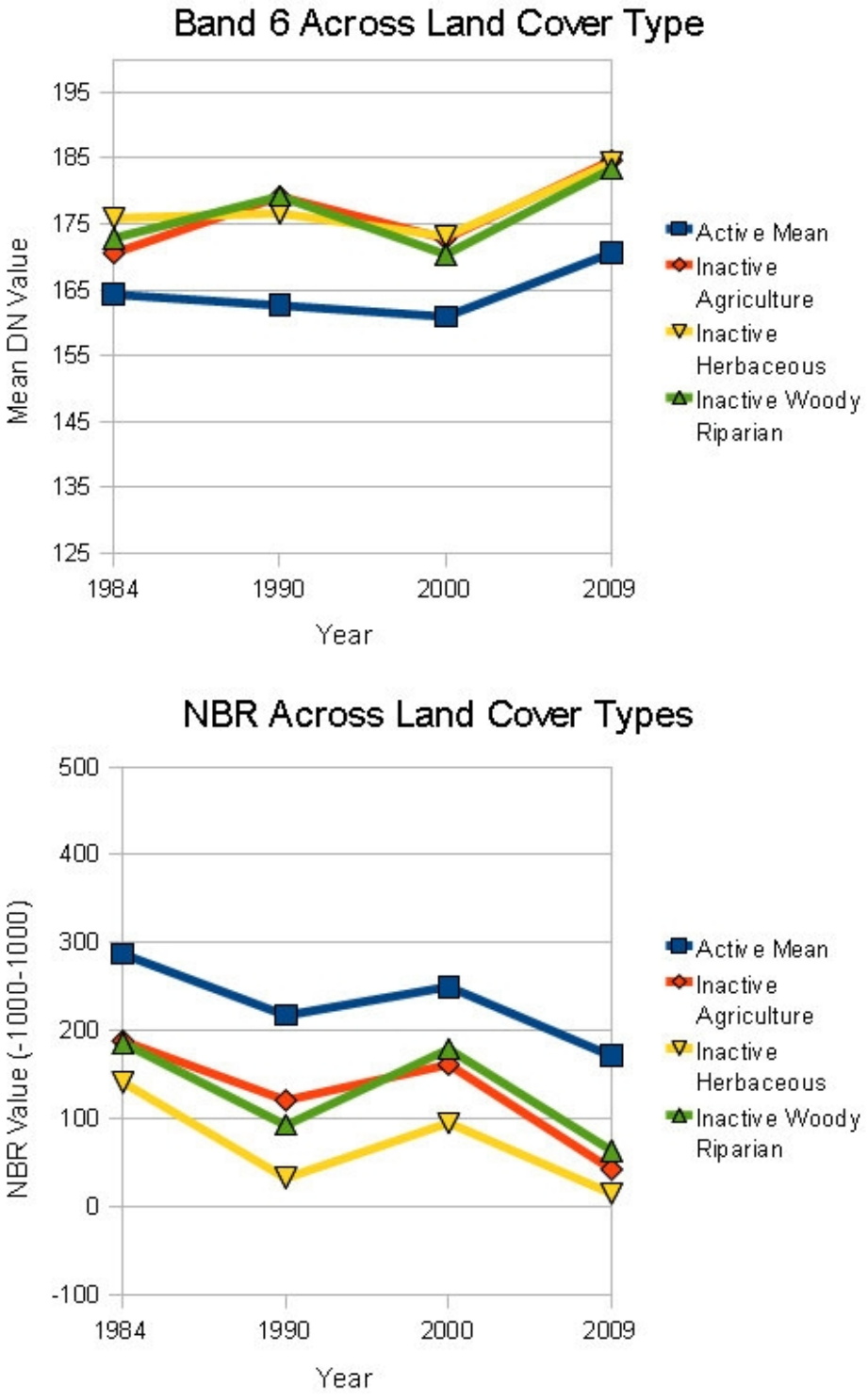

Figure 30: Mean TIR band 6 and NBR values from 1984-2009 of ciénegas classified based on the land cover type succession path

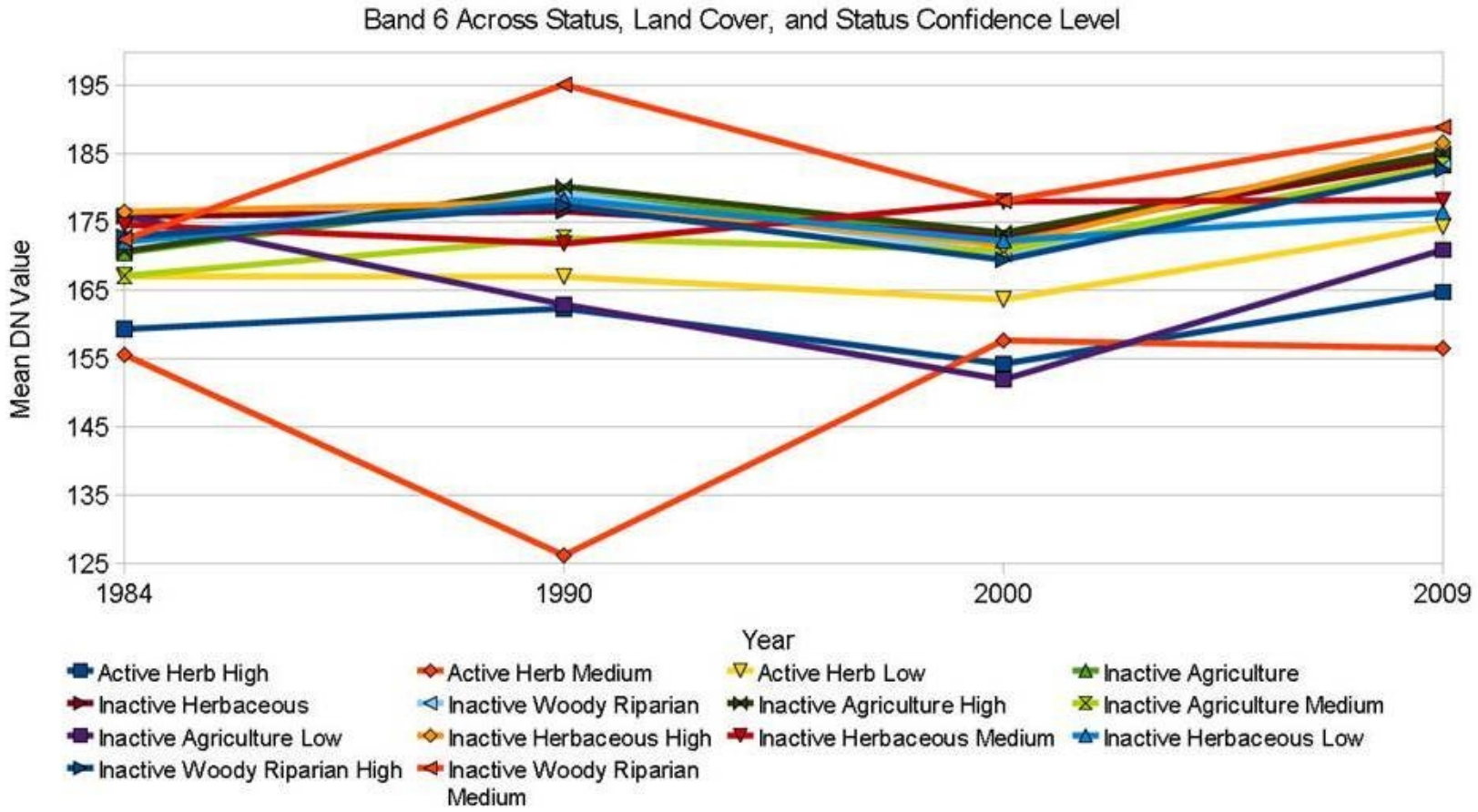

Figure 31: Mean TIR band 6 values from 1984-2009 of ciénegas classified based on status, land cover type, and status confidence level succession paths

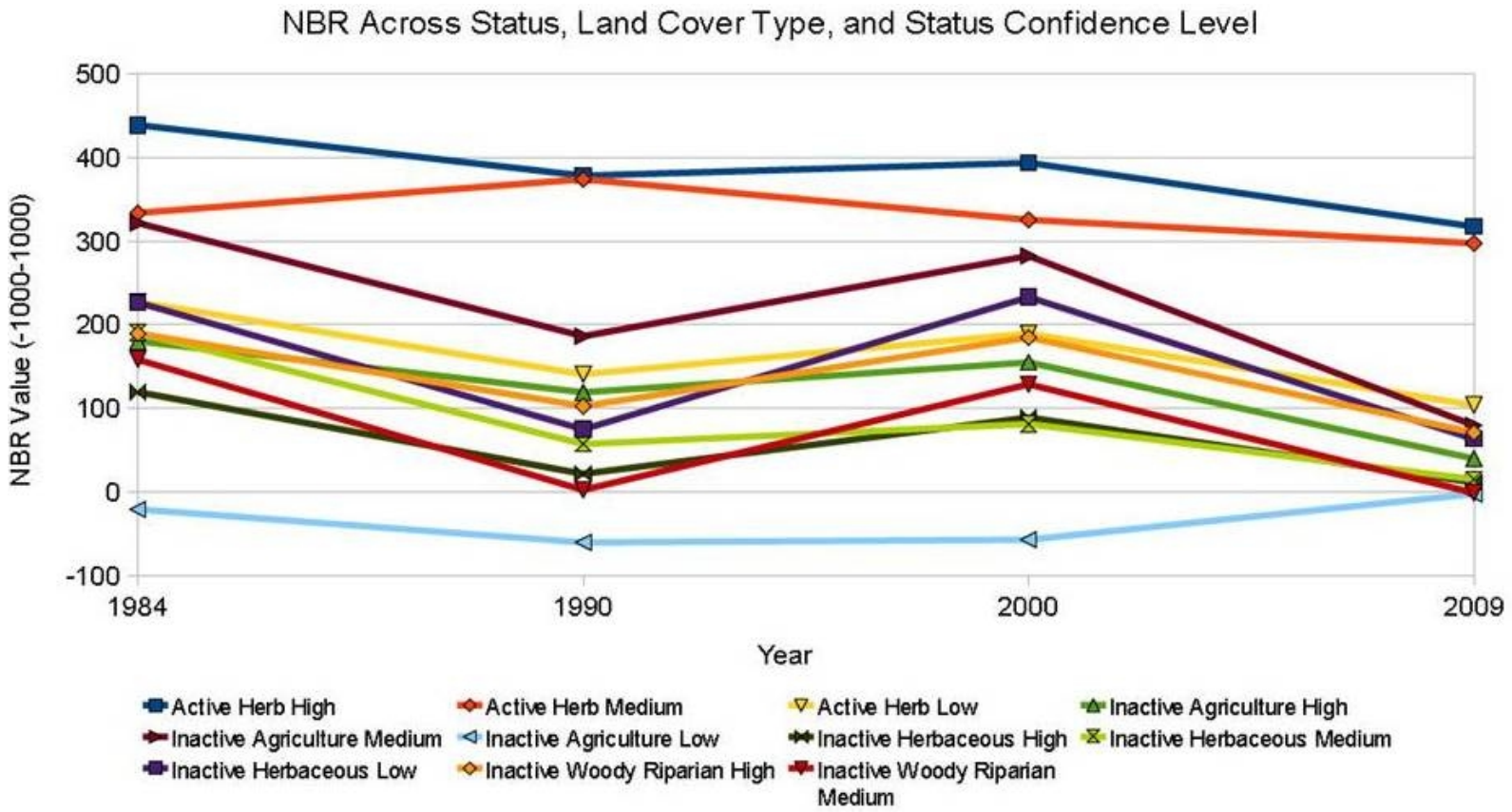

Figure 32: Mean NBR values from 1984-2009 of ciénegas classified based on status, land cover type, and status confidence level succession paths

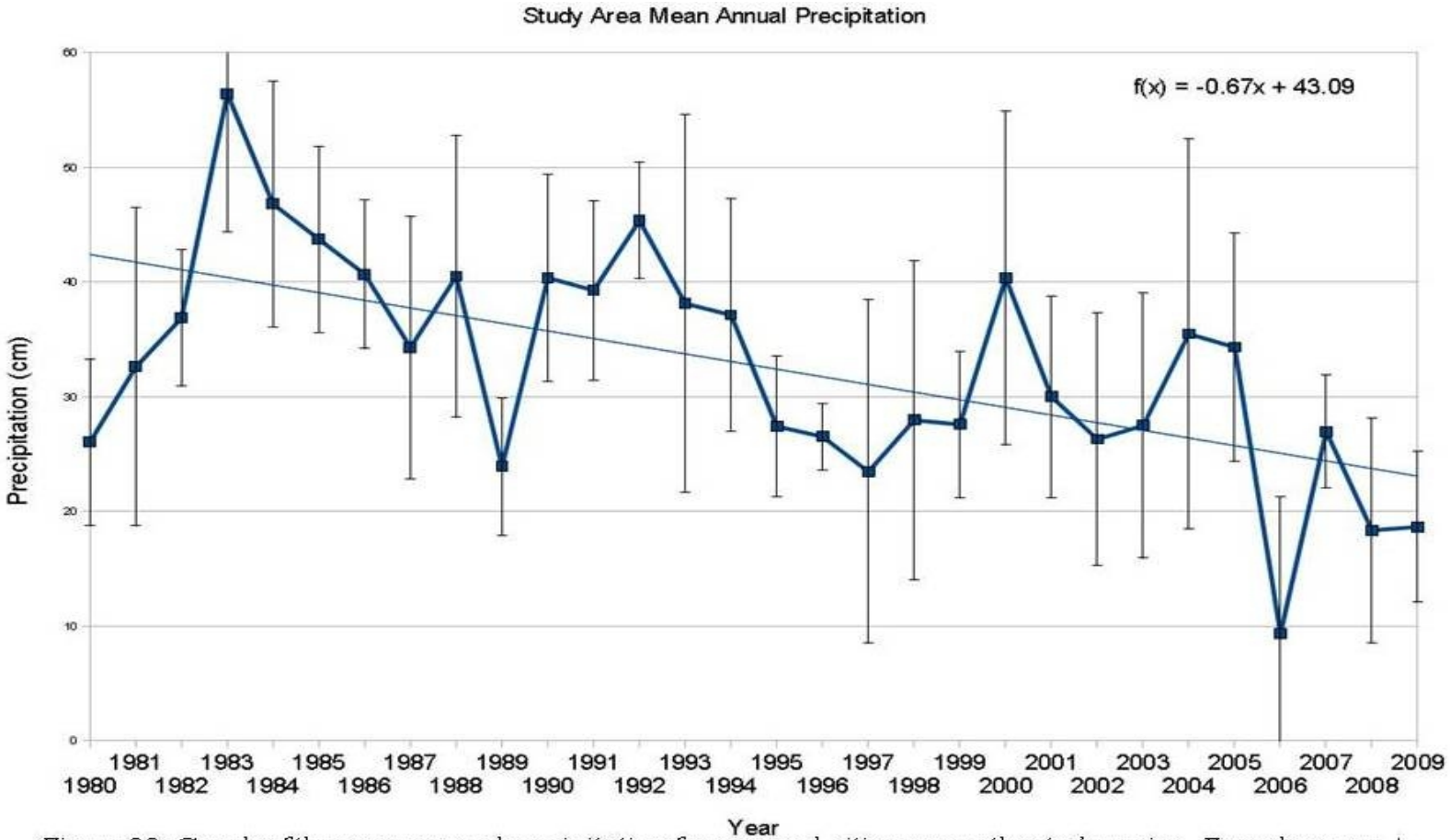

Figure 33: Graph of the mean annual precipitation from several cities across the study region. Error bars are +- 1 standard deviation of the mean values from various cities. Trend line indicates a downward trend across the study area for the time period (Data source: WRCC).

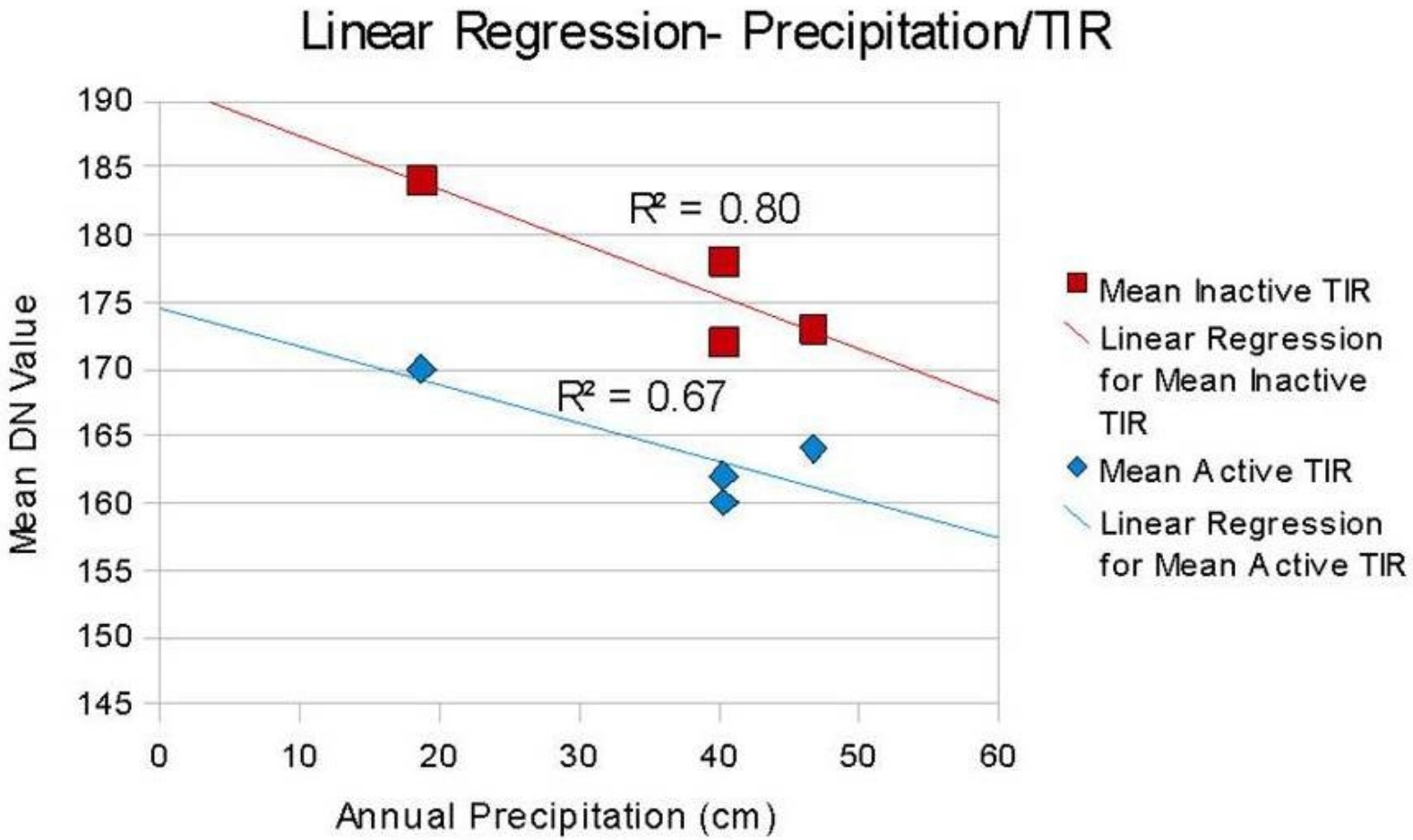

Figure 34: Linear regression of mean TIR values with respect to precipitation for the year of image acquisition

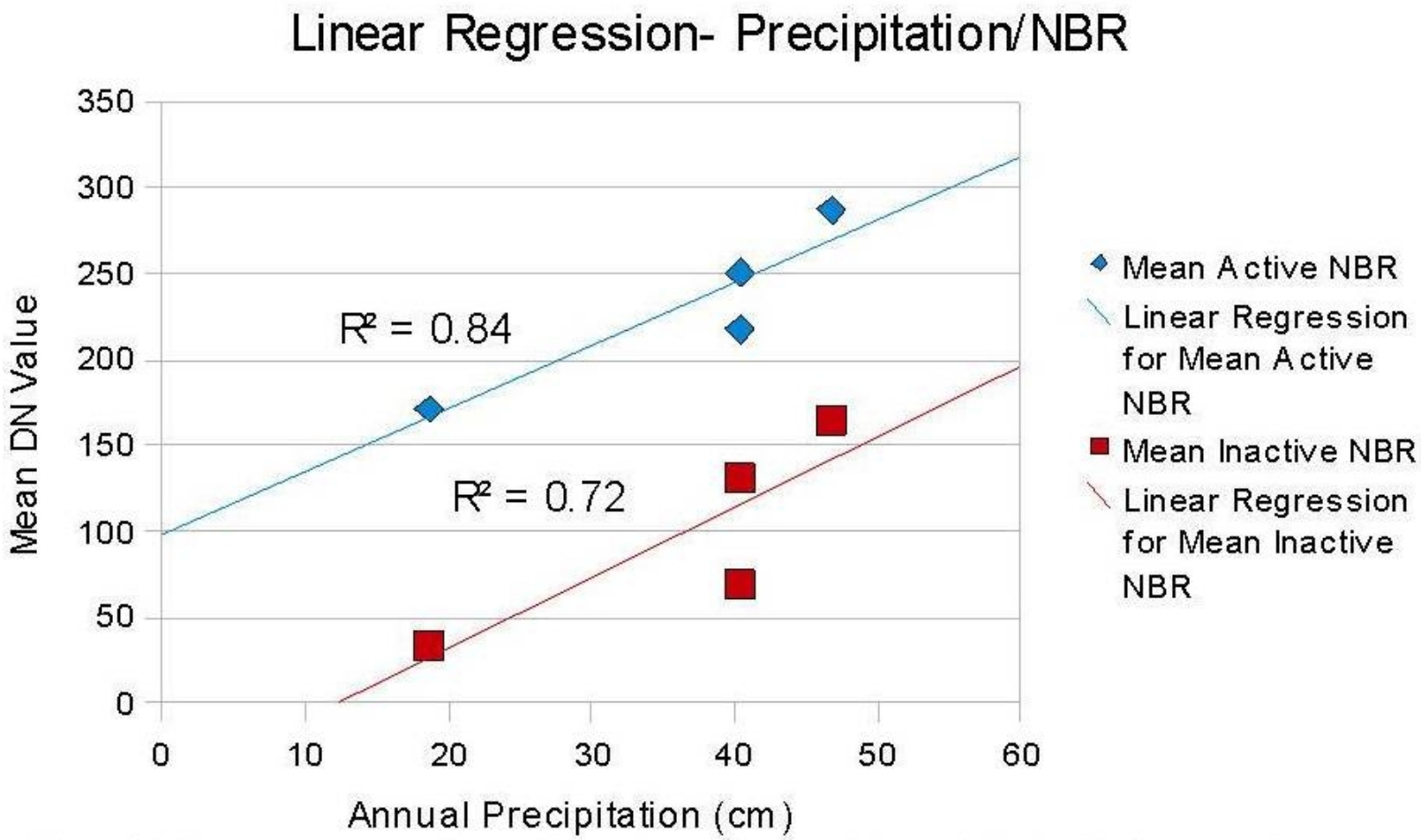

Figure 35: Linear regression of mean NBR values with respect to precipitation for the year of image acquisition

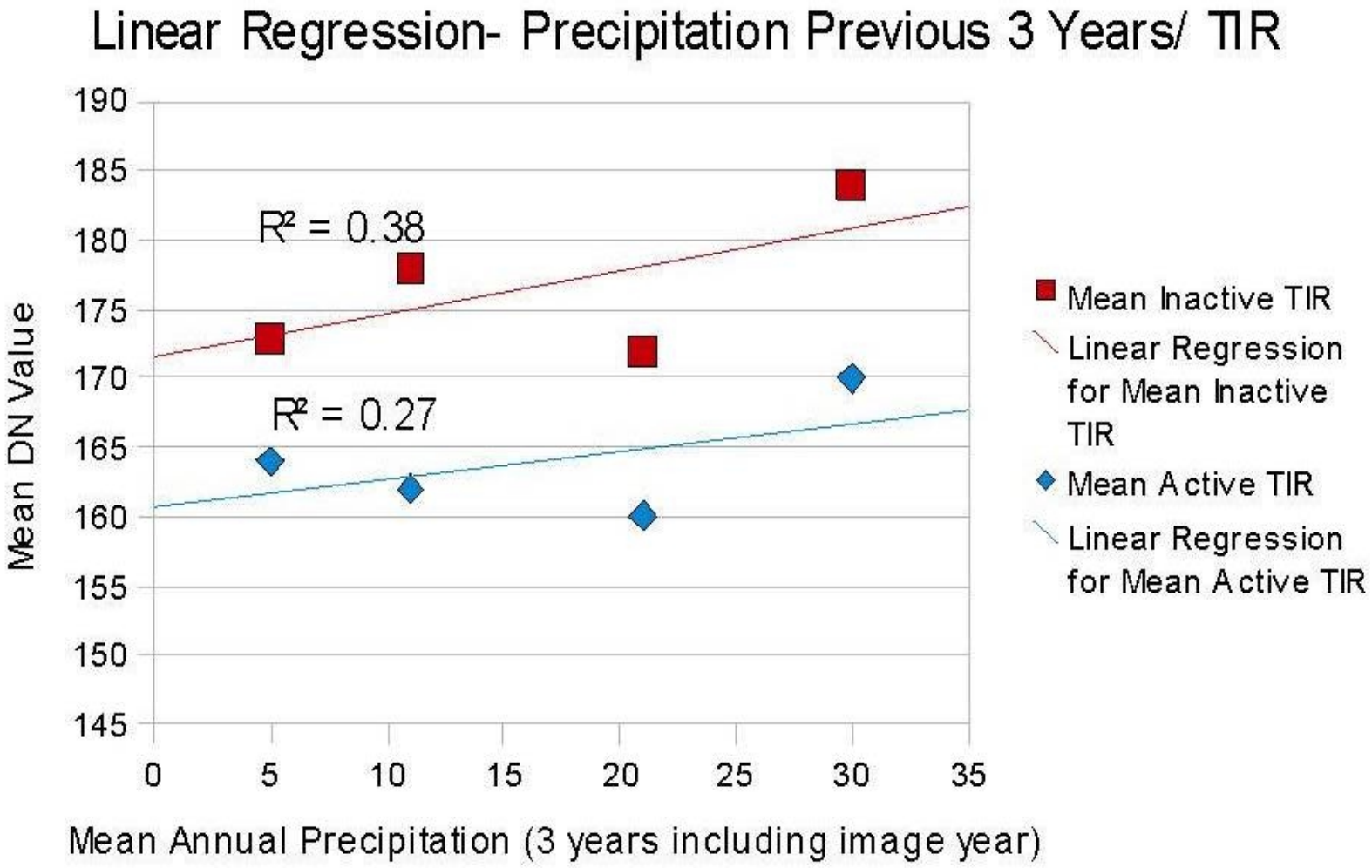

Figure 36: Linear regression of 3-year mean TIR values

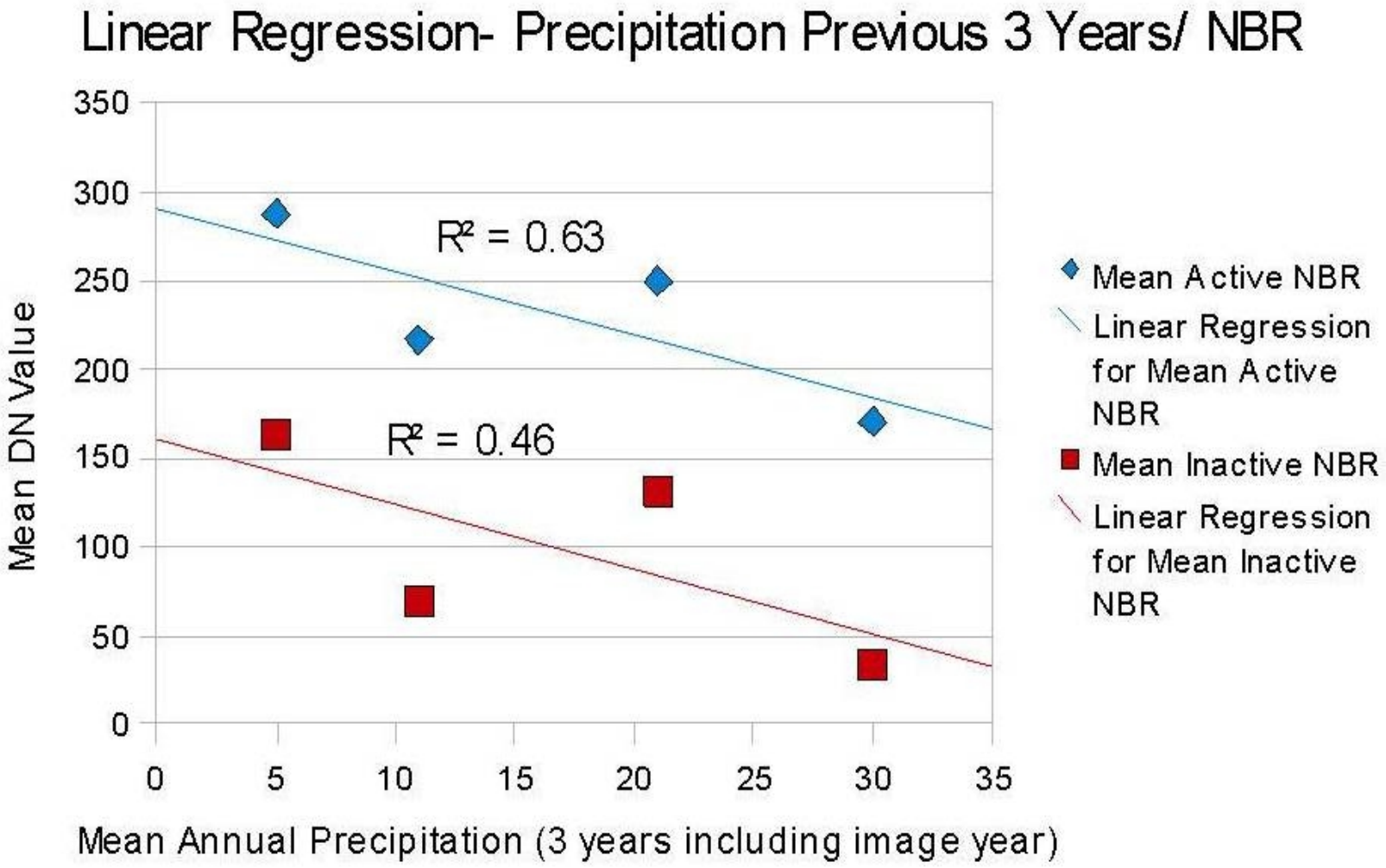

Figure 37: Linear regression of 3-year mean NBR values

DISCUSSION AND CONCLUSIONS

Ciénega Point Inventory

This study has resulted in an improved inventory of historical ciénegas, along with an increased understanding of recent patterns of change of extant and extinct ciénegas. The ciénega point inventory represents a successful synthesis of the review of historical documents, with more modern data sources, and expert knowledge, to arrive at a more comprehensive database of historical ciénega locations.

Ciénega Areal Extent Inventory

Through the use of NAIP imagery, the difficulties with identifying extinct ciénegas that followed different succession paths were circumvented. Future inventories should build on this inventory by relaxing the criteria required for an area to be included as a historical ciénega. This could involve including all areas that meet the image interpretation criteria, but are not located adjacent to a documented ciénega point location. By increasing the errors of commission, a field accuracy assessment would be necessary. The result would be a more complete inventory of the historical extent of ciénegas. Because of the divergent succession paths of ciénegas, validation will likely require coring of the ciénega, to assess the taxa present prehistorically.

The areal extent inventory, along with the methods used to delineate historical ciénega areal extents will allow restoration efforts to concentrate their efforts more effectively. By knowing where a ciénega may have existed historically, restoration can

be devoted to these areas. Because there is a chance that the area that is delineated using the areal extent inventory delineation methods may be larger or smaller than the actual historical extent, these methods should be viewed as a tool to gain an understanding of restoration possibilities, rather than the basis for an entire restoration project's design.

Best Predictor Variable Determination

The use of zonal statistics to determine the best predictor variable for different succession paths introduces many assumptions. Among the most difficult is to assure that the statistic is representative of the entire polygon. Some of the variability that was not representative of the true values of the polygon was eliminated by using a -30 m buffer. This excluded most of the mixed pixels that were influenced by the reflectance of surfaces outside of the polygon. Despite this measure and careful delineation of homogenous land cover types, intrapolygon variability among values of various datasets was unavoidable. In Figure*s* 37 and 38, the Babocamari Ciénega demonstrates the spatial variability of change in both the TIR and NBR. Such variation is difficult to account for with aspatial statistics. Because pixels were the sample source of each polygon, several small polygons did not contain sufficient pixels to be representative. Most ciénega subset polygons were of sufficient size to gather a representative statistic for that polygon, and its respective succession path.

The variability among different ciénega areal extent polygons reiterates the rationale behind the image interpretation method that was employed over data-driven classification methods. If each polygon had a variable that consistently separated the data across all succession paths, the initial studies would have yielded sufficient results to

have promoted the implementation of a more automated classification method.

Elevation did appear as though it was a good variable for separating the ciénegas across various succession paths. Although this relationship was subject to local influences, it was clear when looking at the overall distribution that the active ciénegas had an overall higher elevation. This may be due to the high amount of precipitation in areas at higher elevations. Hendrickson and Minckley (1984) divided ciénegas into three groups, based on their characteristics. They used elevation to make the distinction between which characteristics are more prevalent across different types of ciénegas. If the type of ciénega is dependent on elevation, it cannot be ruled out that the status of a ciénega is somewhat dependent on elevation.

Additional reasoning behind this argument is that ciénegas found at higher elevations are less prone to scouring from flash floods. Minckley and Brunelle (2007) determined that periods of high precipitation can result in an aggradation or degradation trend. When contrasting the San Bernardino ciénega from the Santa Cruz and San Pedro complexes, the largest differences are their distances from headwaters, not elevation. Perhaps a better measure for resiliency of a ciénega would be distance from headwaters, instead of elevation. This allows for removal of the bias the base elevation of the basin introduces, and accounts for the actual characteristics of the hydrological basin, as well as the probability of incision due to flash flooding. This does not account for the spatial variability in the status and subsequent vegetation succession found within almost every ciénega inventoried.

Such a basic attribute as elevation relative to a basin does not account for the

intraciénega spatial variability in the patterns of ciénega change. Restoration methods involve slowing the flow of the river either through the use of dams, dikes, gabions, or deflecting control structures. If the speed of flow is the ultimate determining factor of the resiliency of a ciénega, then a simple slope analysis would suffice to indicate which ciénegas are more prone to desiccation. The slope of all ciénegas in this analysis was <5 degrees. Figure 39 illustrates the distribution of the mean slope values across the status succession paths, to show that the distribution of slope does not differ based on status. Although restoring ciénegas involves slowing flow, the initial catalysts for desiccation and subsequent fluctuations in vegetation and saturation over time are not as simple. A likely influencing variable is the hydraulic conductivity, or rate at which water flows through a substrate with a given change in potential energy, of the subsurface substrate.

Using the best predictor variables to create a classification tree model yielded numerous likely undocumented active ciénegas. Although remote sensing techniques proved limited at identifying historical ciénegas that have desiccated, it proved useful at identifying areas that share the same attributes as active ciénegas . The resulting classification allows for the study of presently active ciénegas, along with the adjacent historical extent to further the understanding of the dynamics of ciénegas. This model can be applied to other regions that contain ciénegas or similar types of groundwater dependent ecosystems.

Recent Trends of Change

The strong relationship between the variation in mean annual precipitation of the study region and both the TIR and NBR mean values was hypothesized. What was

unexpected was the significant decrease in the sensitivity of active ciénegas' mean TIR value to the 3-year mean precipitation. It was speculated that perhaps a cumulative measurement of precipitation would account for the variability better. The hypothesis that there was no relationship between the 3-year mean annual precipitation and NBR or TIR values could not be refuted. Because the influencing variables on the health of ciénegas are apparently quite complex, it warrants further investigation to gain a better understanding as to what is causing these patterns of change. It is clear that precipitation can account for more than half of the variability in the sample used. This leaves almost half of the influencing variables unaccounted for. Other influencing variables could be local influences from humans, recent incision and subsequent desiccation, and the continued succession from herbaceous to woody riparian vegetation.

Future Research Directions

This analysis used surface attributes to infer what was occurring in the subsurface. Because of the inherent difficulties of using surface data as a proxy for what is occurring in the subsurface, actual analyses involving the monitoring of groundwater flow using piezometer transects is warranted. Currently, such data are only being collected on the Burro ciénega. Installation of piezometer transects in various ciénegas of various succession states would allow for a more complete understanding of what is occurring in the subsurface.

This study highlights the need for increased studies investigating contemporary influences on ciénegas, in order to assure that active ciénegas may remain as such, and that inactive ciénegas, where practical, may be effectively restored. This inventory

should be used as a tool for gaining a more geographically complete picture of ciénegas in their various settings. Future research should build on this inventory, while incorporating subsurface data in order to identify areas with the highest probability of being sustainably restored. It is apparent that if future precipitation trends continue on the recent trend, the overall likelihood of successful restoration of extinct historical ciénegas is low. However, with an increased understanding of what has caused the divergent succession paths of extinct ciénegas, as well as the spatial heterogeneity of the succession within each ciénega, will allow for the best chance of successful restoration.

This inventory can also be used as a source for future studies involving coring techniques. A number of core samples from geographically diverse ciénegas will allow for a more complete understanding of the cycles of aggradation and deggredation.

The true number of future research directions this inventory will allow for is difficult to quantify. As the dynamics of precipitation change throughout the region, it is clear that an increased understanding of how ciénegas react to these forcings is essential to ensure that this once widespread desert ecotone does not completely disappear.

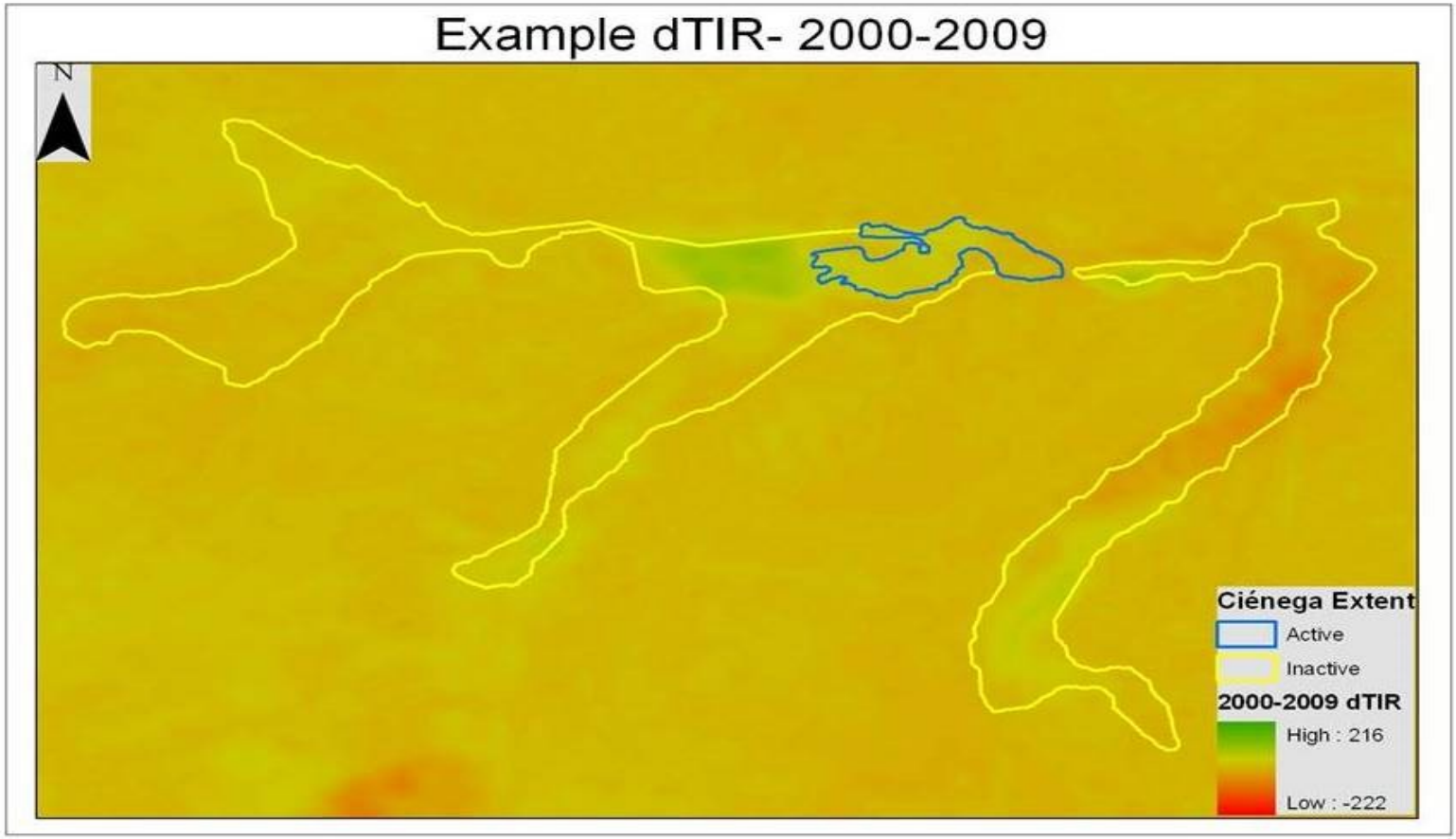

Figure 38: Example of difference in 2000 and 2009 TIR values of the Babocamari ciénega. Both active and inactive areas have heterogeneous patterns of change. This demonstrates the short-fallings of using asapatial zonal statistics to characterize ciénegas.

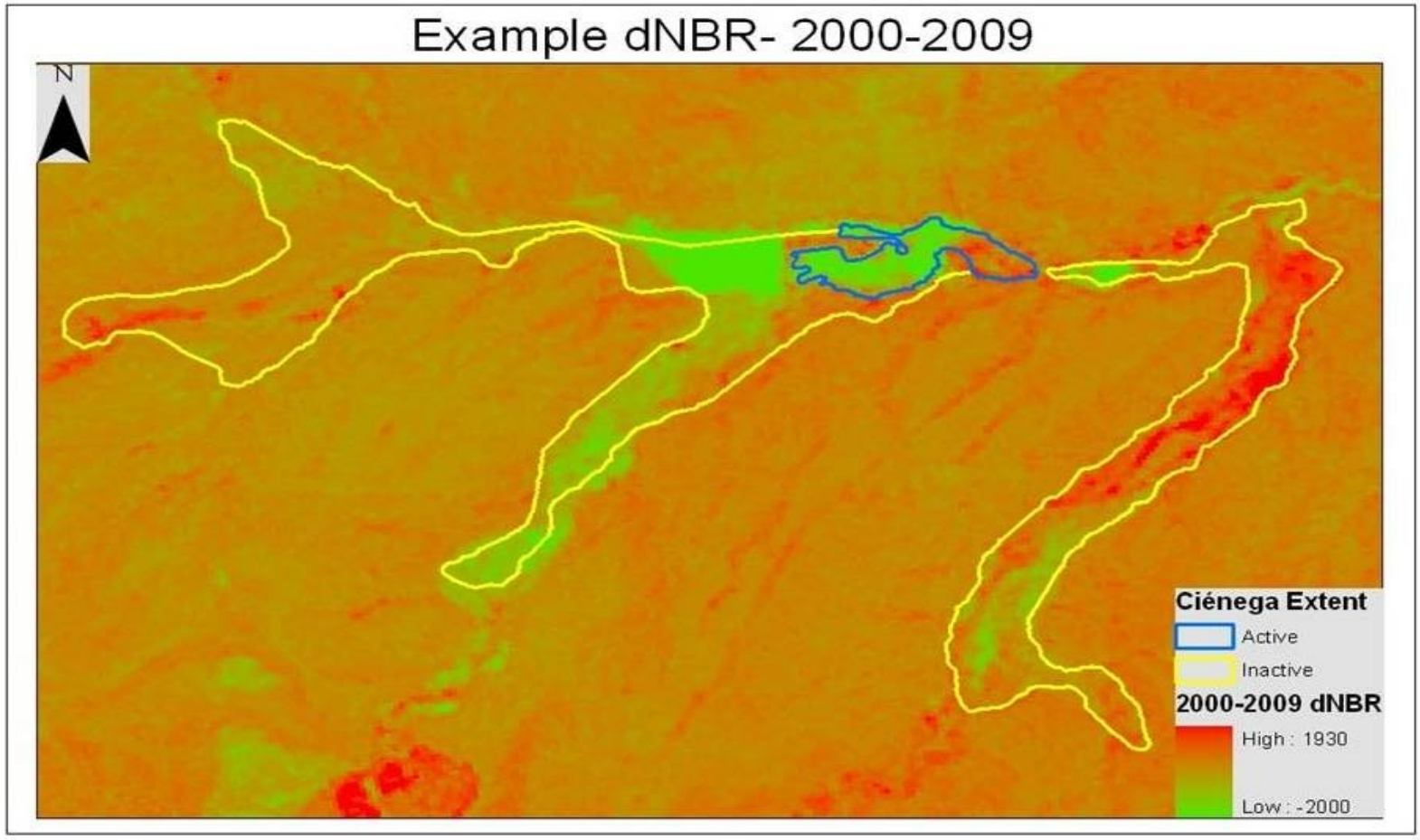

Figure 39: Example of difference in 2000 and 2009 NBR values of the Babocamari ciénega. Both active and inactive areas have heterogeneous patterns of change. This demonstrates the short-fallings of using asapatial zonal statistics to characterize ciénegas.

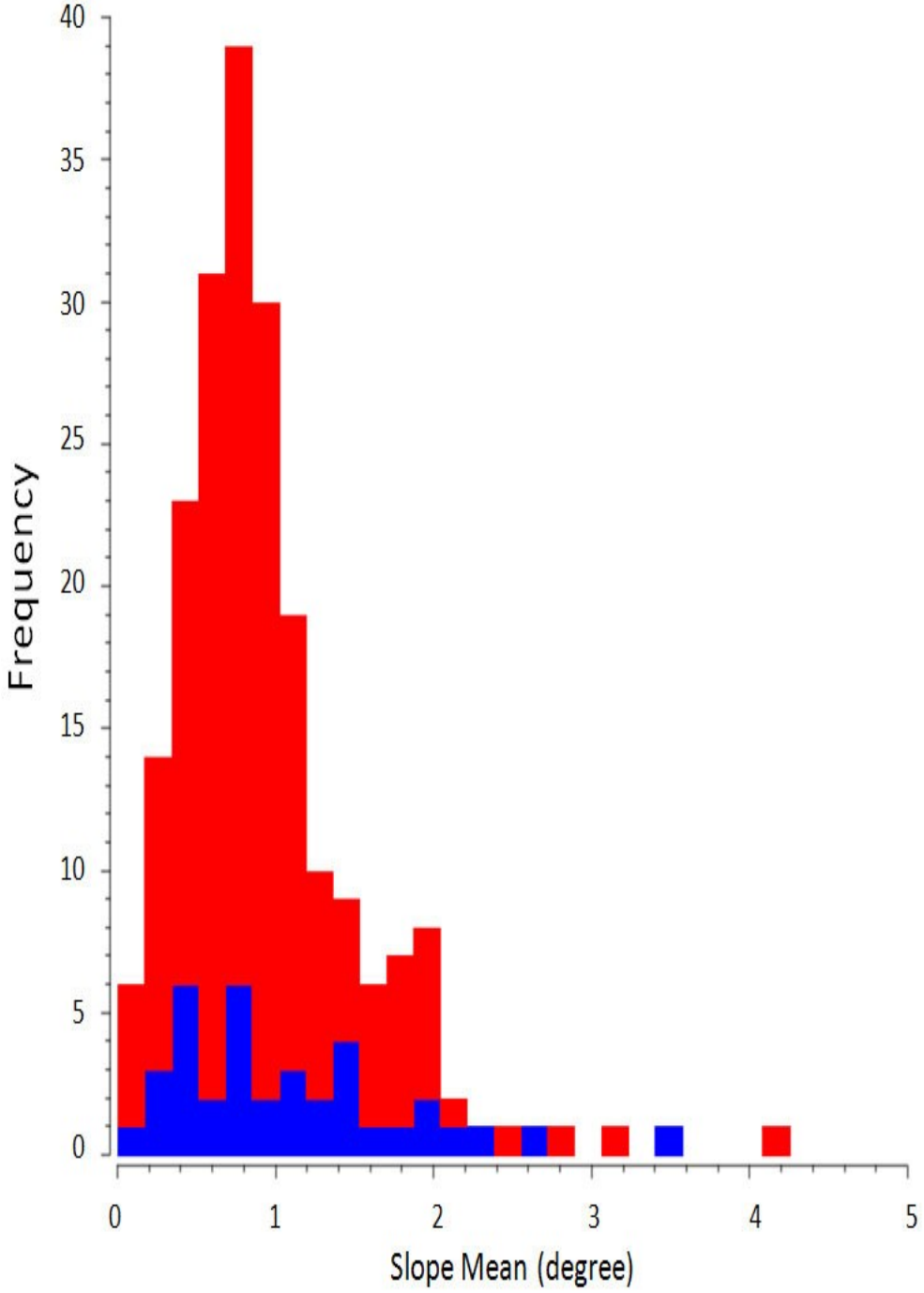

Figure 40: Distribution of mean slope values across active (blue) and inactive (red) ciénegas. There is little difference in mean slope of ciénegas of different status succession paths.

REFERENCES

Allen, R.G., Robison, C.W., Garcia, M., Kjaersgaard, J., & Kramber, W.J. (2008). Enhanced resolution of evapotranspiration by sharpening the Landsat thermal band. *Pecora17- The Future of Land Imaging… Going Operational*. Retrieved February 3, 2010, from http://www.asprs.org/publications/proceedings/pecora17-/0004.pdf .

Baker, C., Lawrence, R., Montagne, C., & Patten, D. (2006). Mapping wetlands and riparian areas using Landsat ETM+ imagery and decision-tree-based models. *Wetlands*, *26*(2), 465-474.

Baker, M.B., Folliott, P.F., & Dbano, L.F. (2004). *Riparian areas of the southwestern United States hydrology, ecology, and management*. Boca Raton, FL: Lewis.

Barnett, T.P., & Pierce, D.W. (2009). Sustainable water deliveries from the Colorado River in a changing climate. *PNAS*, *106*(18), 7334-7338.

Becker, M.W. (2006) Potential for satellite remote sensing of ground water. *Ground Water, 44*(2), 306-318.

Brunelle, A., Minckley, T.A., Blissett, S., Cobabe, S.K., & Guzman, B.L. (2010). A ~8000 year fire history from an Arizona/Sonora borderland ciénega. *Journal of Arid Environments*, *74*, 475-481.

Cooke, R.U., & Reeves, R.W. (1976). Arroyos and environmental change in the American Southwest. *Oxford Research Studies in Geography*. Oxford: Oxford University Press.

Crist, E.P., & Cicone, R.C. (1984). Application of the tasseled cap concept to simulated thematic mapper data. *Photogrammetric Engineering and Remote Sensing*, *50*, 343-352.

Davis, O.K., Minckley, T., Moutoux, T., Jull, T., & Kalin, B. (2002). The transformation of Sonoran Desert wetlands following the historic decrease of burning. *Journal of Arid Environments, 50*, 393-412.

Dobyns, H.F. (1981). From fire to flood: Historic human destruction of Sonoran Desert riverine oases. *Ballena Press Anthropological Papers, 20*, 203-222.

Etheredge, D. (2004). Geomorphic response to seasonal variations in rainfall in the

Southwest United States. *Geological Society of America Bulletin*, *116*(5-6), 606-618.

Hansen, M.K. (2008). *Decision tree classification of Dambo wetlands using remotely sensed multispectral and topographic data.* Master's thesis, University of Utah, Salt Lake City, UT.

Hastings, J.R. (1959). Vegetation change and arroyo cutting in southeastern Arizona. *Journal of the Arizona Academy of Science 1*, 60–67.

Hastings, J.R., & Turner, R.M. (1965). *The changing mile: An ecological study of vegetation change with time in the lower mile of an arid and semiarid region*. Tucson: University of Arizona Press.

Hendrickson, D.A., & Minckley, W.L. (1984). Ciénegas-vanishing climax communities of the American Southwest. *Desert Plants*, *6*, 130–176.

Jha, M.K., Chowdhury, A., Chowdary, V.M., & Peiffer, S. (2006). Groundwater management and development by integrated remote sensing and geographic information systems: Prospects and constraints. *Water Resources Management*, *21*(2), 427-467.

Krankina, O.N., Pflugmacher, D., Friedl, M., Cohen, W.B., Nelson, P., & Baccini, A. (2008). Meeting the challenge of mapping peatlands with remotely sensed data. *Biogeosciences Discussions*, *5*, 2075-2101.

Kustas, W., Anderson, M., Mecikalski, J.R., & Hain, C.R. (2009). A physically-based drought product using thermal remote sensing of evapotranspiration. *International Conference on Land Surface Radiation and Energy Budgets: Observations, Modeling and Analysis*. Retrieved February 4, 2010, from http://www.ars.usda.gov/research/publications/publications.htmseq_no_115=235-962

Leban, G., Zupan, B., Vidmar, G., & Bratko, I. (2006). VizRank: Data visualization guided by machine learning. *Data Mining and Knowledge Discovery*, *13*(2), 119-136.

McCune, B., & Keon, D. (2002). Equations for potential annual direct incident radiation and heat load index. *Journal of Vegetation Science*, *13*, 603-606.

Minckley, T.A., & Brunelle, A. (2007). Paleohydrology and growth of a desert ciénega. *Journal of Arid Environments*, *69*, 420-431.

Minckley, T.A., Clementz, M.T., Brunelle, A., & Klopfenstein, G.A. (2009). Isotopic

analysis of wetland development in the American Southwest. *The Holocene*, *19*(5), 737-745.

Munch, Z., & Conrad, J. (2007) Remote sensing and GIS based determination of groundwater dependent ecosystems in the Western Cape, South Africa. *Hydrogeology Journal, 15*(1), 19-28.

Pflugmacher, D, Krankina, O.N., & Cohen, W.B. (2007). Satellite-based peatland mapping: Potential of the MODIS sensor. *Global and Planetary Change, 56*, 248-257.

Powell, S.L., Pflugmacher, D., Kirschbaum, A.A., Kim, Y., & Cohen, W.B. (2007). Moderate resolution remote sensing alternatives: A review of Landsat-like sensors and their applications. *Journal of Applied Remote Sensing*, *1*, 012506.

Roshier, D.A., & Rumbachs, R.M. (2004). Broad-scale mapping of temporary wetlands in arid Australia. *Journal of Arid Environments*, *56*, 249-263.

Soti, V., Tran, A., Bailly, J., Puech, C., Seen, D.L., & Begue, A. (2009). Assessing optical earth observation systems for mapping and monitoring temporary ponds in arid areas. *International Journal of Applied Earth Observation and Geoinformation*, *11*(5), 344-351.

Southworth, J. (2004). An assessment of Landsat TM band 6 thermal data for analysing land cover in tropical dry forest regions. *International Journal of Remote Sensing*, *25*(4), 689-706.

Stambaugh, M.C., & Guyette, R.P. (2008). Predicting spatio-temporal variability in fire return intervals using a topographic roughness index. *Forest Ecology and Management, 254*, 463-473.

Tiner, R.W. (2003). Geographically isolated wetlands of the United States. *Wetlands*, *23*, 3, 494-516.